The Dissertation Committee for Sarah Anne Wolfe certifies that this manuscript is the approved version of the following dissertation:

MOLECULAR MECHANISMS UNDERLYING ALCOHOL USE DISORDER AND MAJOR DEPRESSIVE DISORDER COMORBIDITY

Committee:

_____

R. Adron Harris, Co-Supervisor

_____

Kimberly Raab-Graham, Co-Supervisor

_____

Nace Golding

_____

Richard Morrisett

_____

Paul Macdonald

MOLECULAR MECHANISMS UNDERLYING ALCOHOL USE DISORDER AND MAJOR DEPRESSIVE DISORDER COMORBIDITY

By

SARAH ANNE WOLFE, B.S.

DISSERTATION

Presented to the Faculty of the Graduate School of

The University of Texas at Austin

in Partial Fulfillment

of the Requirements

for the Degree of

DOCTOR OF PHILOSOPHY

The University of Texas at Austin

May 2017

ACKNOWLEDGMENTS

I would like to thank my advisors Drs. R. Adron Harris, and Kimberly Raab-Graham for their wonderful mentoring, support, and guidance through my graduate career, as well as my fellow lab members for their help and support. I would also like to thank Dr. Marisa Roberto for providing me with an amazing postdoctoral opportunity to continue my career.

ABSTRACT: MOLECULAR MECHANISMS UNDERLYING ALCOHOL USE DISORDER AND MAJOR DEPRESSIVE DISORDER COMORBIDITY

SARAH ANNE WOLFE, Ph.D.

The University of Texas at Austin, 05/2017

Supervisors: R. ADRON HARRIS and KIMBERLY RAAB-GRAHAM

Alcohol Use Disorder (AUD) and Major Depressive Disorder (MDD) are two widespread and debilitating disorders that share a high rate of comorbidity with the presence of either disorder doubling the risk of developing the other. Despite their prevalence, few treatments are available to individuals with comorbid AUD and MDD. Both alcohol and antidepressants promote lasting neuroadaptive changes in synapses and dendrites. With alcohol these changes may provide relief from depressive symptoms, and the initial use of alcohol may be a form of self-medication for individuals with MDD, suggesting ethanol may have antidepressant properties underlying similarities in neurobiological abnormalities. However, the synaptic pathways that are shared by alcohol and antidepressants are unknown. This study aims to identify why acute exposure to ethanol produced lasting antidepressant and anxiolytic behaviors. To understand the functional basis of these behaviors, a molecular pathway activated by rapid antidepressants was investigated. Here ethanol, like rapid antidepressants, altered γ-aminobutyric acid type B receptor ($GABA_BR$) expression and signaling,

to increase dendritic calcium. New $GABA_BRs$ were synthesized in response to ethanol treatment, requiring fragile-X mental retardation protein (FMRP). Ethanol-dependent changes in $GABA_BR$ expression, dendritic signaling, and antidepressant efficacy were absent in Fmr1-knockout (KO) mice. These findings indicate that FMRP is an important regulator of protein synthesis following acute alcohol exposure, and provided a molecular basis for the antidepressant efficacy of acute ethanol exposure. We identify alterations on a global scale with acute alcohol and antidepressant by sequencing the synaptic transcriptome. We identified parallel alterations in exon usage with acute alcohol and antidepressant treatment. These shared differentially expressed exons may give rise to isoforms and proteins with altered function or localization in the synapse. Some of these differentially expressed exons were identified in genes known to have alternative isoforms with AUD and MDD. These data implicate alternative splicing and isoform expression in the acute antidepressant-like effects of ethanol and the development of comorbid alcohol and depression. Understanding the molecular basis for comorbidity may aid in development of treatment options for afflicted individuals with dual disorders, as well as explore the mechanism for the initiation of addiction with acute exposure to alcohol.

TABLE OF CONTENTS

LIST OF FIGURES

LIST OF ABBREVIATIONS

5-HT – 5-hydroxytryptaamine
AAV – Adeno-associated viral vector
Ach – Acetylcholine receptor
ACSF – Artificial cerebral spinal fluid
AMPAR – α-amino-3-hydroxy-5-methyl-4-isoxazolepropionic acid receptor
AP5 – D-(-)-2-Amino-5-phosphonopentanoic acid
ATP9B – ATPase 9B
AUD – Alcohol Use Disorder
BONCAT – Bioorthoganol noncononical amino acid tagging
BSA – Bovine serum album
CaMK-II – Calcium/calmodulin-dependent protein kinase
CHX – Cycloheximide
DEE – Differentially expressed exon
DEG – Differentially expressed gene
DIV – Days *in vitro*
DSM – Diagnostic and Statistical Manual of Mental Disorders
EIF3K – Eukaryotic translation initiation factor 3 subunit K
ETOH – Ethanol
FDA – Federal Drug Administration
FMR1 – Fragile X mental retardation 1 gene
FMRP – Fragile X Mental Retardation Protein
FST – Forced swim test
FXS – Fragile X syndrome
$GABA_AR$ – γ-aminobutyric acid type A Receptor
$GABA_BR1$ – γ-aminobutyric acid type B Receptor 1
$GABA_BR2$ – γ-aminobutyric acid type B Receptor 2
GIRK – G-protein inwardly rectifying potassium channel
GlyR – Glycine receptor
GPCR – G protein coupled receptors
GTP – Green fluorescent protein
i.p. – Intraperitoneal injection
iGluR – Ionotropic glutamate receptor
IPSC – Inhibitory postsynaptic current
KO – Knock out
LGIC – Ligand-gated ion channels
LTD – Long-term depression
LTP – Long-term potentiation
MAP2 – Microtubule associated protein 2
MDD – Major Depressive Disorder
mGluR – Metabatropic glutamate receptor
mTOR – Mammalian target of rapamycin
NMDAR – N-methyl-D-aspartate receptor
PBS – Phosphate buffered saline
PCA – principle component analysis
PFA – Paraformaldehyde
PLA – Proximal ligation assay
qPCR – Quantitative Polymerase Chain Reaction
RAAD – Rapid acting antidepressant
RIP – RNA immunoprecipitation
RNA – Ribonucleic acid
RNA-seq – RNA sequencing
Ro 25-6981 – (α*R*,β*S*)-α-(4-Hydroxyphenyl)-β-methyl-4-(phenylmethyl)-1-piperidinepropanol
ROI – Regions of interest
RT – Reverse transcription
S6K – S6 Kinas
SDS-PAGE – Sodium dodecyl sulfate polyacrylamide gel electrophoresis
SEM – Standard error of the mean
Seq – Sequencing
SN – Synaptoneurosomes
SSRI – Selective serotonin reuptake inhibitor
TCA – Tricyclic antidepressant
Veh – Vehicle
WHO – World Health Organization
WT – Wild Type
3'-UTR – 3'-untranslated region

CHAPTER 1: INTRODUCTION

Disease overview

Alcohol use disorder and major depressive disorder are two wide spread and devastating disorders which often occur together. It is evident that a high rate of comorbidity occurs between these disorders, but how and why they develop together is an unanswered question. Alcohol abuse, depression, and evidence of comorbidity will be discussed in this section.

Alcohol Use Disorder

Alcohol use disorder (AUD) is the medical diagnosis given to individuals with severe problem drinking. AUD affects approximately 7% of adults in the United States, which includes about 11 million men and 6 million women. It is one of the world's leading health risks causing more than 60 major types of diseases and injuries, and resulting in approximately 3.3 million deaths each year or 5.9% of all deaths globally. Alcohol can cause harm and death through its toxic effect on organs and tissues; ability to cause impairment in physical coordination, consciousness, perception, and cognition leading to accidental injury or death to self or others; and reduces self-control affecting a persons behavior (WHO 2014 global status report).

The addictive nature of alcohol is due in part to neuroadaptive changes that occur in response to chronic ethanol exposure (Fig. 1.1). Neuroadaptation alters brain functioning to compensate for constant exposure to alcohol making it difficult for individuals to function in its absence. Neuroadaptation from continued alcohol abuse manifest as tolerance and physiological dependence, and are thought to be crucial to transition from controlled drinking to frequent, uncontrolled and excessive drinking[1]. Remodeling of the synapse in response to alcohol is thought to lead to tolerance and physical dependence in AUD[2]. The initial signaling mechanisms that produce changes in synaptic protein composition that lead to neuroadaptations have yet to be explored, but it appears to be a slippery slope that initiates acute changes that with repeated exposure can lead to addiction. AUD is also a difficult disorder to overcome once diagnosed in an individual due to alcohol withdrawal complications. Withdrawal symptoms can be dangerous and last for prolong periods of time. Symptoms including: seizures, vomiting, hallucinations, and autonomic hyperactivity. Withdrawal symptoms can also make individuals relapse even after periods of abstinence, perpetuating alcohol use and abuse[3]. The widespread and debilitating nature of AUD make the development of more effective treatment options imperative.

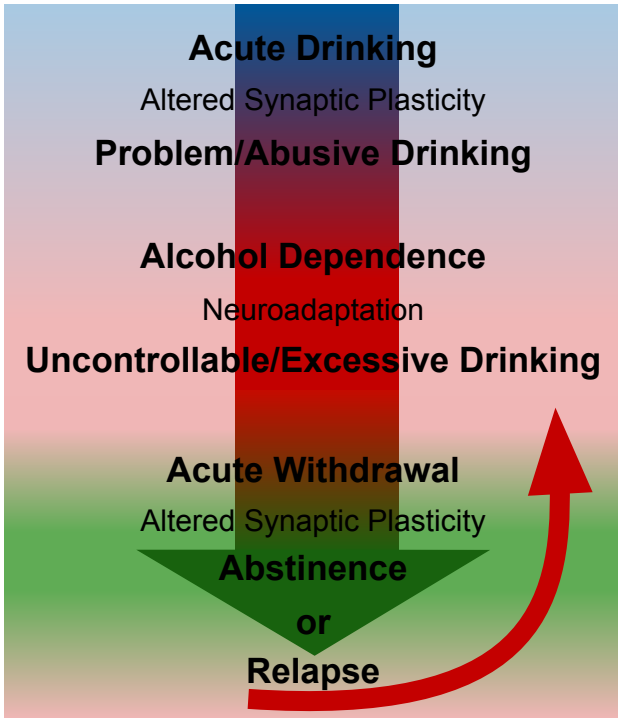

Figure 1.1. Cycle of Alcohol Dependence

Schematic illustrating how acute drinking can develop into alcohol dependence due to neuroadaptation, which in turn causes withdrawal symptoms with alcohol abstinence and enhanced vulnerability to relapse. Altered synaptic protein composition and plasticity with alcohol exposure may be involved in the initial changes that lead to problem drinking and neuroadaptation/dependence. Synaptic plasticity may also be involved in reversing the effects of neuroadaptation with abstinence/withdrawal.

Available pharmacological treatments

Currently there are minimal effective pharmacological treatments for AUD, because AUD is a complex disorder affecting many brain regions and cellular pathways. The most common drugs used to treat chronic alcohol use are

Disulfiram, Naltrexone, and Acamprosate, however there are other available drugs to address symptoms such as benzodiazepines for withdrawal.

Disulfiram has been used for over 50 years and is FDA approved for the treatment of alcoholism. Its mechanism of action causes the natural breakdown of alcohol to produce acetaldehyde, which can be toxic and causes aversive reactions when alcohol is consumed such as vomiting, headache, and anxiety[4]. It acts as a deterrent to drinking for individuals to whom it is administered, however it is difficult for individuals to maintain compliance due to these side effects. In some cases it may also induce psychiatric disorders such as delirium, depression, anxiety, psychosis, and mania. There is little information about the effects of Disulfiram in individuals with comorbid disorders[4].

Naltrexone is also FDA approved for the treatment of AUD and its mode of action is to block the action of ethanol induced chemical signals in the brain from opioids. It has been shown to be effective in treating alcohol dependence in humans, and reported to lower levels of alcohol craving and drinking[5]. Naltrexone is a promising treatment of comorbidity with psychiatric disorders however more research is needed. However, Naloxone a similar opioid antagonist, demonstrated no effect on mood in patients with depression[6].

Lastly Acamprosate is promising in the treatment of AUD and is FDA approved for such a purpose. Acamprosates mode of action is not completely understood but is thought to normalize alcohol-disrupted brain activity through GABA and glutamate neurotransmission[7]. Acamprosate may help individuals

with AUD achieve abstinence and diminish withdrawal symptoms[8]. Symptoms of alcohol and psychiatric disorder comorbidity with Acamprosate still need to be studied, although it has been shown to have some positive effects in patients with comorbid schizophrenia[9]. However, Acamprosate may increase suicide rate with long-term use[10].

Various pharmacological avenues for aiding patients with AUDs have been developed. However issues with existing treatments include side affects, lack of patient compliance, and effectiveness of the drugs with comorbid psychiatric disorders, which is incredibly high in patients with AUDs. Therefore, novel treatment strategies that reduce adverse effects and are applicable across common comorbidities warrant development.

Major Depressive Disorder

Major Depressive Disorder (MDD) is a widespread and debilitating mental disorder effecting approximately 350 million people worldwide. In the United States it will effects about 17% of individuals at some point in their lifetime[11]. Depression can become a serious long-lasting health risk. Depression can result in suffering for the patient and individuals involved with the patient, through an inability to preform daily functions such as caregiving and working. In severe cases depression can lead to suicide. More than 800 thousand people die each year to suicide (WHO global status report).

MDD symptoms can include: depressed mood, irritability, loss of pleasure or interest, reduced energy, and diminished activity, anxiety symptoms, disturbed sleep, appetite or weight change, poor concentration, and low self-worth, depending on the severity of the episode which can last two weeks or more[12](WHO global status report). MDD can interfere and impair with a patients relationships, school or work, stress levels and anxiety and daily activity[12]. Current pharmacotherapies for depression can take weeks to become effective and many individuals are treatment resistant, leaving these people susceptible to self-destructive behavior and suicide[13]. Self-medication with drugs and alcohol can also become an issue, as well as comorbidity to other disorders[14].

The exact cause of MDD is unknown, but certain factors increase the risk of developing the disorder. Factors such as genes and stress can affect brain chemistry and alter mood stability, and changes in hormone balance may contribute to MDD development[12,14]. Additionally external factors can trigger MDD such as alcohol and drug abuse, medical illness like hypothyroidism and cancer, other psychiatric disorders such as bipolar disorder, some medications like steroids, and bereavement[12, 15]. The widespread, complex, and poor treatment options for MDD makes it imperative to research this disorder to find alternative treatment options and to investigate its relationship to other debilitating disorders.

Available pharmacological treatments

The most common pharmacological treatments for MDD are selective serotonin reuptake inhibitors (SSRIs) and tricyclic or tetracyclic antidepressants (TCAs). SSRIs mode of action block the reuptake of serotonin increasing availability of serotonin in synaptic cleft and brain[16]. There are several FDA approved SSRI to treat depression including Citalopram (Celexa), Fluoxetine (Prozac), Paroxetine (Paxil), Escitalopram (Lexapro), and more. SSRIs have few serious side effects, and are the most popular antidepressant used to treat humans[16]. However, SSRIs only alleviate symptoms of MDD in 37% of patients treated[17]. In addition to its affects on MDD, SSRIs have been found to affect alcohol consumption. SSRIs may aid individuals with comorbid AUD by decreasing consumption and preventing relapse with stress[18]. SSRIs were also shown to be effective in reducing alcohol use in individuals with MDD but not without, reducing symptoms of AUD and MDD in comorbid patients[19, 20].

TCAs are the second choice for treating patients with antidepressants as they have more side effects and potential for overdose, but are still effective in treating MDD[21]. TCAs ease depression symptoms by acting on neurotransmitters to regulate brain chemistry. They have a complex pharmacological profile and inhibit multiple neurotransmitter reuptake sites including the reuptake of serotonin and norepinephrine to increase levels at the synaptic cleft[21]. Examples of FDA approved TCAs include: Impiramine (Tofranil), Desipramine (Norpramin), Doxepin, Protriptyline (Vivactil), and more. TCAs have also been shown to treat depression in patients with comorbid AUD[22].

These conventional antidepressant treatments work well for some, but a majority of patients with MDD are resistant to these drugs and find little or no relief from them. Additionally, these drugs can take weeks to decrease MDD phenotypes and leave patience vulnerable to self-harm and suicide during this time, as well as impeding on daily activities[23, 24]. In addition to these standard antidepressant treatments a new class of antidepressants has developed that are rapid acting and have lasting antidepressant behavioral responses.

Rapid acting antidepressants (RAADs) were first identified in the early 1990s to inhibit N-methyl-D-aspartate receptor (NMDAR) activity and promote antidepressant phenotypes[25]. RAADs such as ketamine elicit an antidepressant response by antagonizing NMDARs and engage a cascade of events that includes a surge in glutamate, stimulation of AMPAR and activation of mTOR signaling and synaptic formation[25, 26]. Examples include Ketamine, Ro 25-6981, MK-801, and AP5. Ketamine, and other FDA approved NDMAR antagonist have remarkable efficacy in treating conventional drug resistant depression, however they also have a downside. The addictive nature and side effects of some RAADs make them less desirable for pharmacotherapy and therefore finding alternative drugs is imperative[27]. Atypical NDMAR antagonists specific for the NR2B subunit were discovered to have improved side effects[28-30], making characterization of other NR2B selective antagonists desirable for possible new treatments[31]. Ro 25-6981 (Fig. 1.2) is one of these antagonists studied as an alternative to Ketamine due to Ketamine's undesirable side effects[29]. Ro 25-6981

is a noncompetitive allosteric modulator of the NR2B subunit of NMDARs, and is potent and highly specific for NR2B blocking NMDARs containing this subunit[31, 32 33]. Ro 25-6981 has a slow half-life of dissociation, reported to last greater than 5 hours at 4°C, and inhibits in a concentration dependent manner with high potency at a K_i of 20nM[31]. It is an activity-dependent inhibitor, binding with higher affinity to the activated and desensitized receptor[32]. In this study we chose to use Ro 25-6981 as a novel rapid-antidepressant specific for NR2B antagonism[34].

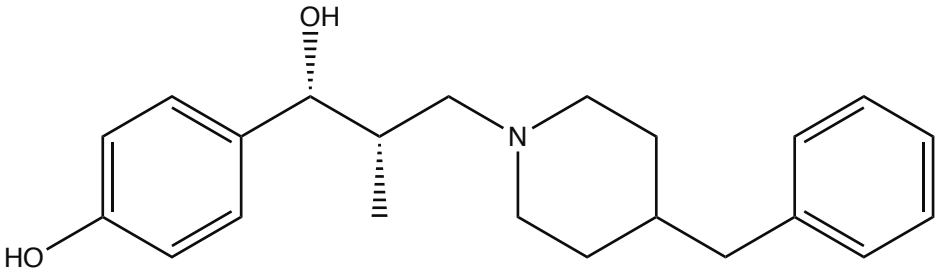

Figure 1.2. Chemical structure of Ro 25-6981 (α*R*,β*S*)-α-(4-Hydroxyphenyl)-β-methyl-4-(phenylmethyl)-1-piperidinepropanol.

Comorbidity

AUD often accompanies other mental disorders, some of which are thought to display aberrant synaptic plasticity[35]. The mechanism underlying the linkage between AUD and MDD is not well understood, but the presence of either disorder in an individual doubles the risk of developing the other disorder[14, 36]. Additionally, AUD and MDD are among the leading cause of disability in the world[14]. Individuals with AUD comorbid MDD have an earlier onset of alcohol dependence and increased rates of lifetime drug dependence[37]. Comorbid MDD

patients entering treatment for alcohol and drug addiction tend to have worse outcomes than those without dual diagnosis[38] including higher relapse rates[39]. Comorbidity is also associated with greater severity and number of both suicide attempts and completed suicides[20, 40].

Epidemiological and clinical studies both support the notion that AUD and MDD are closely linked. AUD and MDD may be caused by similar environmental and genetic factors[14, 36]. One hypothesis suggests that depressed individuals self-medicate with alcohol. This may decrease depressive symptoms acutely, but consistent alcohol abuse may lead to addiction and development of AUD. Therefore, self-medicating with alcohol may also play a role in the development of AUD in individuals with MDD[14, 41].

Treatment failure for co-occurring AUD and MDD might be explained by the theory that patients with comorbidity often do not receive specialized treatment for both conditions. Pharmacological and psychosocial treatments are available for each disorder, but need to be integrated to help comorbid patients, and few established treatments for psychiatric disorders have been evaluated in patients with dual AUD[18]. Additionally, individuals with an AUD and co-occurring psychiatric disorder such as depression may find it more difficult to access and participate in traditional alcohol treatments, which require patient compliance, and self-help groups where most members do not have comorbid disorders[19, 42]. Interestingly, treatment of AUD has been shown to reduce MDD symptoms and vise versa[14]. Specifically the rapid antidepressant Ketamine can has been

observed to reduce ethanol seeking behavior, and NMDAR antagonism may decrease ethanol intake by substituting alcohol and acting as a reinforcing stimulus[43]. More research is necessary for treatment for comorbid patients due to the complexity of the overlapping symptoms, common neurobiological abnormalities and limited dual treatment options.

Molecular Mechanisms

Alcohol and Antidepressants alter a vast and varied array of molecular and cellular processes, and this material is added to continuously. Discussed here are most well known modes of action of alcohol and antidepressants. Particular interest is placed on synaptic pathways and proteins important to the body of work presented in this dissertation.

Acute Alcohol

Acute ethanol exposure can affect the function of ion channels, neurotransmitter receptors, and intracellular signaling proteins. Ion channels are one of the most well studied targets of ethanol action. In particular ligand-gated ion channels bind neurotransmitters or intracellular messengers to activate and open an intrinsic ion pore. In general ethanol exposure facilitates the function of ligand gated ion channels including nicotinic acetylcholine and serotonin receptors, $GABA_AR$, and strychnine sensitive glycine receptors[44, 45]. Ethanol is thought to increase the probability of the opening of some channels and/or increase agonist affinity[46, 47],

such as when ethanol increases amplitude and duration of $GABA_AR$ and Glycine (GlyR) mediated inhibitory postsynaptic currents (IPSCs)[48, 49], which is though to increase neuronal inhibition. Acute ethanol exposure also potentiates 5-HT3 receptors function[45].

Effects of acute ethanol exposure on ionotropic glutamate receptors have also been well studied. These ionotropic glutamate receptors (iGluRs) include AMPA, NMDA, and Kainate receptors. These glutamate receptors are generally inhibited by ethanol[50]. The best-characterized pathway is ethanol's inhibition of NMDR. NMDAR is a ligand, voltage-gated cation channel known for its role in shaping synaptic strength during synaptic plasticity[51]. Ethanol inhibits NMDAR function in a concentration dependent manner at ranges that produces intoxication[52]. Interestingly, synaptic responses mediated by NMDARs have been shown to decrease with acute ethanol exposure[45, 53-55]. NMDARs are heteromeric proteins, with an obligatory NR1 subunit and one or more NR2 subunits [56, 57]. NMDAR receptors containing an NR2B subunit are particularly sensitive to ethanol's effects[58]. Importantly, Ro 25-6981 is selective for the NR2B subunit of NMDAR, binding noncompetitively to a domain of NR2B that promotes stabilization and a closed conformation of the receptor[32]. Ethanol inhibition of these glutamate receptors generally reduces neuronal excitability in most brain regions by reducing excitatory synaptic drive and preventing synaptic plasticity that is dependent upon iGluR activity[45]. Ethanol has been shown to attenuate NMDA induced ion currents in cultured hippocampal neurons and slices, and that

antagonism of NMDAR mediated activity by ethanol may attenuate memory related synaptic plasticity in the hippocampus[59].

The hippocampus is thought to be critically involved in addiction in humans, particularly in synaptic plasticity necessary for drug associated learning and memory[60]. Ethanol related memory retrieval was also observed to cause synaptic protein synthesis, and disruption of these memories by mTORC1 inhibition prevented relapse[61]. MTORC1 is activated by ethanol and is a protein essential to mediating signaling pathways required for local dendritic/synaptic proteins associated with synaptic plasticity and memory processes[61, 62]. These studies indicate that acute ethanol exposure is involved in synaptic plasticity related pathways.

In addition to ionotropic receptors, ethanol also affects G protein-coupled receptors (GPCRS). GPCRs are receptors specialized in binding neurotransmitters and initiating intracellular signaling pathways. GPCRs can affect neurophysiology by indirectly altering protein kinases, ion channels, intracellular signaling, and gene expression down stream. Ethanol inhibits activity of the metabotropic glutamate receptors, Acetylcholine receptors (Ach) and serotonin type 2 receptors. Inhibition to these GPCRs is most likely a downstream effect of ethanol target sites[63, 64]. However it is thought that ethanol weakly affects these protein and their physiologic impact is not yet clear[45]. Ethanol can also potentiate the function of G protein-coupled inwardly-rectifying potassium channels (GIRKs) at intoxicating concentrations[65-67]. GIRKs are

inwardly-rectifying potassium ion channels that through GPCR signaling open and induce hyperpolarization. GIRK channels usually inhibit neuronal activity by hyperpolarizing neurons, and ethanol effects on GIRK2 channels may contribute to intoxication[67].

Neurotransmitters are also affected by ethanol. Monoamine levels in brain increase with acute ethanol exposure[68], and GABA release increases although no change in glutamate occurs[69]. However most neurotransmitter transporters are relatively insensitive to acute ethanol. Acute ethanol exposure has numerous effects on neurons and signaling cascades, and those discussed are only the best studied and relevant. Additional research is required to expand our knowledge of the vast array of effects that ethanol exposure induces as well as understand how these alterations affect individuals on molecular and behavioral levels.

Rapid-Antidepressants

Ketamine, Ro 25-6981, and other FDA approved NDMAR antagonist have remarkable efficacy in treating conventional drug resistant depression. NMDAR blockade at rest is known to cause antidepressant behavioral responses[70]. Acute treatment with Ketamine or Ro 25-6981 can relieve depression symptoms as well as stress induced anhedonia, and anxiogenic behaviors[71]. RAADs ability to alleviate depression quickly and remain effective for long periods is due to their capacity to engage homeostatic mechanisms that trigger protein synthesis

pathways[25]. RAADs can remain in effect long after the drug has cleared the patients system due in part to altered synaptic plasticity and synaptogenesis induced through NMDAR inhibition[72-74]. Acute doses engage numerous synaptic signaling mechanism that can induce protein synthesis and increase synaptic connections long-term, possibly reestablishing brain activity levels that remedy depressed systems[75].

Ketamine has been shown to activate synaptic protein synthesis in an mTOR dependent manner. Increased mTOR activity with NMDAR blockade increases synaptic signaling proteins and the number and function of neuronal spines. Blocking mTOR inhibits ketamine induction of synaptogenesis and antidepressant behavioral responses[76]. Similar to ketamine the rapid-antidepressant Ro 25-6981 inhibits NMDAR activity, however unlike ketamine it is specific for the NR2B receptor subunit[77]. Ro 25-6981 is an effective rapid-antidepressant as determined by numerous behavioral studies[13, 76, 78], and has been shown to mimic some molecular and behavioral phenotypes of alcohol[79].

Synaptic Plasticity and Neuroadaptation

Changes in the efficacy of synaptic signaling contribute to many aspects of development in brain, learning and memory, and addiction[80]. Synaptic plasticity allows synapses to adjust the efficacy of synaptic transmission, strengthening or weakening, in response to synaptic activity and stimulation. Synaptic plasticity commonly manifests in the form of long-term potentiation (LTP), and long-term

depression (LTD). In general, LTP increases synaptic transmission and LTD decreases synaptic transmission. LTP and LTD are induced by repetitive patterns of activation or inputs to a postsynaptic neuron[54]. Acute ethanol exposure suppresses the induction of LTP at synapses[54].

Synaptic plasticity induces changes in protein composition of synapses through local protein translation[81, 82]. mRNAs, and their associated binding proteins or miRNAs, have been shown to be transported from the cell body to dendrites in response to synaptic activity [83,84,85]. Regulation of localization is thought to occur through cis-acting localization elements of the 3'-untranslated region (3'-UTR) of mRNA and RNA binding proteins[81, 86]. Various RNA binding proteins regulate translation and modulate both localization and translation of mRNAs with related functions, such as the Fragile-X mental retardation protein (FMRP)[87-89]. Increasing evidence indicates mRNA localization and translation are tightly linked and regulated[90]. After localization mRNAs are translated in synapses in response to synaptic stimulation by polyribosomes at the base of spines[91]. Individual synapses could independently regulate morphology in a protein synthesis dependent manner in response to stimuli[81]. mRNA localization and translation provides a general mechanism whereby neurons can locally alter protein composition within discrete subcellular compartments[92].

Changes in signaling and neuronal plasticity may be critical components in development of lasting ethanol behavioral phenotypes such as dependence, sensitization, and craving[93]. Transcriptional profiling has been explored acutely to

understand the initial steps that may lead to neuroadaptation. Previous studies have identified that synaptoneurosomes collected from chronic drinking mice had a greater number of alcohol responsive mRNAs and higher fold changes as compared to the total homogenate when sequenced[94]. We have previously identified molecular changes in synaptoneurosomes and dendrites with ethanol and Ro 25-6981[13, 78, 79]. Other rapid-antidepressants such as ketamine have also been shown to effect changes in mRNA at synapses and synaptic plasticity. Ketamine facilitates neuronal plasticity in brain regions implicated in MDD[95]. Interestingly, Ro 25-6981 may have similar effects due to their relatively conserved mechanism of action[78]. Both ethanol and antidepressants have been shown to inhibit NMDARs and facilitate translation of synaptic proteins and synaptic plasticity in an mTORC1 dependent manner[74, 96]. MTOR can be regulated by upstream NMDAR activated pathways[97], and mTOR pathways are known to promote local protein synthesis[55, 98]. In neurons mTOR can be activated by calcium signaling through PI3Kinase and its activity can promote cap-dependent translation by phosphorylating S6 Kinase (S6K) and eIF4E binding protein (4E-BP) to initiate translation[99, 100]. Ethanol and RAADs share some similarities in these pathways and they may underlie a shared antidepressant effect between Ethanol and RAADs.

Neuroadaptation can arise from repeated exposure to drugs or chronic drug abuse. Neuroadaptation arises when lasting changes in neurons such as synaptic protein composition occur to adapt and counter the effects of exposure

to chemicals such as alcohol. With repeated exposure of drug, lasting changes in synaptic plasticity may develop and give rise to addiction. These initial changes in synaptic plasticity with acute exposure have not been fully explored[93, 101].

The $GABA_B$ Receptor Shift

$GABA_B$Rs are G-protein coupled receptors that are typically responsible for depressing neuronal activity[101, 102]. $GABA_B$Rs decrease neurotransmitter release, inhibit presynaptic calcium channels, and activate slow inhibitory postsynaptic potassium channels. The $GABA_B$ Receptor is a heterodimer comprised of two subunits of $GABA_B$R1 and $GABA_B$R2. This receptor has a long extracellular amino terminus, seven transmembrane domains and a short intracellular carboxy terminus responsible for linking the subunits. $GABA_B$R2 functions as a carrier to $GABA_B$R1, transporting $GABA_B$R1 from the endoplasmic reticulum to the cell membrane. $GABA_B$Rs are localized to most brain regions and are at high concentrations in the hippocampus. $GABA_B$Rs are metabatropic receptors and transmit intracellular signals via adaptor proteins capable of producing functional changes including effects on intracellular enzymes and ion channels. These secondary messenger systems operate through binding and activation of guanine nucleotide binding proteins or G proteins. Of particular interest, $GABA_B$R activation can induce GIRK channels and block Ca2+ influx through voltage dependent calcium channels. $GABA_B$R are generally thought to be inhibitory and

reduce calcium signaling pathways[102, 103]. Some evidence also suggests that $GABA_BR$ function may alter alcohol-drinking behaviors[104, 105], but further research is needed to understand the role of $GABA_BRs$ and alcohol dependence.

Recently $GABA_BRs$ have been identified to have an alternative function when NMDARs are inhibited in dendrites and synapses (Fig. 1.3). This shift in $GABA_BR$ function is induced when NMDARs are blocked by the rapid antidepressant Ro 25-6981, AP5[13], and ethanol[79]. Introduction of an NMDA antagonist was demonstrated in mice and cultured hippocampal neurons to induce new dendritic synthesis of $GABA_BR2$, increases formation of new GBA_BARs. These new $GABA_BRs$ operate outside of their canonical role of activating potassium channels and instead shift function to promote dendritic calcium entry. $GABA_BR$-facilitated increases in dendritic calcium promotes a signaling cascade leading to heightened mTOR activity and mTOR dependent translation of plasticity-related proteins that may produce neuroadaptations and long-lasting antidepressant properties. Importantly, $GABA_BR$ antagonism prevents the increase in mTOR activity and thus mTOR dependent protein synthesis, as well as the antidepressant behavioral phenotype with rapid antidepressants[13]. Remarkably, ethanol promotes the same shift in $GABA_BR$ function from reducing to increasing dendritic resting calcium levels with $GABA_BR$ activation. Further dissection of this pathway indicates that the Fragile-X mental retardation protein may play a role in the initial increase in translation of dendritic $GABA_BRs$[79].

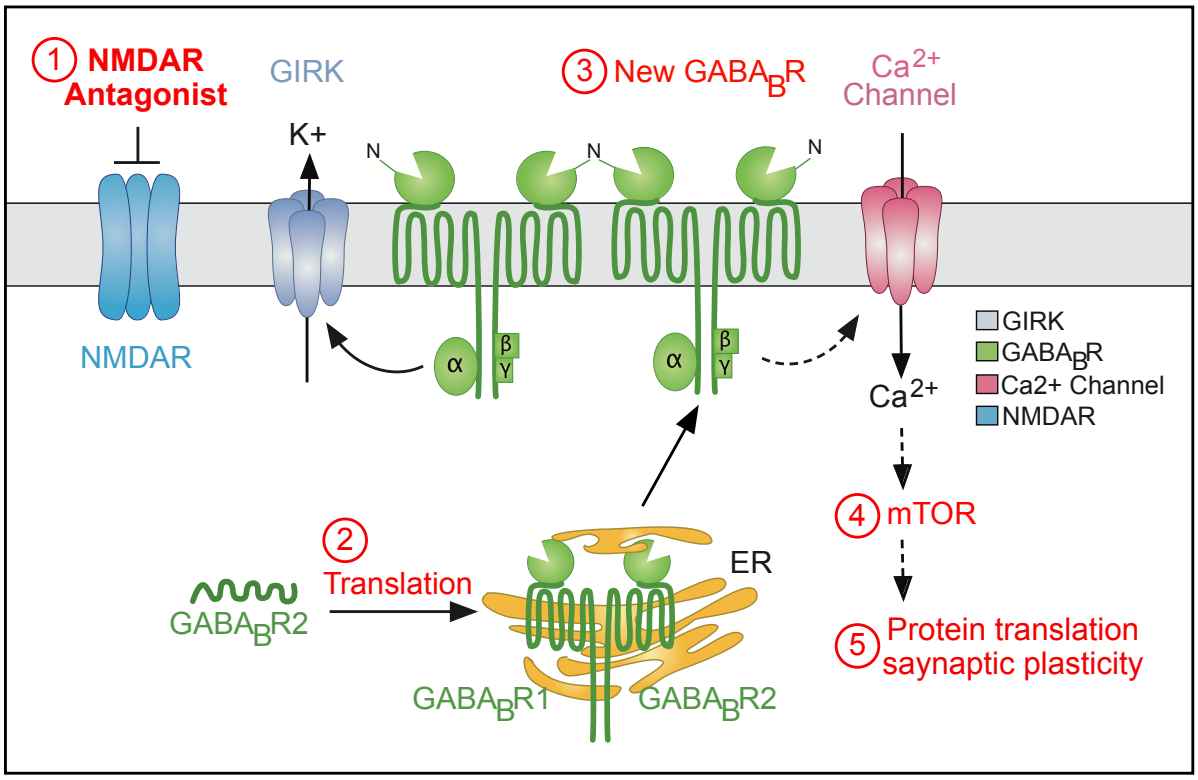

Figure 1.3. Model of acute NMDAR inhibition

This model depicts the proposed pathway initiated by NMDAR antagonism leading to increased synaptic protein synthesis. Numbers indicate the suspected order of events upon inhibition of NMDAR including: initiation of translation of new synaptic $GABA_BRs$, a switch in function of these new receptors, increased intracellular calcium, activation of mTOR and protein translation that may alter synaptic plasticity.

Fragile-X mental retardation protein (FMRP) is an RNA-binding protein that regulates translation by preventing ribosomal translocation of its target mRNA (including the confirmed FMRP targets: $GABA_BR1$ and $GABA_BR2$)[106]. FMRP is thought to influence synaptic plasticity of specific proteins by regulating activity dependent protein synthesis. Neuroadaptations require the translation of

pre-existing dendritic mRNA, and FMRP is a key regulator of synaptic mRNA translation[107]. Synaptic changes produced by ethanol exposure may require translation of proteins from localized mRNAs[93]. An investigation comparing FMRP targets and differentially expressed genes in the hippocampus of human alcoholics identified using RNA-seq data shows a significant overlap. This suggests that the differentially expressed genes in human alcoholics may be regulated by FMRP. This overlap was observed in the hippocampus, but not in other brain regions (Fig. 1.4). Furthermore, $GABA_BRs$ are known to correlate with lifetime consumption of alcohol in humans[108], and FMRP was discovered to play a role in mediating cocaine induced behavioral and synaptic plasticity[109]. These data indicate that FMRP may be a key regulator of differential protein expression in alcohol and other drugs of addiction that may contribute to neuroadaptive changes with addiction. It is clear that regulation of protein translation is important to drug induced neuroadaptive changes; however, mechanisms that induce translation with alcohol remain undiscovered.

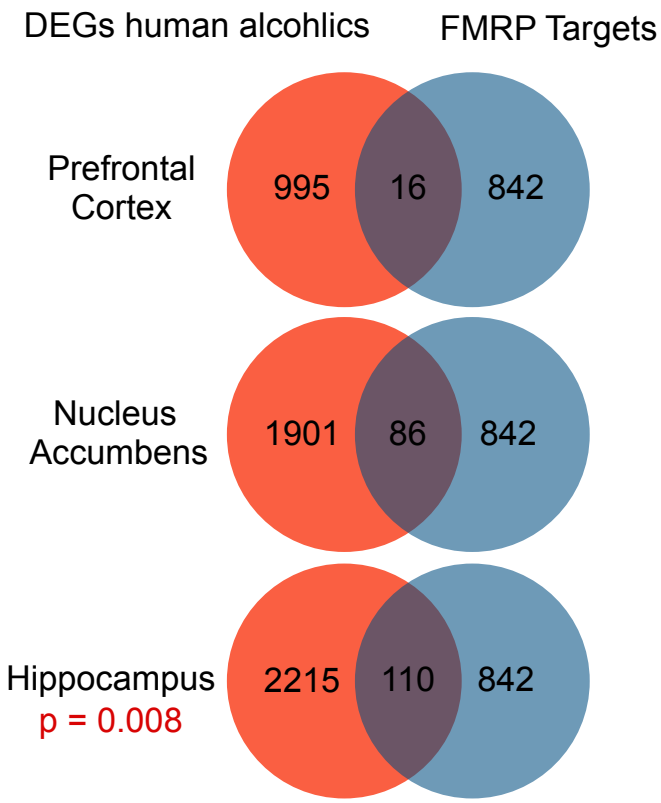

Figure 1.4. Differentially expressed genes in human AUD overlap with FMRP targets

Differentially expressed genes (DEGs) from humans affected by an AUD in the prefrontal cortex, nucleus accumbens, and hippocampus (p=0.01) was found to significantly overlap only in the hippocampus with known FMRP targets (p=0.05) at a p value of 0.008 as determined by Chi^2 test with Yates. This implicates the hippocampus as an important brain region for altered gene expression and possible FMRP regulation.

The Alcohol and Antidepressants Transcriptome

The effect of alcohol and antidepressants on protein translation and synaptic pathways has been discussed; however upstream mRNA transcription is vital to the changes seen in protein expression with drug exposure. Gene expression

studies provide evidence for alcohol- and antidepressant-induced changes in mRNA transcription. A powerful approach to characterizing the transcriptome is RNA sequencing. RNA sequencing is a method that can be used to estimate gene and alternative exon expression levels, allowing for identification of novel genes and exons[110, 111]. In this section we will discuss transcriptome studies associated with alcohol and antidepressant studies using methods such as RNA sequencing.

Acute Alcohol

Drug induced changes in gene expression are proposed as critical molecular adaptations leading to addiction with repeated drug exposure[60]. RNA-sequencing of postmortem human tissue shows consistent differences in transcriptome organization linked with lifetime consumption of alcohol[112]. Particularly, RNA-sequencing of human hippocampal tissue identified differentially expressed genes related to alcohol and addiction[60, 113]. Chronic drinking in humans and animals provide evidence for the association of alcohol-induced changes in genes expression[114]. Human studies often yield complementary results and tend to validate animals models of exposure[60]. Some acute alcohol treatment studies in animals have also identified alterations in the transcriptome. Acute ethanol exposure for 4 hours alters gene expression in mice, including genes involved in neuroplasticity[114]. Alcohol and other drugs of abuse acutely administered to mice identified modules of drug-induced genes that may play a critical role in early

stages of addiction[115]. Current evidence suggests that investigating acute effects on brain gene expression could provide insight into mechanisms of reward, as well as short- and long-term behaviors associated with addiction[116].

Rapid-Antidepressants

Deficits associated with psychiatric disease including MDD have been found in many brain regions including the hippocampus[117], and these deficits may be tied to consistent changes in gene expression observed across brain regions and disorders in individuals with psychiatric disorders[117]. Specifically in depression, transcriptome studies have found altered gene expression in human postmortem tissue between control, individuals with MDD, and MDD suicides[118]. In a particular study individuals with MDD were found to have altered expression of synapse related genes[119], which suggest that synaptic plasticity may play a role in depression. To study the acute use of rapid-antidepressants, animal models are often used due to the availability of human tissue. Although no previous transcriptome sequencing studies have been preformed with the rapid antidepressant Ro 25-6981, RAADs that use a similar mechanism such as ketamine have been explored in animals. Gene expression following a single dose of ketamine was altered in the striatum and hippocampus at acute time points[95]. Patterns of gene expression changes provided novel molecular classification of ketamine, and reflect its multi-target pharmacological nature[95]. Analysis of gene regulation of rat hippocampus treated acutely with several

antidepressants identified a large array of genes involved in various cellular processes suggesting that he therapeutic effect is very complex[120]. However, some RAADs have negative side effects and the potential for abuse making alternative drugs for MDD attractive[13].

Alternative splicing

Alternative splicing can generate isoforms that differ in function and localization[110]. Isoforms are important or development, differentiation and disease[110]. Alternative or differential splicing occurs when exons are recombined in multiple ways to generate different mRNAs, allowing encoding of multiple proteins from a single gene. These splice events allow for increased biodiversity of proteins, regulation of gene expression, and is widespread in mammalian genomes. In proteins alternative splicing can be important for altering binding properties, localization, enzymatic activity, posttranslational modifications, and stability[111]. Splicing can affect determination of mRNA localization and stability, and translation efficiency. Alternative splicing can cause changes in exon expression and composition, allowing the production of new protein isoforms without observed alterations of original protein expression[111]. In addition to studying differential gene expression we also sought to identify changes in exon expression to explore alterations in protein isoforms that were not observable with gene expression studies alone. Many studies have identified alternative

splicing in proteins of interest with alcohol or depression[118, 121-125], but few have identified splicing on a more global, whole genome wide scale.

Research Rational

AUD and MDD are both debilitating and widespread disorders with limited treatment options. The strong comorbidity between these two disorders suggests a connection and warrants further investigation to identify these connections and provide an explanation for the overwhelming rate of comorbidity. Understanding these disorders may eventually help alleviate the progression to comorbid disorders or aid in identification of effective treatment strategies for individuals with dual diagnosis. It is well known that AUD and MDD often occur together but determining the basis for this requires investigation of co-occurring molecular changes with alcohol and antidepressants. This study will provide possible molecular changes that cause depressed individuals to self medicate with alcohol, and provide the first evidence that acute alcohol can induce an antidepressant like behavioral response in mice. The molecular changes we have identified may provide targetable avenues for treatment of either or both disorders for future study.

CHAPTER 2: FMRP REGULATES AN ETHANOL-DEPENDENT SHIFT IN $GABA_BR$ FUNCTION AND EXPRESSION WITH RAPID ANTIDEPRESSANT PROPERTIES

Abstract

Alcohol promotes lasting neuroadaptive changes that may provide relief from depressive symptoms, often referred to as the self-medication hypothesis[41]. However, the molecular/synaptic pathways that are shared by alcohol and antidepressants are unknown. In the current study, acute exposure to ethanol produced lasting antidepressant and anxiolytic behaviors. To understand the functional basis of these behaviors, we examined a molecular pathway that is activated by rapid antidepressants. Ethanol, like rapid antidepressants, alters γ-aminobutyric acid type B receptor ($GABA_BR$) expression and signaling, to increase dendritic calcium. Furthermore, new $GABA_BRs$ are synthesized in response to ethanol treatment, requiring fragile-X mental retardation protein (FMRP). Ethanol-dependent changes in $GABA_BR$ expression, dendritic signaling, and antidepressant efficacy are absent in *Fmr1* knockout (KO) mice. These findings indicate that FMRP is an important regulator of protein synthesis following alcohol exposure, providing a molecular basis for the antidepressant efficacy of acute ethanol exposure.

Introduction

The presence of major depression increases the risk of alcohol use disorders (AUD) by ~2 fold (and vice versa)[14]. The self-medication hypothesis suggests AUDs may develop when the initial antidepressant actions of alcohol are shifted to depressant allostatic states with chronic abuse[101]. The molecular mechanism underlying the initial anti-depressant effects of alcohol is unknown.

A major advance in understanding and treating depression is the recognition that NMDA receptor (NMDAR) antagonists act as rapid and effective antidepressant drugs[126]. A single injection of an NMDAR antagonist or "rapid antidepressant" is effective within 2 hours and has sustained antidepressant efficacy for 2 weeks[25]. These long-lasting properties depend on the activity of mammalian target of rapamycin (mTOR)[13, 74], a serine/threonine kinase essential for mRNA translation[98]. Recently, we demonstrated that activation of mTOR-dependent protein synthesis by NMDAR antagonists requires a shift in $GABA_BR$ signaling from opening potassium channels to facilitating an increase in dendritic calcium[13, 78]. Interestingly, both acute ethanol and rapid antidepressants block NMDARs[25, 52]. In light of these data, we propose that ethanol has lasting antidepressant efficacy, shares the same downstream molecular signaling events as rapid antidepressants, and requires *de novo* protein synthesis (Supplementary Fig. 2.1).

Studies suggest that antidepressant efficacy requires two phases— an induction phase and a sustained phase[127, 128]. Notably, $GABA_BR$-mediated, mTORC1-dependent protein synthesis is required for the long-lasting sustained

phase of rapid antidepressants. Our previous work indicates that both new protein synthesis and an increase in protein stability are required for the $GABA_BR$ shift in function necessary to increase mTORC1 activity[78]. However, the mechanism that initiates such dynamic changes in protein expression by rapid antidepressants remains unclear.

FMRP is an RNA binding protein that has been characterized as a repressor of mRNA translation. Some forms of synaptic activity trigger FMRP to release its targets, allowing them to be translated[129, 130]. Moreover, degradation and new protein synthesis of FMRP creates a window for the translation of specific mRNAs, facilitating long-lasting changes in synaptic function[131, 132]. Complete loss of FMRP results in Fragile X syndrome (FXS), the single most common genetic cause of autism[87]. Moreover, reduced levels of FMRP, caused by a pre-mutation, lead to a higher incidence of tremors, ataxia, memory loss, and neuronal neuropathy in older men[133]. These findings argue that precise levels of FMRP protein and its target mRNAs are required for normal neuronal function.

Drugs of abuse promote profound changes in gene expression, mRNA translation rates, and synaptic protein composition[134, 135]. Some studies suggest that drugs and alcohol highjack the molecular mechanisms that underlie synaptic plasticity[45, 136]. In agreement with this premise, FMRP has been implicated in cocaine addiction[109]. However, little is known about the mRNA targets and the signaling mechanisms involved. Here we describe a critical role for FMRP in

mediating $GABA_BR$ synthesis and plasticity following acute ethanol exposure, a mechanism required for antidepressant efficacy.

Methods

Cell culture

Primary hippocampal neurons were prepared as previously described by Niere et al., 2012[137] . Briefly, hippocampi were extracted from postnatal day 1-3 Sprague-Dawley rat pups, wildtype C57BL/6 mouse pups, or *Fmr1*-knockout (*Fmr1* KO) mouse pups on a C57BL/6 background. The tissue was dissociated and plated in neurobasal A medium supplemented with B27, glutamine, and 1% fetal bovine serum. Cultures were plated at a density of ~100,000 cell/12mm on glass coverslips that had been coated overnight with 50 µg/ml poly-D-lysine and 25 µg/ml laminin in borate buffer. Cultures were fed after 1 day *in vitro* (DIV), and media was replaced approximately once a week with either fresh rat culture media (neurobasal A supplemented with B27, glutamine, and 3 µM AraC) or fresh mouse culture media (glial-conditioned media with 3 µM AraC) until cultures were used at DIV 14-21.

In vitro pharmacology

Primary hippocampal neurons were treated in ethanol vapor chambers according to a method adapted from Chandler et al., 1993[138]. Ethanol vapor chambers were prepared by placing a reservoir of 31.5 mM ethanol (105% of the desired ethanol

concentration, i.e., 30 mM) in a plastic container with 24-well culture plates containing neuronal cultures in which 30 mM ethanol was added to the culture media. Chambers were filled with 95% O_2/5% CO_2 and cultures were incubated for 2 hours at 37^{o}C. Cultures treated with vehicle (H_2O) were incubated in the same manner but in the absence of ethanol. For calcium imaging ethanol was added directly to HEPES-based artificial cerebral spinal fluid (ACSF in mM: 100 NaCl, 10 HEPES (pH 7.4), 3 KCl, 2 CaCl2, 1 MgCl2, 10 glucose) that was adjusted to match the osmolarity of cell culture media for live-imaging. For $GABA_BR$ activation neurons were treated with (R)-baclofen (50 μM, Tocris). For Fig. 2.5 and 2.6, cultured hippocampal neurons were pre-treated for with cycloheximide (50 μM, Tocris) for 10 minutes before ethanol treatment. For Supplementary Fig. 2.3 neurons were treated with Ro 25-6981 (10 μM, Tocris) or Veh (H2O) for 2 hours. All cultures were treated at 14-21 DIV. Following treatment, cultures were immediately fixed or live imaged.

In vivo pharmacology

Male C57BL/6 mice (Charles Rivers) or *Fmr1* knockout (*Fmr1* KO*)* mice on a C57BL/6 background (at least 7 weeks old) were given intraperitoneal (i.p.) injections of either 200 μl saline or 2.5 g kg^{-1} ethanol (in a volume of 200 μl saline)[23] . For Fig. 2.8 CGP-35348 (100 mg kg^{-1}) was i.p. injected with or without ethanol (in a volume of 200 μl saline). All animals were housed 4 mice per cage according to genotype. All treatments were administered to one mouse per home

cage. At the time of drug treatment, animals were coded by number. During the behavioral tasks, animal performance was video recorded, and then later blindly scored. In certain tasks (e.g. open field), the animals were scored by a computer program and blinding was not necessary during that process. For Western blots the hippocampi were isolated 30 minutes post-injection and flash frozen. All experiments were carried out in accordance with the National Institutes of Health's Guide for the Care and Use of Laboratory Animals and approved by the UT-Austin Institutional Animal Care and Use Committee (IACUC).

Immunofluorescence

Primary neuronal cultures on glass coverslips were fixed with 4% paraformaldehyde (PFA) at room temperature (RT) for 20 minutes, washed 3 times with phosphate buffered saline (PBS), and permeabilized in 0.25% Triton X-100 in PBS for 5 minutes. For FMRP staining, neurons were fixed and permeabilized in 100% methanol at -20^{o}C for 10 minutes. Neurons were washed 3 times in PBS and then blocked (10% normal goat serum in PBS) for 30 minutes at RT. Primary antibodies were incubated in blocking buffer at 4^{o}C overnight. Neurons were washed 3 times for 10 minutes with PBS, and then incubated in secondary antibody in blocking buffer for 1 hour at RT, and washed 3 times for 10 minutes with PBS before mounting in Fluoromount with DAPI (SouthernBiotech, 0100-20) as outlined in Sosanya et al., 2013[139]. Surface staining was performed similarly to Workman et al., 2013[13]. Neurons were first

fixed in 4% PFA for 10 minutes on ice, washed 3 times in PBS, blocked with 3% normal goat serum, and then incubated in primary surface antibody in 3% blocking buffer overnight at 4°C. Following primary surface antibody incubation, neurons were washed 6 times for 10 minutes each in PBS, then permeabilized with 0.25% Triton X-100 in PBS for 5 minutes, followed by 3 washes for 10 minutes each in PBS, and again incubated in primary total antibody in 3% blocking buffer overnight at 4°C. Neurons were washed 3 times for 10 minutes each with PBS, and then incubated in secondary antibody in 3% blocking buffer for 1 hour at RT, and finally washed 4 times for 10 minutes with PBS before mounting in Fluoromount with DAPI to slides. The primary antibodies used were: Total $GABA_BR1$ (1/50 dilution; Santa Cruz, sc-14006), Surface $GABA_BR1$ (1/200 dilution; Abcam, ab55051), $GABA_BR2$ (1/100; Neuromab 75-124), FMRP (1/500 dilution; Abcam ab17722), MAP2 (1/2000 dilution; Abcam ab5392), GFP (1/1,000 dilution; Aves, GFP-1020). Secondary antibodies included: Alexa488, 555, and 647 developed in goat (1/500 dilution; Life Technologies, A-11039, A-11017, A-31621, A-21430, A-21449, A-21240, A-21237).

Adeno-associated viral vectors

The FMRP and tdTomato coding sequences were cloned into separate adeno-associated viral (AAV) vectors containing a mouse synapsin promoter, a woodchuck post-transcriptional regulatory element (WPRE), and SV40 poly-adenylation sequence between flanking AAV2 inverted terminal repeats. rAAVs were assembled using a modified helper-free system (Stratagene) as serotype

2/1 (*rep*/*cap* genes) viruses, and harvested and purified over sequential cesium chloride gradients as previously described[140]. Viral titers were greater than $1x10^9$ infectious particles per microliter. For FMRP and tdTomato co-infections, rAAV:mSYN-FMRP and rAAV:mSYN-tdTomato were mixed at a ratio of 4:1. One microliter of the resulting rAAV mix was used per coverslip of primary cultured neurons. Imaging was performed ~1 week after infection.

Live calcium imaging

Dissociated hippocampal cultures were prepared from wildtype (WT) and *Fmr1* KO mice as described[137]. Neurons at 14-21 DIV were used for live calcium imaging. Neurons were treated as outlined in *in vitro pharmacology* above. Before imaging, cells were incubated in ACSF with Oregon Green 488 BAPTA-1 AM (OGB, 200 μM; 30 min; 37°C; ThermoFisher) as described[13]. After OGB incubation, cells were transferred to fresh ACSF (37°C) for imaging (1 frame/20 s). Baseline calcium signal was imaged (1 min), after which (R)-baclofen (50 μM, Tocris) or vehicle (H_2O) was added. For ethanol-treated cells, the neurons were incubated with OGB and imaged in ACSF containing ethanol (30 mM). Neurons were imaged for 800 s at RT. Quantification of the calcium signal was performed using Metamorph (Molecular Devices) as described[13]. Briefly, dendritic regions of interest (ROI) that were at least 5 μm from the soma were analyzed. The mean intensity values for each ROI at each time were averaged as baseline (F_0). The ROI intensity values obtained at each time point after the addition of baclofen or vehicle were averaged (F). The equation, $\Delta F/F = ((F - F_0)/F_0)$, was used to

measure the change in signal and data were plotted as a percentage of the baseline.

BONCAT-PLA

BONCAT-PLA was performed using Click-it Metabolic Labeling AHA, Biotin-Alkyne, and Click-iT Reaction buffer kit (Life Technologies). Proximity ligation assay (PLA) was performed using Duolink kit (Duolink, Sigma)[141]. Briefly, primary hippocampal neuronal cultures were incubated in a methionine-free artificial cerebral spinal fluid (ACSF) media for 30 minutes. AHA was then added to the media just before neurons were treated with ethanol for 2 hours as previously described. Neurons were fixed in 4% PFA for 15 minutes, washed 2 times for 5 minutes with 3% Bovine Serum Albumin (BSA) in PBS, followed by permeabilization with 0.25% Triton X-100 in PBS for 15 minutes, and washed as before. Neurons were incubated for 30 minutes at RT in Cell Buffer Additive/Click-it Cocktail according to manufacturer directions. Neurons were washed as before and then blocked and incubated with primary antibody as previously described. Next, neurons were incubated in the appropriate PLA probes diluted in blocking buffer and secondary antibody at 37^{o}C for 1 hour. Neurons were washed in RT Buffer A 2 times for 5 minutes, and incubated in ligation solution at 37^{o}C for 30 minutes, and washed again in Buffer A. Neurons were incubated in amplification solution at 37^{o}C for 2-3 hours, followed by washing in RT Buffer B 2 times for 10 minutes and 1% buffer B for 1 minute. Lastly, neurons were mounted to slides in Duolink mounting media for imaging.

Primary and secondary antibodies included: $GABA_BR1$ (1/50 dilution; Santa Cruz, sc-14006), $GABA_BR2$ (1/100; Neuromab 75-124), MAP2 (1/2000 dilution; Abcam, ab5392), biotin/α-rabbit (1/500; Sigma, SAB3700857), Alexa488 (1/500; Life Technologies, A-11039). PLA probes used: Rabbit Minus (1/5; Duolink, 82005), Mouse Plus (1/5; Duolink, 82001).

Microscopy and analysis

Images were acquired with a Leica SP5 confocal microscope under a 63X oil immersion lens for fixed tissue or a 63X water immersion lens for live imaging. Max projected images were used for immunostaining analysis from 10 μm Z-stacks of 1024 x 1024 pixels obtained using a 400-Hz scan rate[139]. For each experiment, all images were collected using the same settings. Fixed images were analyzed using NIH imaging software *ImageJ,* and live imaging quantification was performed with Metamorph (Molecular Devices, Sunnyvale, CA). Background signal was determined by shifting the ROI adjacent to the dendrite being traced, but void of all processes. Dendritic signal was background subtracted and averaged every 10 μm using a customized R script.

Western blot analysis

Protein was isolated from hippocampal synaptoneurosomes (SN) prepared from male mice age 7-8 weeks treated with ethanol or vehicle as previously described. SNs were prepared by homogenizing hippocampal tissue in homogenization buffer (20 mM HEPES pH 7.4, 5 μM EDTA pH 8.0, and protease inhibitor

cocktail). Homogenate was filtered through a 100-µm nylon filter followed by a 5-µm filter, and centrifuged at 14000 x g for 20 minutes at 4°C[142]. The pellet was resuspended in RIPA buffer (150 mM NaCl; 10 mM Tris pH 7.4, 0.1% SDS, 1% Triton X-100, 1% deoxycholate, 5 mM EDTA, and protease inhibitor cocktail) and centrifuged for 10 minutes. The supernatant was used for Western blot analysis. Protein was separated on a 4-20% gradient SDS-polyacrylamide gel. The gel was then transferred to a nitrocellulose membrane, blocked in 5% non-fat dry milk in tris-buffered saline and 0.1% tween20 (TBST) for 1 hour, and incubated with primary antibody in blocking buffer overnight at 4°C. The blot was washed in TBST 3 times for 10 minutes each, incubated in secondary antibody for 1 hour, and washed as before. Blots were imaged using a LICOR Odyssey imaging system, and ImageJ was used for densitometry analysis. Representative images are pseudocolored with black (lowest intensity at 0 pixels) to red (highest intensity at 255 pixels) using LICOR Image Studio software. Primary antibodies used consisted of: $GABA_BR1$ (1/400 dilution; Santa Cruz, sc-14006), $GABA_BR2$ (1/800; Neuromab 75-124), alpha-Tubulin (1/2000 dilution; Sigma, T6074). Secondary antibodies included: anti-mouse-IR-Dye 800 (1/5000 dilution excluding tubulin at 1/10,000 dilution; LICOR, 96-32210) and anti-rabbit Alexa680 (1/5000 dilution; Invitrogen, A-21084).

RNA Immunoprecipitations

Cortices from 6-week old C57BL/6 and *Fmr1* KO male mice were harvested and flash frozen on dry ice. RIP was performed by modified method of Jain et al.,

2011 and Keene et al., 2006[143, 144]. Tissue was homogenized and lysed with a cordless pestle motor and disposable pellet mixers (VWR) in polysome lysis buffer (10 mM HEPES pH 7.0, 100 mM KCl, 25 mM EDTA, 5 mM $MgCl_2$, 1mM DTT, 0.5% NP-40) in a 1:1 tissue-buffer ratio. RNaseOUT (Thermo) and protease/phosphatase inhibitors (Halt™ Protease and Phosphatase Cocktail, Pierce Biotechnology) were freshly added to samples. Samples were rotated for 10 minutes at 4°C to induce swelling and then flash frozen on dry ice. Samples were thawed by holding between fingers at RT to lyse and nuclei were pelleted at 3000 x g for 10 minutes. Lysates obtained above were pre-cleared by adding 50 µl of washed magnetic bead slurry (Protein A Dynabeads, Thermo) and rotating for 30 minutes at 4°C. To bind the antibody to the beads, 50 µl of magnetic beads slurry was washed and then resuspended in 8 volumes of NT-2 buffer (50 mM Tris-HCl pH 7.4, 150 mM NaCl, 1 mM $MgCl_2$, 1mM DTT, 0.05% NP-40 with RNaseOUT/protease & phosphatase inhibitors added fresh) + 5% BSA. 10 µg of either FMRP (Abcam, ab17722) or IgG (Santa Cruz Biotechnologies, sc-2027) antibodies were added to the beads and rotated for 10 minutes at RT. Antibody-bound beads were washed 4 times with ice-cold NT-2 buffer. For the immunoprecipitation, 4.5 mg of protein from pre-cleared lysates was added to an RNase-free microcentrifuge tube containing the antibody-bound beads. Input collected at this step for downstream analysis was either 1% of the final pre-cleared lysate volume in the immunoprecipitation reaction (for immunoblotting) or 10% of the final pre-cleared lysate volume (to normalize in qPCR). The antibody-

bead-lysate mixture was then diluted at a ratio of 1:5 with NET-2 buffer (20 mM EDTA pH 8.0, and 1 mM DTT in NT-2 buffer; RNaseOUT and protease/phosphatase inhibitors added fresh) and rotated for 1 hour at room temperature. Beads were quickly washed 6 times in ice-cold NT-2 buffer and immediately resuspended in 350 µl TRI Reagent® Solution (Ambion) for 10 minutes at RT. Beads were pelleted and the supernatant was removed and resuspended in 350 µl of absolute ethanol. RNA was extracted by applying ethanol-resuspended samples to spin column from the Direct-zol RNA MiniPrep Kit (Zymogen) according to manufacturer's instructions. Eluted RNA (25 µl) was DNase treated using the TURBO DNA-free kit (Thermo).

cDNA Synthesis and Quantitative Real-Time PCR (qRT-PCR)

DNase-treated RNA samples were reverse-transcribed to cDNA using the iScript cDNA Synthesis Kit (Bio-Rad) in a 20 µl volume according to manufacturer's instructions. qRT-PCR was performed in 20 µl reaction volume using the iQ™ SYBR® Green Supermix (Bio-Rad) and primers for $GABA_BR1$, $GABA_BR2$, CaMKIIα, and Cacna2δ2 (GeneCopoeia). qRT-PCR was run with the following protocol: 95°C for 10:00, 40 cycles of 95°C for 0:15 followed by 60°C for 1:00, 95°C for 1:00, and 55°C for 1:00. Relative fold-enrichment was determined by the equation $\Delta\Delta Ct = 2^{-(Ct\ FMRP\ RIP - Ct\ IgG\ RIP) - (Ct\ FMRP\ input - Ct\ IgG\ input)}$ [145].

Forced Swim Test

Male mice were tested in the forced swim test 24 hours post-injection as

described previously[13, 78]. Mice were individually placed into a cylinder containing 3 L of water (25°C) for 6 minutes. Each session was video recorded and the last 4 minutes of the sessions were later scored blindly for immobility. Animals were scored for escape-directed behaviors. The water was replaced between animals. Experiments were repeated by 3 independent experimenters. Data was normalized by experimenter. Power analysis was performed in R Programming[146] to predict sample size for all behavioral tests. This sample size was used as a guideline for the wild type animals, however since transgenic animals were used, the exact sample size for each group may not have been possible. Transgenic animal sample size was as close as possible to that which was calculated, due to limitations of litter size.

Open Field

Twenty-four hours after animals were injected i.p. with either saline or ethanol, they were studied in the open field test similar to Treit et al, 1988[147]. Mice were individually placed in a 40 cm x 40 cm x 35 cm arena with opaque walls. Each test session lasted 30 minutes under 85 lux illumination. Sessions were video recorded and analyzed via ANY-Maze (Stoelting, Wood Dale, IL). Mice were considered to be in the center of the maze if they entered a 18.5 cm x 18.5 cm area in the center of the apparatus. Mice were returned to their home cage at the end of the test session, and the arena was wiped down with 70% ethanol before the start of each run.

Splash Test

Two and a half hours after open field testing, animals underwent the splash test[148, 149]. Cage mates were moved from their home cage to a holding cage, and each animal was individually tested in its home cage. Two hundred microliters of 10% sucrose was applied to the dorsal fur of the mouse. Mice were monitored and video recorded for 5 minutes and then moved to a different holding cage. Videos were later scored blindly for latency to initiate grooming and for total time spent grooming. Grooming behavior included licking, grooming with forepaws, and scratching.

Statistical analysis

Power analysis was performed in R Programming[146] to predict sample size. Prism software (GraphPad) was used for all statistical analyses. Statistical comparisons were made using one-way ANOVA, two-way ANOVA, Student's t-test, or Chi^2 test with Yates. Outliers were determined using Grubbs' test (alpha=0.05). All data are expressed as mean ± Standard Error of the Mean (SEM).

Results

Antidepressant and anxiolytic effects of ethanol on behavior

To determine if acute alcohol has antidepressant properties, as predicted by the self-medication hypothesis, we first assessed the efficacy of alcohol on

antidepressant- and anxiolytic-like effects on behavior. The forced swim test (FST) is a rodent behavioral test predictive of antidepressant activity in humans[150]. Rodents treated with a single injection of NMDAR antagonists or rapid antidepressants swim longer and thus have reduced immobility relative to controls. Notably, these positive effects on behavior last long after the drug has been metabolized[13, 70, 74, 78]. Therefore, we considered the possibility that ethanol, which blocks NMDARs[52], could also act like an antidepressant at 24 hours, well beyond the intoxication period[151]. To test this, C57BL/6 mice were injected with ethanol (2.5 g kg^{-1}, intraperitoneal (i.p.)), a concentration that is achieved during self-administration in mice[152]. Twenty-four hours after injection, the immobility of ethanol-treated mice was reduced by ~15% relative to controls (Fig. 2.1a), similar to our previous observation in mice that had been exposed to the rapid antidepressant Ro 25-6981[13, 78]. These results demonstrate that acute ethanol elicits a lasting antidepressant effect on behavior similar to that seen with rapid antidepressants[78].

As another measure of antidepressant effect of ethanol on behavior, we assessed the grooming behavior of mice using the splash test after ethanol or saline administration. The splash test measures latency to groom and dedicated grooming time as indicators of self-care and motivational behavior[148, 149]. Lack of self-care is often observed in humans with depressive disorder[12]. We have previously shown that mice receiving a single i.p. injection of the rapid antidepressant Ro 25-6981 spend more time grooming compared to control

mice[78]. We hypothesized that ethanol would produce similar effects on grooming behavior. Indeed, ethanol-treated mice spent more time grooming and displayed shorter latency to initiate grooming relative to controls (Fig. 2.1b and c).

Ethanol is a well-known anxiolytic substance[67]. However, the anxiolytic effect of a single dose of ethanol 24 hours after administration has not been determined. We subjected ethanol- and saline-injected mice to the open-field test to assess the influence of ethanol on anxiety-like behaviors after 24 hours. Mice that spend more time in the center of the open field are scored as having reduced anxiety-like behavior relative to mice that remain close to the perimeter[147]. Indeed, mice that received a single dose of ethanol (2.5 g kg^{-1}, i.p.) had reduced anxiety-like behavior, spending ~40% more time in the center relative to controls (Fig. 2.1d). There was no significant difference in total distance traveled or average speed between the groups (Fig. 2.1e-f). These data suggest that the anxiolytic effects of ethanol last up to 24 hours post-injection.

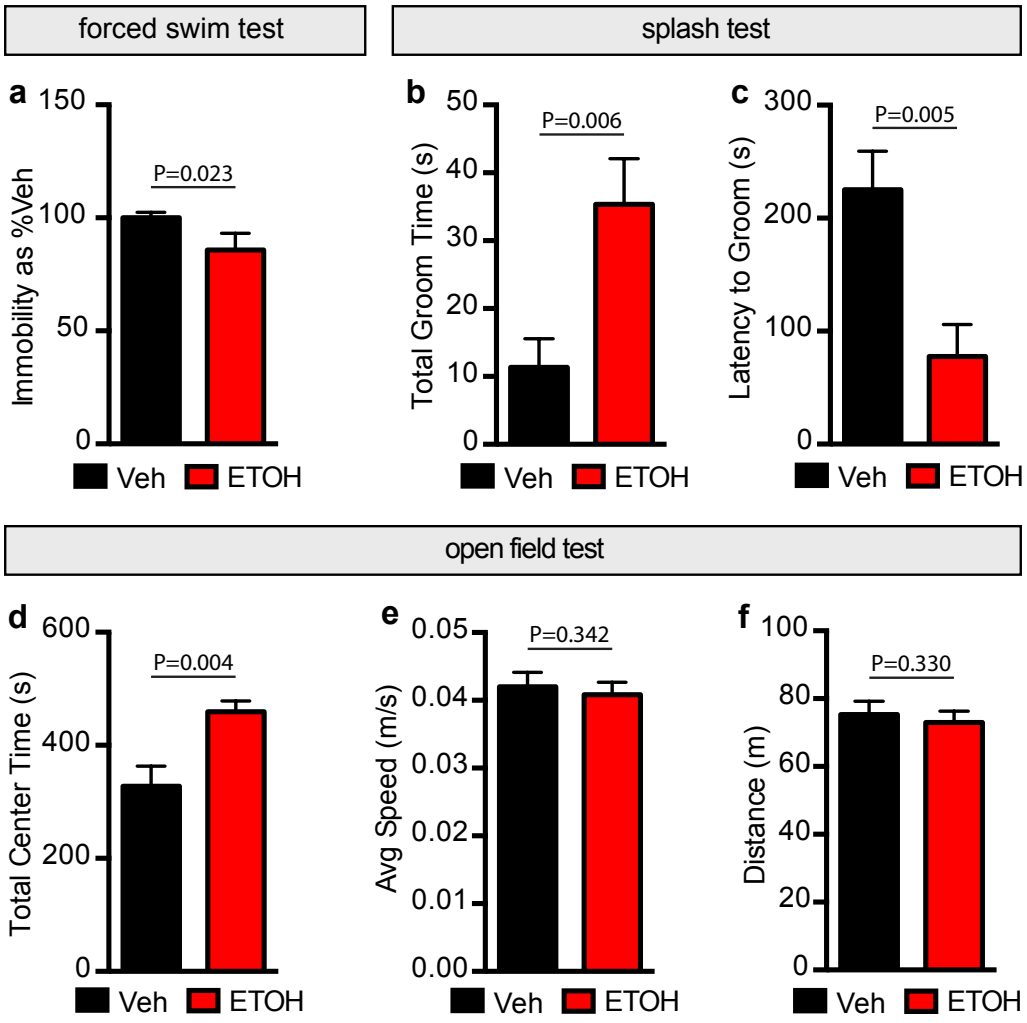

Figure 2.1. Ethanol elicits a lasting antidepressant-like effect on behavior

(a) C57BL/6 male mice were subjected to the forced swim test 24 hours after i.p. injection with vehicle (Veh; saline) or ethanol (ETOH; 2.5g kg^{-1}). Ethanol treatment reduced immobility, indicating antidepressant efficacy. Veh=100 ± 2.5, n=10 mice; ETOH=86 ± 7.4, n=6. (b-c) In the splash test, male C57BL/6 mice groomed longer and took less time to initiate grooming 24 hours post-ethanol (2.5 g kg^{-1}, i.p.) compared to 24 hours post-vehicle (saline, i.p.) treatment. Total groom time: Veh=11.34 ± 4.23 s, n=6; ETOH=35.37 ± 6.72 s, n=5. Latency to groom: Veh=225.2 ± 34.13 s, n=6; ETOH=77.55 ± 28.44 s, n=5. (d-f) Total center time, speed, and distance were measured in the open field test 24 hours post-injection. Ethanol-treated (2.5 g kg^{-1}, i.p.) mice spent more time in the center,

while speed and distance were unaffected compared to vehicle-treated (saline, i.p.) mice, indicating an ethanol-induced anxiolytic effect without altering mobility. Total center time: Veh=327.5 ± 35.62 s, n=6; ETOH=459.2 ± 19.13 s, n=6. Average speed: Veh=0.042 ± 0.002 m/s, n=6; ETOH=0.041 ± 0.002 m/s, n=6. Total distance: Veh=75.35 ± 3.92 m, n=6; ETOH=73.00 ± 3.35 m, n=6. Significance determined by one-tailed t-test. Values represent mean ± SEM.

Acute ethanol increases $GABA_BR2$ and surface $GABA_BRs$

Both ethanol and rapid antidepressants block NMDARs in the hippocampus[25, 52]. One of the first events triggered by NMDAR antagonism is increased dendritic $GABA_BR2$ protein expression[78]. $GABA_BRs$ are obligate heteromultimers, consisting of $GABA_BR1$ and R2. $GABA_BR2$ is required for expression of receptors at the surface by masking an endoplasmic reticulum retention sequence on $GABA_BR1$[153]. Similarly, treatment with a rapid antidepressant leads to (1) increased dendritic expression of $GABA_BR2$ but not $GABA_BR1$[78], and (2) a corresponding increase in surface expression of $GABA_BR1$[13, 78].

To determine if acute ethanol exposure *in vivo* rapidly increases the levels of $GABA_BR1$ and/or $GABA_BR2$, hippocampal synaptoneurosomes were isolated from mice that had been injected with a single dose of ethanol (2.5 g kg^{-1}, i.p.) or saline for Western blot analysis. The hippocampi were collected within the initiation phase (30 minutes post-injection), a phase where molecular changes facilitate increased downstream mTORC1 activity[128]. Consistent with rapid antidepressants, acute ethanol injection increased the protein expression of

$GABA_BR2$ by ~37% in the hippocampus with no significant change in $GABA_BR1$ (Fig. 2.2a-c; uncropped blots, Supplementary Fig. 2.7a).

To further identify the subcellular localization of ethanol-induced increase in $GABA_BR2$, we examined $GABA_BR$ expression in cultured hippocampal neurons. $GABA_BR1$ and R2 were immunostained and quantified in the dendrites. A concentration of 30 mM ethanol was chosen, as it has been shown to reduce NMDAR activity in hippocampal neurons and reflects that achieved *in vivo* following i.p. injection[52, 154]. Acute ethanol exposure (30 mM, 2 hours) increased the dendritic levels of $GABA_BR2$ by ~47%, but did not affect $GABA_BR1$ levels (Fig. 2.2d-g). We did not observe a difference in the diameter of the primary dendrites between vehicle- and ethanol-treated neurons, demonstrating that ethanol does not modify dendritic caliber (Supplementary Fig. 2.2). These *in vivo* and *in vitro* findings establish a role for ethanol in increasing $GABA_BR2$ protein expression.

Since $GABA_BR2$ is required for the surface expression of the heteromultimeric receptor, we predicted that the ethanol-induced elevation in $GABA_BR2$ levels would increase expression of receptors at the surface. We measured the surface expression of dendritic $GABA_BRs$ using an antibody directed against the extracellular domain of $GABA_BR1$ in unpermeabilized hippocampal neurons. The surface signal was normalized by the total dendritic $GABA_BR1$ levels after permeabilization[13]. As predicted, surface expression of $GABA_BRs$ in ethanol-treated neurons was significantly higher (~66% increase)

relative to controls (Fig. 2.2h-i). This ethanol effect was consistent with what we previously observed following rapid antidepressant treatment of cultured hippocampal neurons[13]. Collectively, these results suggest that ethanol promotes the surface expression of $GABA_BRs$, and this is likely achieved by increasing $GABA_BR2$ protein levels[13, 78, 153].

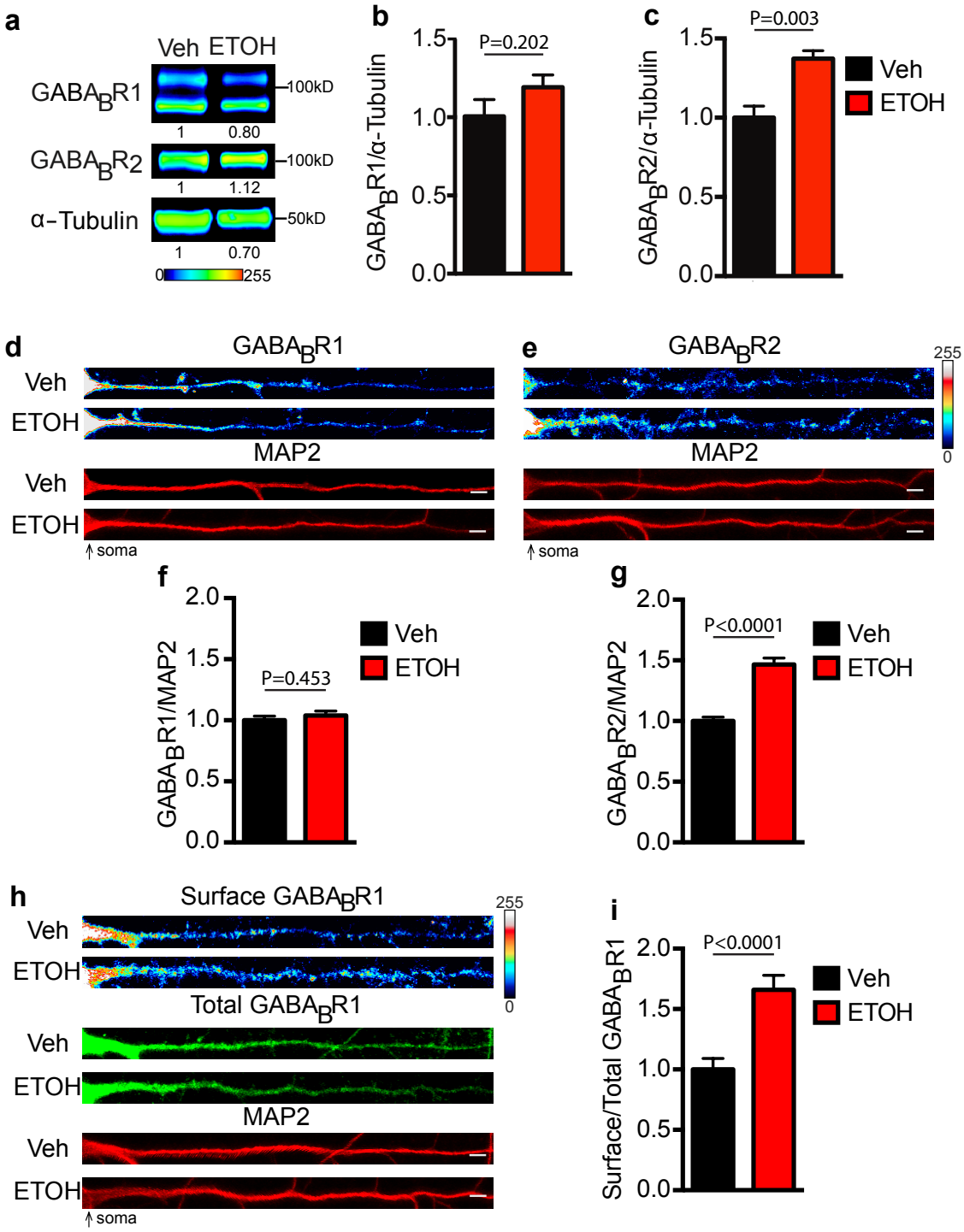
a
Veh ETOH
GABABR1
100kD
1 0.80
GABABR2
100kD
1 1.12
α-Tubulin
50kD
1 0.70
0 255
b
P=0.202
GABABR1/α-Tubulin
1.5
1.0
0.5
0.0
c
P=0.003
GABABR2/α-Tubulin
Veh
ETOH
d
GABABR1
Veh
ETOH
MAP2
Veh
ETOH
soma
e
GABABR2
255
0
MAP2
soma
f
P=0.453
GABABR1/MAP2
2.0
1.5
1.0
0.5
0.0
Veh
ETOH
g
P<0.0001
GABABR2/MAP2
h
Surface GABABR1
255
0
Veh
ETOH
Total GABABR1
MAP2
soma
i
P<0.0001
Surface/Total GABABR1

Figure 2.2. Acute ethanol increases dendritic $GABA_BRs$ in hippocampus

(a-c) Western blot analyses of $GABA_BR1$ and $GABA_BR2$ in isolated hippocampal synaptoneurosomes from ethanol-treated (ETOH; 2.5g kg^{-1} i.p.), and vehicle-treated (Veh; saline i.p.) C57BL/6 male mice 30 minutes post-injection. (a) Pseudocolored representative Western blots to show intensity with normalized optical density for each band indicated below blot (Lookup table, below Western blot). No significant change was observed in (b) $GABA_BR1$, but a significant increase was found in (c) $GABA_BR2$ with ethanol treatment. Western blots were normalized to the loading control, α-Tubulin. $GABA_BR1$: Veh=1.00 ± 0.11; ETOH=1.19 ± 0.08. Experiment was repeated 5 times. $GABA_BR2$: Veh=1.00 ± 0.07; ETOH=1.37 ± 0.05. (d-e) Representative immunostaining images of $GABA_BR1$ and $GABA_BR2$ in cultured rat hippocampal dendrites normalized to microtubule associated protein 2 (MAP2) as volume control. There was no change in (f) $GABA_BR1$ and a significant increase in (g) $GABA_BR2$ in ethanol-treated (30 mM, 2 hours) compared to vehicle-treated (H2O, 2 hours) dendrites: Total $GABA_BR1$: Veh=1.00 ± 0.03, n=46 dendrites; ETOH=1.04 ± 0.04, n=51 dendrites. Total $GABA_BR2$: Veh= 1.00 ± 0.03, n=46 dendrites; ETOH=1.47 ± 0.05, n=51 dendrites. (h-i) Immunofluorescence shows a significant increase in surface $GABA_BR1$ expression in dendrites of cultured rat hippocampal neurons treated with ethanol (30 mM, 2 hours); (i) Surface expression of $GABA_BR1$ in vehicle-treated (H_2O, 2 hours) and ethanol-treated (30 mM, 2 hours) dendrites. Veh=1.00 ± 0.09, n=43 dendrites; ETOH=1.66 ± 0.12, n=47 dendrites. Significance determined by Student's t-test. Values represent mean ± SEM. Scale bars=5 μm. Uncropped version of western blots, with size markers are available in Supplementary Figure 7a.

FMRP regulates the protein expression of $GABA_BR1$ and $GABA_BR2$

Next we sought to identify the mechanism by which NMDAR antagonism increases $GABA_BR2$ expression. $GABA_BR2$ mRNA is present in the dendrites of hippocampal neurons[92], suggesting that this mRNA may be locally regulated at the translational level. Thus, we examined RNA-binding factors that may regulate $GABA_BR2$ mRNA expression in dendrites. Notably, both $GABA_BR1$ and

$GABA_BR2$ mRNAs are reported targets of FMRP, an RNA binding protein that stalls translational elongation of its targets[106, 155].

To test the hypothesis that FMRP regulates $GABA_BR$ mRNA translation, we first verified that (1) $GABA_BR$ mRNAs bind to FMRP, and that (2) the absence of FMRP in knockout mice results in aberrant expression of $GABA_BRs$. Using a specific antibody against FMRP, bound mRNAs were isolated using RNA immunoprecipitation (RIP). $GABA_BR1$ and $GABA_BR2$ binding were assessed by reverse transcription (RT) and quantitative PCR. Indeed, $GABA_BR1$ and $GABA_BR2$ mRNAs were detected in the immunoprecipitate, along with CaMKIIα, a well-known FMRP mRNA target (Fig. 2.3a-b; uncropped representative qPCR gels, Supplementary Fig. 2.7d). The calcium channel accessory subunit Cacnα2δ2 mRNA is not a reported target for FMRP[106] and was used as a negative control. Cacnα2δ2 mRNA was not detected in the FMRP RIP (Fig. 2.3b). In parallel, we used lysates isolated from brains of mice with a genetic deletion of the *Fmr1* gene. We did not observe amplification of any of the mRNAs in *Fmr1* KO brains, providing additional evidence for specific binding of FMRP to $GABA_BR1$ and $GABA_BR2$ mRNAs (Fig. 2.3a-c; uncropped blots, Supplementary Fig. 2.7b).

Next, we determined if FMRP regulates $GABA_BR1$ and $GABA_BR2$ protein levels. Genetic deletion of *Fmr1* leads to the constitutive translation of FMRP target mRNAs and the loss of activity-dependent translation[87]. Protein levels of $GABA_BR1$ and $GABA_BR2$ were compared in hippocampal synaptoneurosomes

from *Fmr1* KO and wildtype (WT) mice (Fig. 2.3c-g). $GABA_BR2$ basal protein levels were elevated by ~53% in *Fmr1* KO hippocampi (Fig. 2.3g). $GABA_BR1$ protein levels also increased, albeit to a lesser extent than $GABA_BR2$ (Fig. 2.3f). Collectively, these data suggest that FMRP regulates the expression of $GABA_BR1$ and $GABA_BR2$.

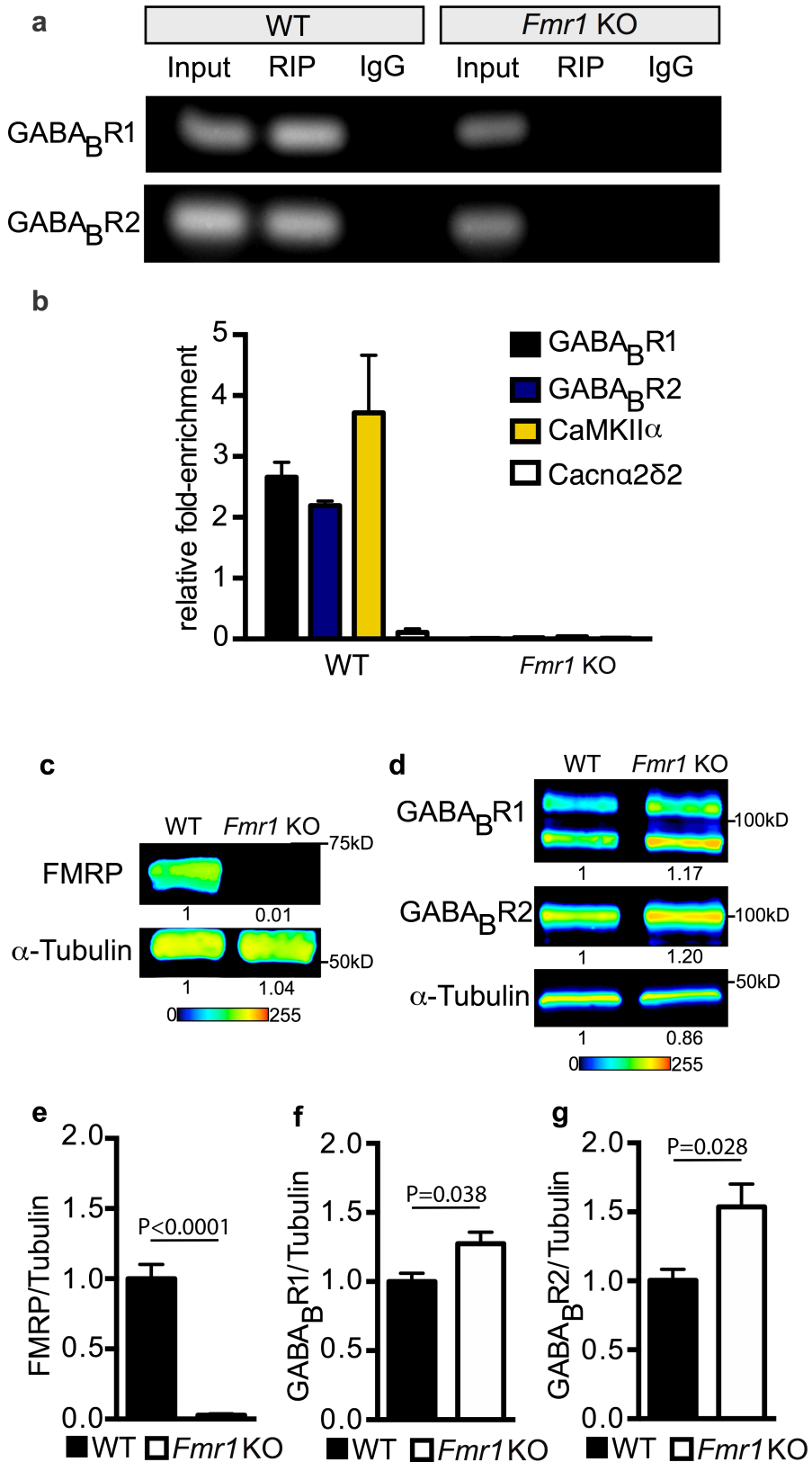
a
WT
Fmr1 KO
Input
RIP
IgG
Input
RIP
IgG
GABABR1
GABABR2
b
relative fold-enrichment
5
4
3
2
1
0
GABABR1
GABABR2
CaMKIIα
Cacnα2δ2
WT
Fmr1 KO
c
WT
Fmr1 KO
FMRP
75kD
1
0.01
α-Tubulin
50kD
1
1.04
0
255
d
WT
Fmr1 KO
GABABR1
100kD
1
1.17
GABABR2
100kD
1
1.20
α-Tubulin
50kD
1
0.86
0
255
e
FMRP/Tubulin
2.0
1.5
1.0
0.5
0.0
P<0.0001
WT
Fmr1KO
f
GABABR1/Tubulin
2.0
1.5
1.0
0.5
0.0
P=0.038
WT
Fmr1KO
g
GABABR2/Tubulin
2.0
1.5
1.0
0.5
0.0
P=0.028
WT
Fmr1KO

Figure 2.3. $GABA_BR1$ and $GABA_BR2$ mRNAs are FMRP targets

(a-b) RNA immunoprecipitation (RIP) for FMRP was performed using brains from wildtype (WT) and *Fmr1* KO male mice. (a) Gels showing RT-qPCR amplified product of input sample, FMRP RIP, and IgG control for $GABA_BR1$ and $GABA_BR2$. (b) Relative fold-enrichment as determined by real-time qPCR relative to input control ($\Delta\Delta Ct = 2^{-(Ct\ FMRP\ RIP - Ct\ IgG\ RIP) - (Ct\ FMRP\ input - Ct\ IgG\ input)}$). FMRP binds $GABA_BR1$, $GABA_BR2$, and the positive control CaMKIIα mRNA as detected in the RIP sample by real-time qPCR. Cacnα2δ2 served as a negative control and was not detected above background. WT: $GABA_BR1$=2.66 ± 0.248, n=2; $GABA_BR2$=2.19 ± 0.08, n=2; CaMKII=3.72 ± 0.94, n=2; Cacnα2δ2=0.11 ± 0.6, n=2. *Fmr1* KO: $GABA_BR1$=0.01 ± 0.0002, n=2; $GABA_BR2$=0.02 ± 0.00006, n=2; CaMKII ± 0.04±0.01, n=2; Cacnα2δ2=0.012 ± 0.005, n=2. (c-g) Western blot analysis of hippocampal synaptoneurosomes isolated from C57BL/6 WT and *Fmr1* KO mice on a C57BL/6 background indicates the absence of (e) FMRP and increased protein expression of (f) $GABA_BR1$ and (g) $GABA_BR2$. Representative Western blots are pseudocolored to indicate intensity of bands, and the normalized optical density for each band is indicated below blot (Lookup table, below Western blot). Western blots were normalized to the loading control, α-Tubulin. WT: FMRP=1.00 ± 0.10; $GABA_BR1$=1.00 ± 0.06; $GABA_BR2$=1.00 ± 0.08. *Fmr1* KO: FMRP=0.03 ± 0.01; $GABA_BR1$=1.27 ± 0.08; $GABA_BR2$=1.54 ± 0.17. Experiment was repeated 3 times. Significance determined by Student's t-test. Values represent mean ± SEM. Uncropped versions of qPCR gel, with size markers, are available in Supplementary Figure 7d. Uncropped version of western blots, with size markers are available in Supplementary Figure 7b.

Ethanol and rapid antidepressants reduce dendritic FMRP

As an initial test to determine if FMRP-regulated translation is linked to alcohol exposure, we compared FMRP target mRNAs[106] with mRNAs that are differentially expressed in the hippocampi of alcohol-dependent humans[60]. Remarkably, 225 or ~25% of verified FMRP target mRNAs overlap with mRNAs that are altered in alcohol-dependent individuals, suggesting a role for FMRP in aberrant protein levels observed in humans with AUD (Fig. 2.4a)[60, 106]. We then determined if exposure to acute ethanol (30 mM, 2 hours) or Ro 25-6981 (10 μM,

2 hours) alters FMRP expression in the dendrites of hippocampal neurons. Using immunofluorescence, we found that ethanol and Ro 25-6981 reduced FMRP levels by ~38% and 45%, respectively (ethanol: Figure 2.4b-c; Ro-25-6981: Supplementary Fig. 2.3). These data suggest that ethanol and Ro 25-6981 alter protein expression in an FMRP-dependent manner.

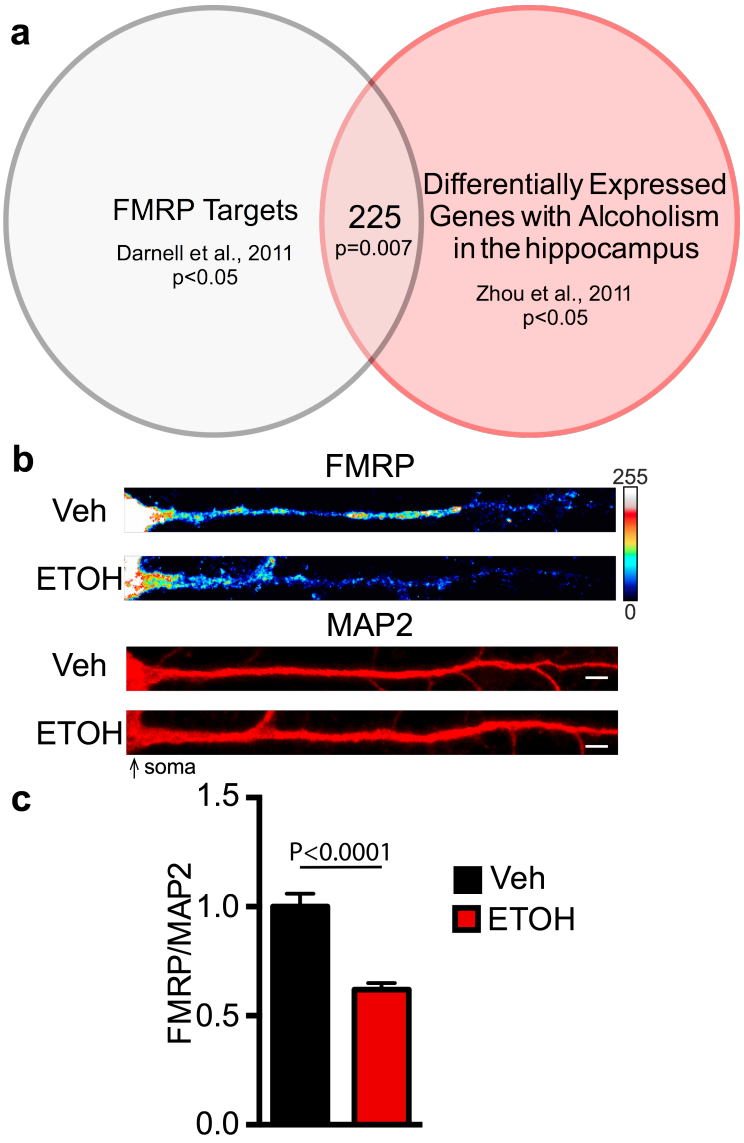

Figure 2.4. FMRP and AUD share target mRNAs and ethanol decreases FMRP

(a) Venn diagram illustrating the significant overlap between FMRP mRNA targets and differentially expressed genes in the hippocampus of humans with AUDs. Significance determined with Chi^2 test. (b-c) Immunofluorescence images normalized to MAP2 as volume control and quantification summary shows a significant decrease in FMRP expression in dendrites of cultured hippocampal neurons treated with ethanol (ETOH; 30 mM, 2 hours) compared to vehicle-treated (Veh; H_2O, 2 hours). Veh: FMRP =1.00 ± 0.06, n=32 dendrites; ETOH: FMRP =0.62 ± 0.03, n=31 dendrites. Significance determined by Student's t-test. Values represent mean ± SEM. Scale bars=5 μm.

Ethanol-induced synthesis of $GABA_BR2$ requires FMRP

Due to the ethanol-induced decreases in FMRP, we hypothesized that FMRP is required for ethanol-induced expression of $GABA_BRs$. Specifically, if expression of $GABA_BRs$ is constitutive and unregulated in *Fmr1* KO mice, then ethanol-induced changes in $GABA_BR$ expression should be absent in *Fmr1* KO mice. Hippocampal synaptoneurosomes were isolated from WT and *Fmr1* KO mice 30 minutes after i.p. injection of ethanol (2.5g kg^{-1}). Western blot analysis indicated that both $GABA_BR1$ and $GABA_BR2$ expression remained constant in vehicle- and ethanol- treated *Fmr1* KO mice. As observed in Fig. 2.2, WT hippocampal synaptoneurosomes showed an ~23% increase in $GABA_BR2$ but no change in $GABA_BR1$ expression (Fig. 2.5a-c; uncropped blots, Supplementary Fig. 2.7c). These data suggest that ethanol-induced changes in $GABA_BR$ expression are dependent on FMRP translational regulation.

To determine whether protein synthesis is essential for the FMRP-dependent changes in $GABA_BR$ expression, we measured ethanol-induced $GABA_BRs$ in the presence of cycloheximide (CHX), a protein synthesis inhibitor. As demonstrated previously, ethanol did not influence the dendritic expression of $GABA_BR1$; however, co-treatment with cycloheximide increased $GABA_BR1$ expression by ~22%. FMRP deletion did not affect the basal, ethanol-, or cycloheximide-induced dendritic protein expression of $GABA_BR1$ (Fig. 2.5d-e and h). For $GABA_BR2$, we again saw a significant ~28% increase in dendritic

expression with acute ethanol treatment; however, in the presence of cycloheximide the ethanol-induced increase was abolished. Notably in *Fmr1* KO cultures, no change was observed with ethanol or ethanol+cycloheximide (Fig. 2.5f-g and i).

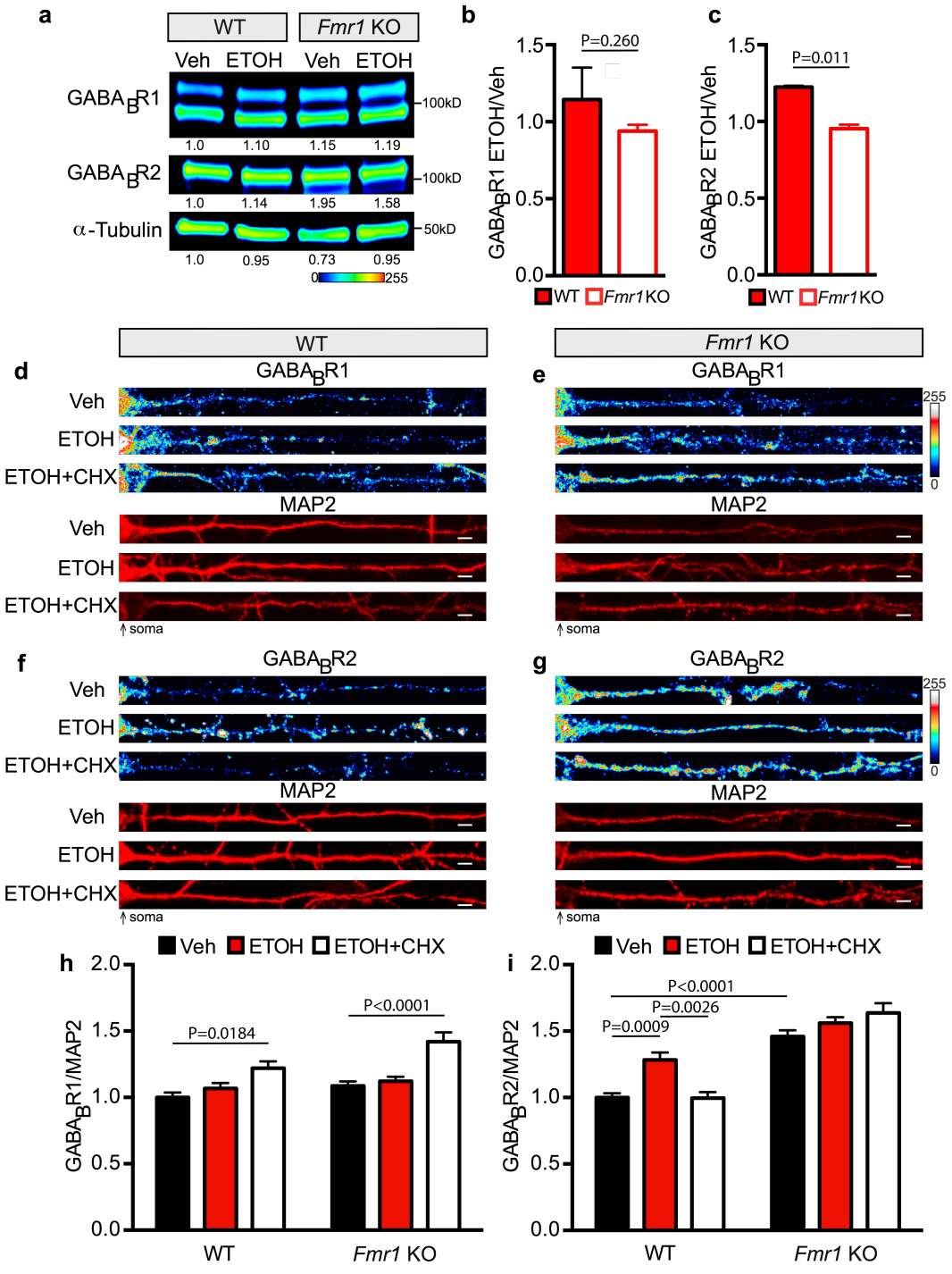

Figure 2.5. *Fmr1* KO prevents ethanol-induced altered $GABA_BR$ expression

a-c) Western blot analysis of $GABA_BR1$ and $GABA_BR2$ in wildtype (WT) and *Fmr1* KO C57BL/6 hippocampal synaptoneurosomes after vehicle (Veh; saline i.p., 30 minutes) or ethanol (ETOH; 2.5 g kg^{-1} i.p., 30 minutes) treatment. (a) Pseudocolored representative Western blots showing band intensity, and normalized optical densities to WT-vehicle are reported below each image (Lookup table, below Western blot). Western blots were normalized to the loading control, α-Tubulin. No change was found in (b) $GABA_BR1$ after ethanol treatment in either genotype as shown by ethanol/vehicle comparison. A significant increase in (c) $GABA_BR2$ expression was observed in WT mice after ethanol, but no change was observed in *Fmr1* KO mice (shown as ethanol/vehicle). WT ETOH/Veh: $GABA_BR1$=1.15 ± 0.21; $GABA_BR2$=1.22 ± 0.01. *Fmr1* KO ETOH/Veh: $GABA_BR1$=0.94 ± 0.04; $GABA_BR2$=0.95 ± 0.03. Experiment was repeated 3 times. Significance determined by Student's t- test. Values represent mean ± SEM. Representative immunofluorescent images (d-g) and quantification summaries (h-i) of dendritic expression of $GABA_BR1$ and $GABA_BR2$ from WT and *Fmr1* KO primary mouse hippocampal cultures normalized to MAP2. (h) $GABA_BR1$ expression was not changed in either genotype after 2-hour treatment with vehicle (Veh; H_2O), ethanol (ETOH; 30 mM), or ethanol and cycloheximide (30 mM ETOH+ 50 μM CHX). WT $GABA_BR1$: Veh=1.00 ± 0.04, n=44 dendrites; ETOH=1.07 ± 0.04, n=29 dendrites; ETOH+CHX=1.22 ± 0.05, n=34 dendrites. *Fmr1* KO $GABA_BR1$: Veh=1.09 ± 0.03, n=72 dendrites; ETOH=1.12 ± 0.03, n=41 dendrites; ETOH+CHX=1.42 ± 0.07, n=43 dendrites. (i) $GABA_BR2$ expression in WT neurons increased after ethanol (ETOH; 30 mM, 2 hours) compared to vehicle (Veh; H_2O, 2 hours) treatment, and was rescued with co-treatment of cycloheximide (CHX; 50 μM, 2 hours). $GABA_BR2$ expression in *Fmr1* KO dendrites was not significantly altered between neurons treated with Veh, ETOH, or ETOH+CHX. WT $GABA_BR2$: Veh=1.00 ± 0.03, n=41 dendrites; ETOH=1.28 ± 0.06, n=40 dendrites; ETOH+CHX=0.99 ± 0.05, n=33 dendrites. *Fmr1* KO $GABA_BR2$: Veh=1.46 ± 0.05, n=73 dendrites; ETOH=1.56 ± 0.04, n=45 dendrites; ETOH+CHX=1.63 ± 0.07, n=36 dendrites. Significance determined by two-way ANOVA with Tukey's post-test. Value represent mean ± SEM. Scale bars=5 μm. Uncropped version of western blots, with size markers are available in Supplementary Figure 7c.

We next examined the requirement for protein synthesis and FMRP in ethanol-dependent surface expression of $GABA_BRs$. Using WT and *Fmr1* KO hippocampal neurons, we measured ethanol-induced surface expression of $GABA_BR1$ with or without cycloheximide. Co-assembly of $GABA_BR1$ and R2 is

required to express $GABA_BR$ heterodimers in the membrane[153]. Thus, we predicted that the ethanol-induced increase in surface $GABA_BRs$ would require FMRP-regulated synthesis of $GABA_BR2$. Again, acute ethanol increased dendritic surface $GABA_BRs$ by ~76%, and this was blocked by cycloheximide. In *Fmr1* KO neurons there was no significant ethanol-induced change in surface $GABA_BRs$, but a decrease was observed with ethanol+cycloheximide (Fig. 2.6a-c). These data suggest that $GABA_BR2$ protein synthesis is required for the increased surface expression of the hetermultimeric receptor with ethanol exposure.

FMRP is reported to repress new protein synthesis. Considering the effects of the protein synthesis inhibitor, these data suggests that the ethanol-mediated reduction in FMRP results in the increase in dendritic $GABA_BR2$ by *de novo* protein synthesis. To provide more direct evidence, we performed bioorthogonal noncanonical amino acid tagging (BONCAT) in conjunction with proximity ligation assay (PLA-Duolink)[141]. BONCAT+PLA can be used to detect new synthesis of proteins of interest, such as $GABA_BR1$ and $GABA_BR2$. Through click chemistry, noncanonical amino acids that are incorporated during mRNA translation are biotinylated. PLA, on the other hand, generates a fluorescent signal when two antibodies are within 30-40 nm of each other (i.e., anti-$GABA_BR1$ or $GABA_BR2$ and anti-biotin). By combining these methods, we determined that ethanol treatment increases new protein synthesis of $GABA_BR2$ by ~40%, but does not alter $GABA_BR1$ synthesis, similar to the $GABA_BR$ changes

induced by rapid antidepressants[78]. In *Fmr1* KO dendrites, basal levels of $GABA_BR2$s increased by ~48%, while a significant decrease was observed in $GABA_BR1$ levels. Additionally, ethanol-induced translation of $GABA_BR2$ was lost in *Fmr1* KO dendrites (Fig. 2.6d-i). These data provide additional evidence that the ethanol-induced increase in $GABA_BR2$ expression is due to new protein synthesis that requires the release of translational repression by FMRP.

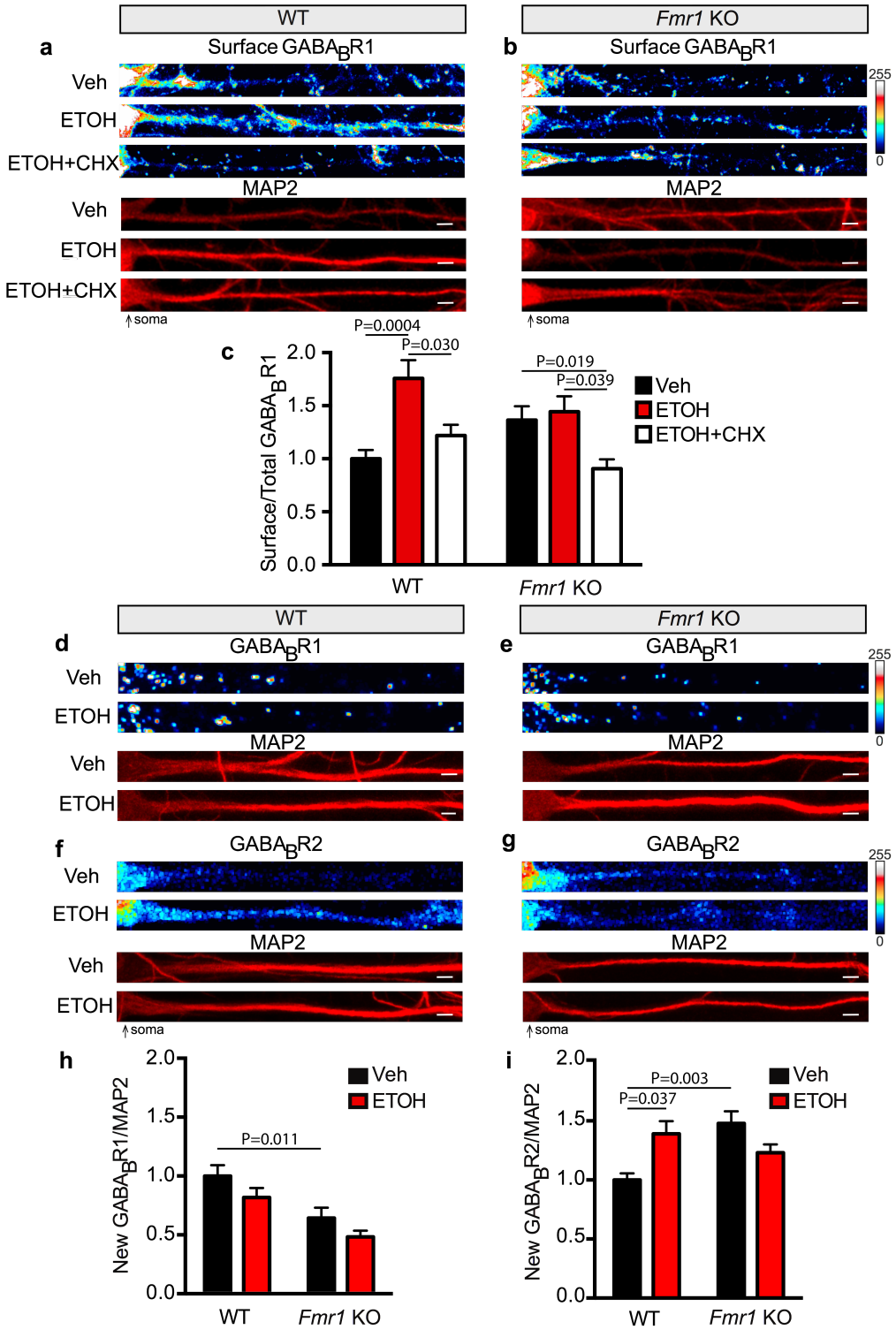

Figure 2.6. New $GABA_BR2$ protein and surface expression requires FMRP

Immunofluorescent images and quantification summary of $GABA_BR1$ surface expression in wildtype (WT) and *Fmr1* KO primary hippocampal cultures normalized to MAP2 as volume control. (a-b) Representative images of immunostaining. (c) Increased expression of surface $GABA_BR1$ in WT dendrites after ethanol (ETOH: 30 mM, 2 hours) compared to vehicle (Veh: H_2O, 2 hours) or ethanol-cycloheximide (30 mM ETOH+ 50 μM CHX, 2 hours) treatment. No significant change in surface $GABA_BR1$ expression in *Fmr1* KO cultures treated with ETOH or ETOH+CHX was observed. WT Surface $GABA_BR1$: Veh=1.00 ± 0.08, n=28 dendrites; ETOH=1.76 ± 0.17, n=37 dendrites; ETOH+CHX=1.22 ± 0.1, n=36 dendrites. *Fmr1* KO Surface $GABA_BR1$: Veh=1.36 ± 0.13, n=39 dendrites; ETOH=1.44 ± 0.15, n=42 dendrites; ETOH+CHX=0.91 ± 0.09, n=29 dendrites. (d-i) BONCAT combined with PLA, a method to detect newly synthesized proteins. (d-g) Representative images for $GABA_BR1$ and $GABA_BR2$ expression. Pixels were equally dilated by 1 using ImageJ software for enhanced visualization as described by Cajigas et al., (2012)[92]. In WT and *Fmr1* KO primary hippocampal cultures (h) $GABA_BR1$ synthesis in dendrites was not altered by ethanol (30 mM, 2 hours) compared to vehicle (H_2O, 2 hours) treatment normalized to MAP2. WT $GABA_BR1$: Veh=1.00±0.09, n=47 dendrites; ETOH=0.82±0.08, n=39 dendrites. *Fmr1* KO $GABA_BR1$: Veh=0.64±0.09, n=38 dendrites; ETOH=0.48±0.05, n=36 dendrites. (i) In contrast, ethanol induced a significant increase in new $GABA_BR2$ synthesis in WT hippocampal dendrites but not in *Fmr1* KO dendrites. WT $GABA_BR2$: Veh=1.00 ± 0.06, n=21 dendrites; ETOH=1.39 ± 0.11, n=25 dendrites. *Fmr1* KO $GABA_BR2$: Veh=1.48 ± 0.10, n=32 dendrites; ETOH=1.23 ± 0.07, n=41 dendrites. Significance determined by two-way ANOVA with Tukey's post-test. Values represent mean ± SEM. Scale bars=5 μm.

Ethanol-induced $GABA_BR$ plasticity requires FMRP

We previously demonstrated that rapid antidepressants shift $GABA_BR$ signaling from opening potassium channels to increasing dendritic calcium[13]. To determine if ethanol (30 mM, 2 hours) causes the same plasticity in $GABA_BR$ signaling, we performed fluorescence calcium imaging in cultured WT and *Fmr1* KO hippocampal neurons. A transient rise or fall in calcium in dendritic compartments

can be detected using a fluorescent indicator that exhibits changes in fluorescent properties depending on the amount of bound calcium[156]. We used baclofen, a $GABA_BR$ agonist, to activate $GABA_BRs$ in the presence or absence of ethanol. After establishing a baseline measurement, baclofen reduced dendritic calcium fluorescence in saline-treated WT neurons by ~11%, a characteristic signature of $GABA_BR$ signaling increasing outward potassium conductance[78]. However, in ethanol-treated WT neurons, baclofen induced distinct calcium waves and an overall averaged increase in calcium signal of ~9% (Fig. 2.7a-c and Supplementary Fig. 2.4a and c). These results recapitulate our previous observations with NMDAR antagonists[13]. In addition, these findings in WT mouse neurons are consistent with what we observed in rat cultured hippocampal neurons treated with ethanol or the clinically relevant rapid antidepressant Ro 25-6981 (Supplementary Fig. 2.5). Unexpectedly, $GABA_BR$ activation in saline-treated *Fmr1* KO neurons failed to reduce the calcium signal. Moreover, in ethanol-treated *Fmr1* KO neurons, $GABA_BR$ activation failed to increase dendritic calcium signal (Fig. 2.7 b-c and Supplementary Fig. 2.4b and c). These findings suggest that the loss of FMRP in *Fmr1* KO dendrites decouples $GABA_BRs$ from potassium channels. These results also suggest that the dynamic, ethanol-induced plasticity in $GABA_BR$ signaling, which is observed with rapid antidepressants, requires FMRP[13].

To further substantiate that FMRP regulates ethanol-dependent $GABA_BR$ plasticity, we overexpressed FMRP in rat hippocampal neurons. Overexpression

of FMRP did not alter the $GABA_BR$ activation in saline-treated neurons because baclofen reduced the dendritic calcium signal. However, in ethanol-treated neurons, overexpressing FMRP blocked the ethanol-induced $GABA_BR$ plasticity (Fig. 2.7d and Supplementary Fig. 2.4d-e). These results provide additional evidence that the dynamic reduction of FMRP with ethanol exposure is important for the expression of $GABA_BR$ plasticity.

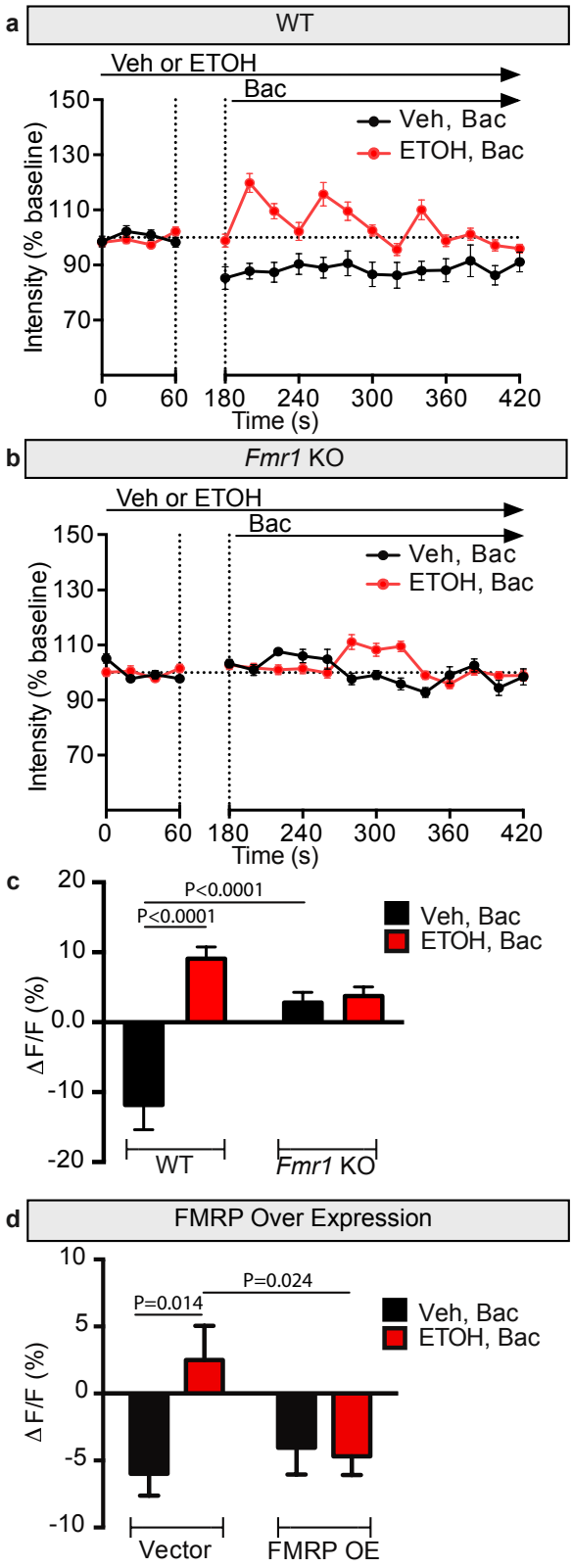
a
WT
Veh or ETOH
Bac
Veh, Bac
ETOH, Bac
Intensity (% baseline)
150
130
110
90
70
0
60
180
240
300
360
420
Time (s)
b
Fmr1 KO
Veh or ETOH
Bac
Veh, Bac
ETOH, Bac
Intensity (% baseline)
150
130
110
90
70
0
60
180
240
300
360
420
Time (s)
c
P<0.0001
P<0.0001
Veh, Bac
ETOH, Bac
ΔF/F (%)
20
10
0.0
-10
-20
WT
Fmr1 KO
d
FMRP Over Expression
P=0.024
P=0.014
Veh, Bac
ETOH, Bac
ΔF/F (%)
10
5
0
-5
-10
Vector
FMRP OE

Figure 2.7. $GABA_BR$ plasticity and signaling is absent in *Fmr1* KO mice

(a-c) Mouse hippocampal cultured neurons were pre-treated for 2 hours with either vehicle (Veh: H_2O) or ethanol (ETOH: 30 mM). Line graphs represent the average fluorescent calcium signal in dendrites over time from (a) wildtype (WT) and (b) *Fmr1* KO mice. Baseline was established for 1 minute before the addition of the $GABA_BR$ agonist baclofen (Bac: 50 μM) in vehicle- or ethanol-exposed neurons. Baclofen was allowed to equilibrate as indicated by the break between dotted lines. (c) Summary graph shows significant increase in dendritic calcium signal (ΔF/F) with the addition of baclofen in WT neurons pre-treated with ethanol, which was not observed in *Fmr1* KO neurons. WT: Veh+Bac= -11.82 ± 3.55, n=8; ETOH+Bac=9.10 ± 1.65, n=14. *Fmr1* KO : Veh+Bac=2.81 ± 1.48, n=12; ETOH+Bac=3.74 ± 1.30, n=12. (d-e) Dendritic calcium imaging was performed as before in hippocampal cultured neurons infected with either vector (rAAV:mSYN-tdTomato) or FMRP overexpression (rAAV:mSYN-FMRP and rAAV:mSYN-tdTomato). Ethanol-induced increase in dendritic calcium is prevented by FMRP overexpression. Vector: Veh+Bac: -6 ± 1.6, n=17 dendrites; ETOH+Bac: 2.5 ± 2.5, n=17 dendrites. FMRP overexpression: Veh+Bac: -4 ± 2, n=11 dendrites; ETOH+Bac: -4.7 ± 1.4, n=27 dendrites. Significance determined by two-way ANOVA, followed by Tukey's multiple comparison. Values represent mean ± SEM.

Antidepressant effect of ethanol on behavior requires FMRP

Since FMRP is important for ethanol-induced $GABA_BR$ plasticity, we examined antidepressant and anxiolytic-like effects of ethanol on behavior in *Fmr1* KO mice. Interestingly, ethanol administration did not affect the behaviors of *Fmr1* KO mice in the splash and open field tests compared to saline-treated mice (Supplementary Fig. 2.6a-e). Surprisingly, the basal state of immobility in the FST in *Fmr1* KO mice is equivalent to ethanol-injected WT mice (Fig. 2.8). To explore this paradox, we examined the requirement of $GABA_BR$ activation in ethanol-induced decreases in immobility by using CGP-35348 to inhibit

postsynaptic $GABA_BRs$. We previously showed that $GABA_BR$ antagonism blocked the antidepressant-like behavior produced by NMDAR antagonist in the FST[13]. $GABA_BR$ inhibition alone did not affect the immobility of saline-injected WT mice in the FST, similar to what we observed previously (Fig. 2.8)[13]. CGP-35348, however, abolished the ethanol-induced antidepressant behavior, demonstrating a requirement for $GABA_BR$ activation in ethanol-triggered reduction of immobility. Neither ethanol, CGP-35348, or ethanol + CGP-35348 treatment in *Fmr1* KO mice produced immobility scores that were significantly different from saline-treated *Fmr1* KO mice. These findings collectively demonstrate that $GABA_BRs$ and FMRP are necessary to elicit the ethanol-mediated antidepressant response.

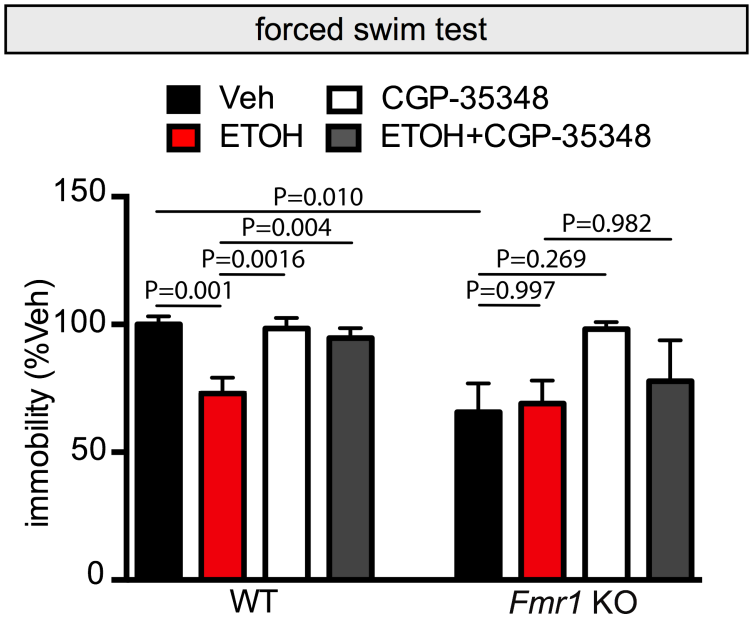

Figure 2.8. Ethanol's antidepressant effect requires $GABA_BR$ activation

Wildtype (WT) C57BL/6 and *Fmr1* KO male mice were subjected to the forced swim test (FST) 24 hours post-injection of vehicle (Veh: saline), ethanol (ETOH: 2.5 g kg^{-1}), CGP-35348, a $GABA_BR$ antagonist (CGP: 100 mg kg^{-1}), or ethanol+CGP-5348. Ethanol induced-decrease in immobility was absent in *Fmr1* KO mice. WT: Veh=100 ± 3.19 s, n=9 mice; ETOH=72.97 ± 6.23 s, n=7 mice; CGP-35348=98.38 ± 4.2 s, n=10; ETOH+CGP-35348=94.73 ± 3.77 s, n=7 mice. *Fmr1* KO : Veh=58.75 ± 10.33 s, n=9; ETOH=69.02 ± 8.99 s, n=3; CGP-35348=88.00 ± 9.56 s, n=3; ETOH+CGP-35348=77.78 ± 16.04 s, n=3. Significance determined by two-way ANOVA Tukey's multiple comparison test. Values represent mean ± SEM.

Discussion

Emerging behavioral and molecular evidence demonstrate that NMDAR antagonists act as rapid antidepressants[13, 70, 74, 78, 157]. Because it has long been speculated that individuals with major depressive disorders self-medicate with alcohol, we examined whether ethanol, which blocks NMDARs[52], acts through the same synaptic pathways as NMDAR antagonists. Until this study, the molecular mechanisms shared by alcohol and antidepressants were unexplored. Here, we provide molecular and behavioral evidence that acute alcohol exposure elicits antidepressant-like behaviors that persist up to 24 hours after administration (Fig. 2.1), supporting the hypothesis that ethanol initiates lasting antidepressant activity. We have previously demonstrated that NMDAR inhibition by rapid antidepressants induces two key molecular changes that are responsible for the rapid antidepressant response, namely (1) an increase in $GABA_BR$ protein synthesis and (2) a shift in $GABA_BR$ function that increases dendritic calcium signaling[13, 78]. Our current work shows that these same signature changes are produced by acute ethanol exposure (Fig. 2.5-2.7).

Surface expression of functional $GABA_BRs$ requires the dimerization of $GABA_BR1$ and R2 subunits. Without $GABA_BR2$, $GABA_BR1$ is retained in the endoplasmic reticulum[153]. Our current studies show that the release of $GABA_BR2$ mRNA translational repression by FMRP is necessary for the ethanol-induced increase in surface $GABA_BRs$ with NMDAR blockade (Fig. 2.4,2.6,2.8, Supplementary Fig. 2.3). Reduction of FMRP, as seen in animal models of FXS, is associated with elevated protein synthesis of target mRNAs[87]. While we have demonstrated that FMRP associates with $GABA_BR1$ and R2 mRNAs, the loss of FMRP has a profound effect on $GABA_BR2$ protein expression in dendrites. Constitutive loss of FMRP, as observed in many of its targets, abrogates stimulus-dependent mRNA transport and translation of target mRNAs[88, 137, 158, 159]. We show that the ethanol-induced increase in $GABA_BR2$ protein is also absent in *Fmr1* KO mice.

The question of why $GABA_BR2$ is uniquely affected by acute ethanol and its dependence on reduced FMRP levels is intriguing. Both $GABA_BR1$ and $GABA_BR2$ mRNA were detected in the FMRP RIP (Fig. 2.3). Interestingly, *in vivo* FMRP influences $GABA_BR1$ expression to a lesser extent compared to $GABA_BR2$, suggesting that FMRP may act in concert with other repressors such as microRNAs to tightly regulate $GABA_BR1$ expression[160]. Moreover, our immunostaining and protein synthesis assays suggest that the increased protein levels of $GABA_BR1$ are not due to new protein synthesis in the dendrites, even in *Fmr1* KO mice (Fig. 2.5 and 2.6). These results indicate that the overall increase

in synaptic $GABA_BR1$ expression in *Fmr1* KO mice may be due to an increase in presynaptic $GABA_BR1$ expression, either through protein synthesis or increased protein stability. Notably, FMRP has been localized to axons and presynaptic terminals[161, 162]. Further exploration into presynaptic and postsynaptic $GABA_BR$ expression and function in AUD and FXS is warranted.

The "GABA hypoinhibition theory" posits that loss of inhibition is a leading cause in many of the neurological symptoms observed in FXS[163]. While studies showing reduced inhibition in models of FXS have focused on decreased expression of $GABA_AR$ subunit mRNA and protein[164], $GABA_BR$ protein expression and dendritic signaling has not been explored. Interestingly, the $GABA_BR$ agonist baclofen has shown promise in treating FXS. (R)-baclofen administration *in vitro* corrects the elevated basal protein synthesis normally seen in *Fmr1* KO mice, and rescues synaptic abnormalities such as increased spine density[165]. Additionally, baclofen administration reduced symptoms related to FXS in *Fmr1* KO mice[165, 166]. Recent studies have shown that the excitatory drive to fast spiking inhibitory neurons is reduced in the cortex of *Fmr1* KO mice[167]. Our data expands upon these findings by suggesting that postsynaptic $GABA_BR$ coupling to inwardly rectifying G protein-coupled potassium channels (GIRK) is absent in *Fmr1* KO neurons (Fig. 2.7). Collectively, these results may imply that the therapeutic effects of baclofen in the *Fmr1* KO mouse may be due to activation of presynaptic $GABA_B$ receptors that may in turn reduce glutamate

release and reduce hyperactive metabatropic glutamate receptor mGluR signaling in the hippocampus[168].

Changes in gene expression and protein synthesis are essential for normal neuroplasticity, but these crucial processes are dysregulated by drug addiction[134, 169]. Several lines of evidence support parallel changes in $GABA_BR$ mRNA translation/signaling as a result of NMDAR blockade that may be critical for alcohol actions. First, NMDAR antagonists mimic some effects of ethanol in humans[170], suggesting common biochemical/electrophysiological signaling pathway(s). Second, changes in $GABA_BR2$ brain gene expression correlates with lifetime alcohol consumption, supporting a role for altered $GABA_BR$ signaling in AUD[112]. Third, although controversial, the $GABA_BR$ agonist baclofen may decrease alcohol consumption in some alcoholics[171]. In summary, our data defines a common molecular paradigm for alcohol and rapid antidepressants and identifies a mechanism for the initial antidepressant effects of alcohol. A shift in $GABA_BR$ signaling is observed with both rapid antidepressants and acute ethanol treatment, which may provide insight into the molecular basis for the high comorbidity between major depressive disorder and AUD.

CHAPTER 3: ACUTE ALCOHOL AND RAPID ANTIDEPRESSANT INFLUENCE ON THE SYNAPTIC TRANSCRIPTOME

Abstract

Alcohol use disorder (AUD) and major depressive disorder (MDD) are prevalent, debilitating, and highly comorbid. The dual development of these disorders has been speculated, but underlying molecular changes that could account for the high rate of comorbidity are undetermined. Recent evidence suggests that acute alcohol exposure has rapid antidepressant behavioral and molecular properties. To explore parallels between alcohol and rapid antidepressants on a genomic scale, we interrogated transcriptional changes induced with acute treatment of ethanol or the N-methyl-D-aspartate receptor (NMDAR) antagonist, Ro 25-6981 in hippocampal synapses. Ethanol and Ro 25-6981 distinctly altered differential gene expression with only select genes exhibiting similar changes in expression, and acute ethanol exposure induced alterations in gene expression largely independent of NMDAR antagonism. To explore parallel alterations between ethanol and Ro 25-6981 treatment that alter synaptic function, but not necessarily gene expression, we interrogated differential exon usage. Notably both ethanol and antidepressant induced similar alterations in exon usage, suggesting that ethanol and rapid antidepressants induce differential splicing of synaptic related genes. Additionally, predominant genes associated with alternative splicing in AUD and MDD were identified within differential exon expression data with both ethanol and Ro 25-6981. Finally, our analysis highlights the profound effect acute NMDAR inhibition exerts on differential exon use at the synapse. This altered exon use likely contributes to the mechanism of acute Ro 25-6981 and other NMDAR antagonists providing important context for

their biological and pharmacological implications. These data implicate alternative splicing and isoform expression in the acute antidepressant-like effects of ethanol and the development of comorbid alcohol and depression. Understanding the molecular basis for comorbidity may aid in development of treatment options for afflicted individuals with dual disorders, as well as explore the mechanism for the initiation of addiction with acute exposure to alcohol.

Introduction

Alcohol use disorders display high comorbidity with other psychiatric disorders in particular major depressive disorder. The relationship between AUD and MDD is not fully understood, but the two disorders are closely linked through epidemiological and clinical studies[14, 36, 38]. The connection between AUD and MDD may be caused by similar environmental and genetic factors[14, 36, 38]. The self-medication hypothesis proposes that depressed individuals drink to alleviate symptoms initially, but chronic use leads to comorbid AUD. This chronic abuse can induce neuroadaptive changes manifesting as tolerance and physiological dependence[1]. In particular, synaptic remodeling in response to alcohol is thought to lead to tolerance and physical dependence with continued alcohol abuse[2]. Some studies suggest that alcohol and other addictive drugs alter molecular mechanisms underlying synaptic plasticity[45, 136], and drug induced changes in gene expression are proposed as critical molecular adaptations leading to addiction with repeated exposure[60]. These initial changes in synaptic remodeling

may be key to understanding the development of comorbid AUD. Our previous studies in animals have identified that acute alcohol and antidepressant can elicit the same synaptic signaling pathway, thought to lead to activation of synaptic plasticity related pathways[79]. Alcohol was also shown to induce a lasting antidepressant like response in behavioral assays for antidepressant efficacy[79]. To address the continued mystery surrounding the acute antidepressant effects of ethanol and the development of comorbid AUD and MDD, we sought to identify acute alcohol and antidepressant effects on a global scale by analyzing parallels between the acute ethanol and rapid antidepressant synaptic transcriptome.

Alcohol and other drugs of abuse promote profound changes in gene expression, mRNA translation rates, and synaptic protein composition[134, 135]. Genome-wide expression studies show that transcriptional profiling is important to understand brain effects of alcohol exposure in both humans and mice. RNA-Sequencing (RNA-Seq) analysis of postmortem brain tissue from human alcoholics revealed that differences in transcriptome organization is linked with lifetime consumption of alcohol[112]. Both MDD and rapid antidepressants alter the transcriptome of humans and animals. RNA-Seq studies of postmortem depressed human tissues find altered expression of genes with MDD, and MDD suicides[118], and enrichment for particular synapse related genes in human MDD tissues[119]. Analysis of gene regulation of rat hippocampus treated acutely with antidepressants identified a variety of genes involved in various cellular

processes suggesting that the therapeutic effect is very complex[120]. It is evident that both AUD and MDD alter gene expression, however little is known about their acute effects on the transcriptome and even less is known about shared alterations in gene expression between these two disorders.

The effect alternative splicing has on acute alcohol or antidepressant behavior is undetermined. This is an important avenue of study because, alternative splicing can generate isoforms that differ in function and localization[110], and these Isoforms can be important for development, differentiation, and disease[110]. Alternative splicing and exon composition play an important role in the complexity of the proteome and are widely implicated in physiological and pathophysiological processes[172-174]. Alternative splicing can induce altered exon expression and composition in RNA, allowing new protein isoforms to be translated without observed alterations of basal mRNA or protein expression. Ethanol exposure has been shown to affect splice patterning of several transcripts including NMDAR[121], γ-aminobutyric acid type A receptor ($GABA_AR$)[122], and γ-aminobutyric acid type B receptor ($GABA_BR$)[123], however, transcriptome-wide RNA-Seq has not been used to define synaptic effects of acute alcohol exposure. Differential exon usage occurs in individuals with MDD with the strongest evidence for splicing in ATPase class II type 9B (ATP9B) and eukaryotic translation initiation factor 3 subunit K (EIF3K) genes[118]. The significance of splice patterning in AUD and MDD in development of these disorders, or the effects that altered isoforms may have on neuroadaptation with

alcohol is unknown. In addition to identifying parallel gene expression changes between ethanol and rapid antidepressant; we sought to identify altered exon usage to further investigate possible shared transcriptome changes that may lead to altered synaptic function through isoform expression.

We focused on alterations in the hippocampus due to previous studies of ethanol and antidepressants affecting this brain region. Studies of human hippocampus demonstrate that this brain region shows changes in transcription patterns with chronic drinking[60, 113]. Animal studies of rapid antidepressants, including ketamine, identified altered gene expression after as little as one dose in the hippocampus and other brain regions[95]. Additionally, our previous work identified shared molecular mechanisms induced by both ethanol and rapid antidepressant in the hippocampus[79]. Additionally, we selected the rapid antidepressant Ro 25-6981 for it's highly selective and potent inhibition of the NR2B subunit of the NMDAR[31, 32] as opposed to other rapid antidepressants that some of which have adverse side effects[27], or alternative convoluting mechanisms of action[175].

RNA sequencing allows for the detection of most mRNAs, including those that map to the same gene due to splice variation[176]. RNA sequencing paired with differential expression tools like DEXSeq can provide information on differential exon-usage of gene products[177]. Here we applied next generation RNA sequencing to identify the differentially expressed genes (DEGs) and differentially expressed exons (DEEs) for mice treated acutely with alcohol or the

rapid acting antidepressant, Ro 25-6981. We isolated RNA from hippocampal synaptoneurosomes to evaluate parallel gene and exon usage patterns between acute alcohol and antidepressants that may play a role in synaptic plasticity. Our results suggest that limited parallel alterations in gene expression occur between both ethanol and Ro 25-6981 acute treatment; however, exon usage analysis showed pronounced alterations with both treatments and an abundance of shared genes containing DEEs between both treatments.

Methods

Animals

Male C57BL/6NCrl mice at least 8 weeks old were given intraperitoneal (i.p.) injections of 200 µl vehicle (saline), ethanol (2.5 g kg^{-1} in saline), or Ro 25-6981 (10 mg kg^{-1} in saline, Tocris). All animals were housed 4 mice per cage. All treatments were administered to one mouse per home cage. At the time of drug treatment, animals were coded by number. Animals were sacrificed 30 minutes after inject to harvest tissue. Hippocampi was immediately flash frozen in liquid nitrogen after dissection. All experiments were carried out in accordance with the National Institutes of Health's Guide for the Care and Use of Laboratory Animals and approved by the UT-Austin Institutional Animal Care and Use Committee (IACUC).

Synaptoneurosome preparation and RNA isolation

RNA was isolated from hippocampal synaptoneurosomes (SN) prepared from male mice age 7-8 weeks treated with vehicle (saline), Ethanol (2.5g kg^{-1}), or Ro-25-6981 (10 mg kg^{-1}) as previously described. SNs were prepared by homogenizing hippocampal tissue in homogenization buffer (20 mM HEPES pH 7.4, 5 µM EDTA pH 8.0, and RNase inhibitor). Homogenate was filtered through a 100-µm nylon filter followed by a 5-µm filter, and centrifuged at 14000 x g for 20 minutes at 4°C[142]. The pellet was resuspended in Buffer RLT for processing with an RNeasy micro Kit (Qiagen, 74004). RNeasy micro kit procedure was followed as supplied by the company. Briefly, sample was homeginzed in RLT buffer. 1 volume of 70% ethanol was added to precipitate RNA and sample was centrifuged for 15 seconds at 8000xg in microcentrifuge through RNeasy MinElute spin column. Buffer RW1 was added to column and centrifuged as before. Sample was DNAse treated and centrifuged as before with buffer RW1. Column was then washed in buffer RPE and spun as before. Column was dried by adding 80% ethanol and centrifuging for 2 minutes at 8000 xg and then again with column lid open for 5 min at full speed. RNA was then eluted in nuclease free water. RNA quality was determined using a 2200 AgilentTapeStation Instrument(Agilent Technologies, G2965AA), and yield was determined using Qubit fluormetric quantitation (ThermoFisher, Q33216).

RNA-Sequencing

RNA samples were sequenced by the genome sequencing and analysis facility at the University of Texas at Austin. Poly-A-mRNA was captured with

MicroPoly(A) Purist Kit (Life Technologies). Samples were processed with whole transcriptome library preparation kit (NextSeq 500/550 High Output Kit, FC-404-2002) and sequenced on a NextSeq 500 system (Illumina) at a depth of ~20million reads with paired-end reads. Read quality was assessed using FASTQC (version 0.11.5). One ethanol treated sample was discarded due to low sequencing reads. Sequencing reads were mapped to the mouse genome (*Mus musculus* version GRCm38 rel.80, Ensemble) with Splice Transcripts Alignment to a Reference (STAR, version 2.5.0a). HTSeq (version 0.5.3p9) was used to quantify raw counts[178], followed by DESeq2 (version 1.14.1) to identify differentially expressed genes with treatment[179], and DEXSeq (version 1.20.2) to identify differentially expressed exons[177, 180]. Enrichment analysis for gene ontologies was preformed with Enrichr[181, 182]. Data processing and statistics was preformed with R programming[146].

Results

Ethanol and Ro 25-6981 treatment induce differential expression of genes

Ethanol and the rapid antidepressants Ro 25-6981 display some similar features acutely including: the induction of synaptic plasticity related pathways[96], acute inhibition of the NMDAR[52, 74, 183], lasting antidepressant like behavioral responses in mice[78, 79], and altered gene expression[95]. To better understand these similar phenomena of the acute effects of both ethanol and rapid antidepressant, we

investigated the synaptic transcriptome through RNA sequencing of hippocampal synaptoneurosomes of mice treated acutely (30 minutes) with ethanol (2.5g kg^{-1}) or Ro 25-6981 (10 mg kg^{-1}).

The differential gene expression analysis tool DESeq2 was used to detect genes significantly altered by ethanol exposure (Fig 3.1a) and Ro 25-6981 exposure (Fig. 3.1b). For quality control purposes, isolation purity, batch affect, and sample outliers were assessed. Synaptoneurosome preparations were assessed for purity and were highly enriched in synaptic genes (Supplemental Fig. 3.1). No differences in batch effect were identified when assessed with principle component analysis (PCA; supplemental Fig. 3.2), and no sample outliers were detected with hierarchical clustering and correlation plotting (Supplemental Fig. 3.3).

Differentially expressed genes were identified between saline and ethanol or Ro 25-6981 treatment. DEGs were plotted in volcano plots comparing p-value and fold-change for each gene, and colored points indicate DEGs with a significance bellow 0.05. With ethanol treatment 1031 genes were identified as significantly differentially expressed (red), and with Ro 25-6981 treatment 2623 genes were identified (yellow). Cellular component gene ontologies were assessed for these DEGs with ethanol treatment (Fig. 3.1c) and Ro 25-6981 treatment (Fig. 3.1d) using the enrichment ontology tool Enrichr[181, 182]. With both ethanol and Ro 25-6981 treatments, we observed ontologies highly enriched for synaptic genes as expected from the hippocampal synaptoneurosomes (Fig.

3.1e-f). We identified parallels between the alcohol and antidepressant DEGs by examining the genes altered in both treatments. There were 178 shared genes differentially expressed with both treatments, comprising ~17% of the ethanol induced DEGs and ~7% of the Ro 25-6981 induced DEGs (Fig. 3.1e). These DEGs were enriched for synaptic and dendritic genes as well as those involved in protein kinase signaling (Fig. 3.1f). The observed alterations in these synaptic ontologies may indicate alterations in synaptic function with both treatments.

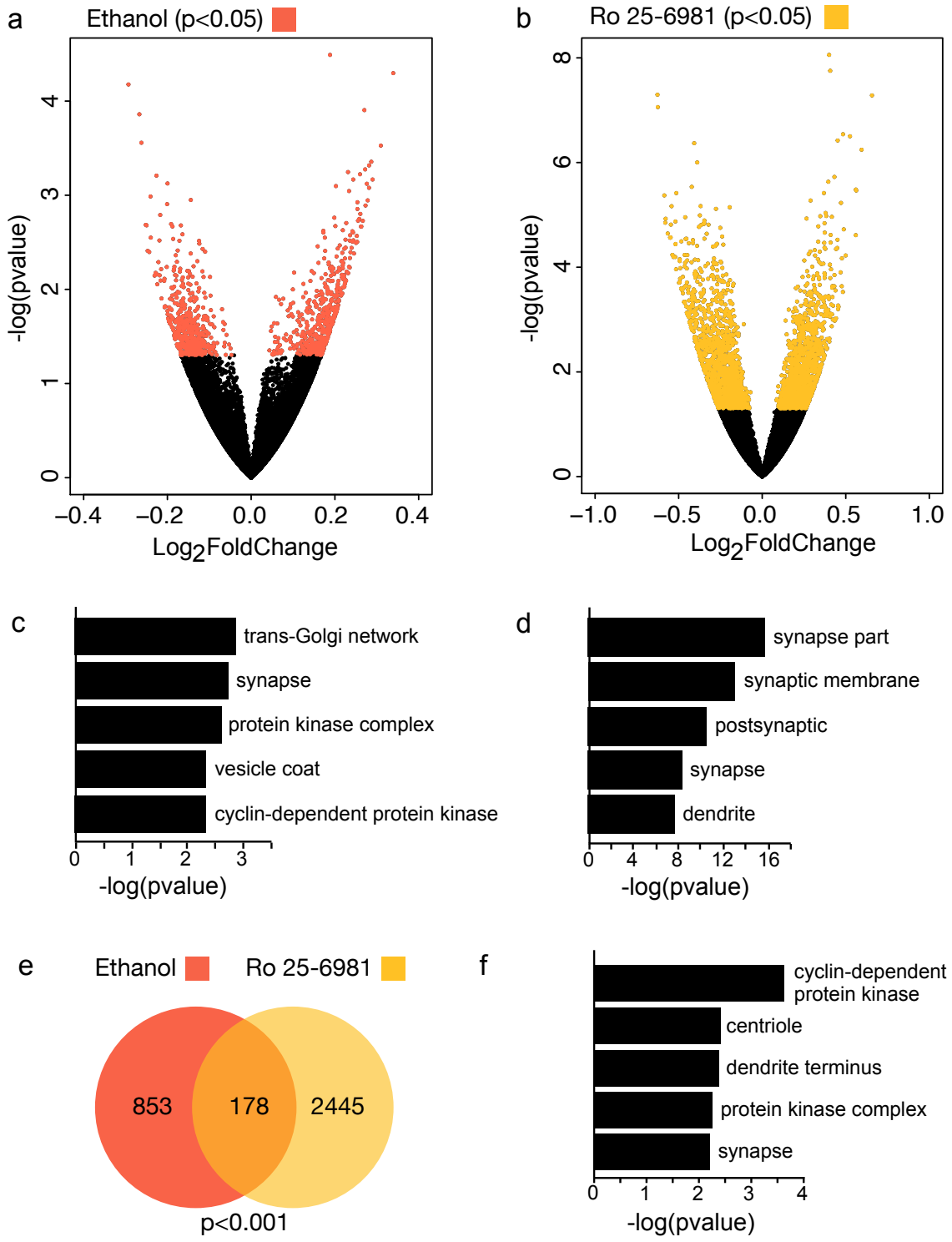

Figure 3.1. RNA-seq results of differentially expressed genes (DEGs) from synaptoneurosomes

C57Bl/6 mice were treated with vehicle (saline; n=8), ethanol (2.5g/kg; n=7), or Ro 25-6981 (10mg/kg; n=8). a) Volcano plot of differentially expressed genes with ethanol (n=7) compared to vehicle (saline, n=8) reveal a significant number of genes (1031; red) both up- and down-regulated with ethanol exposure shown as positive of negative log_2fold change with treatment ($p \leq 0.05$). b) Volcano plot of differentially expressed genes with Ro 25-6981 compared to vehicle reveal a significant number of genes (2623; yellow) both up- and down-regulated with Ro 25-6981 exposure shown as positive of negative log_2fold change with treatment ($p \leq 0.05$). c) Cellular component gene ontologies for DEGs ($p \leq 0.05$) with ethanol were identified with Enrichr gene enrichment analysis software. The 5 most significant ontologies determined by p value are shown in the summary bar graphs. d) Cellular component gene ontologies for DEGs ($p \leq 0.05$) with Ro 25-6981. The 5 most significant ontologies determined by p value are shown in the summary bar graphs. e) Venn diagram compared DEGs found in ethanol and Ro 25-6981 treatment groups, and found 178 genes that overlapped between both treatment groups ($p \leq 0.0001$), suggesting these genes may be implicated in the acute antidepressant like effects of alcohol exposure. f) Cellular component gene ontologies for these 178 overlapping DEGs were identified with Enrichr gene enrichment analysis software. The 5 most significant ontologies determined by p value are shown in the summary bar graphs.

To examine these findings further we investigated the co-occurring DEGs for up-regulation and down-regulation for both treatments. A heat map of the fold change of the 178 overlapping DEGs was generated where red indicates up-regulation and blue down-regulation (Fig. 3.2a), and many genes were observed to have opposite directionality. We identified 50 genes with parallel expression patterns, meaning they were either up-regulated (Fig. 3.2b) in both treatment groups, or down-regulated (Fig. 3.2c) in both treatment groups. The limited parallel effects we observed with DEGs between ethanol and Ro 25-6981 may be due to alternative targets of ethanol in neurons, and differences in binding specificity and affinity between ethanol and Ro 25-6981 for the NR2B subunit of

the NMDAR. Our data emphasizes the selective and potent binding of Ro 25-6981 to the NR2B subunit compared to ethanol. Where Ro 25-6981 is a highly selective noncompetitive antagonist of the NR2B subunit[32, 33, 184], ethanol transiently inhibits NMDARs, and affects many other cellular targets[45, 185]. NMDAR inhibition with acute ethanol exposure is thought to affect synaptic plasticity[96, 186, 187], conversely most of our DEGs with ethanol are not conserved with NR2B antagonism. To explore this further we analyzed ethanol induced DEGs independent of NR2B antagonism.

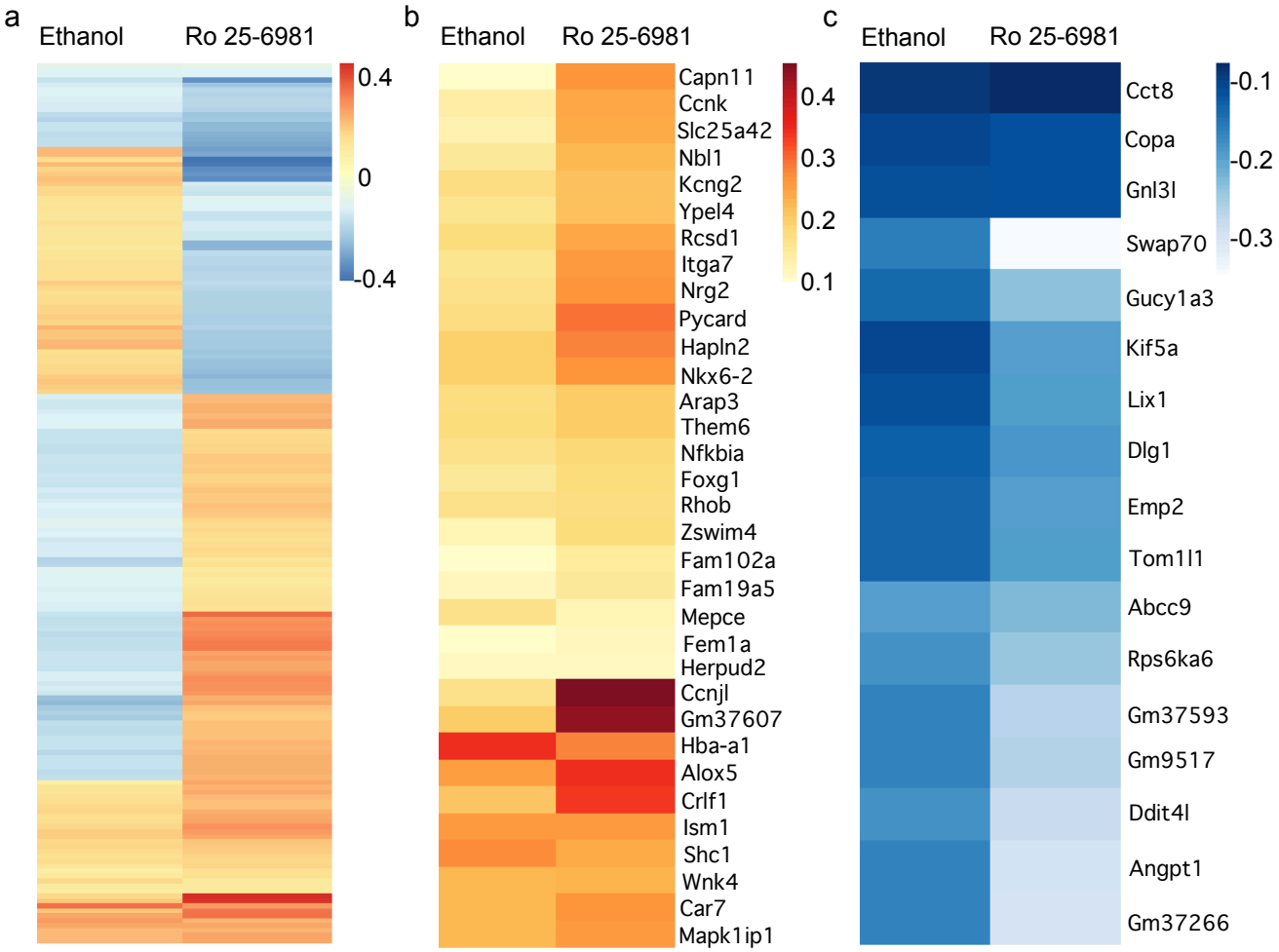

Figure 3.2. Parallel expression of DEGs with ethanol and antidepressant

DEGs in each treatment group were compared for similarities in fold change directionality using a heat map of log_2fold changes. a) The log_2fold changes of the 178 co-occurring DEGs between ethanol and Ro 25-6981 were clustered and visualized in a heat map. Scale bar indicates log_2fold changes ranging from blue (down-regulated with negative fold change) to red (up-regulated with positive fold change). b) Simultaneously occurring up-regulated DEGs in both treatment groups were plotted together in a heat map with gene labels displayed. Scale indicates positive log_2fold changes. c) Simultaneously occurring down-regulated DEGs were plotted together in a heat map with gene labels displayed. Scale indicates negative log_2fold changes. 50 genes were identified to have similar regulation between both ethanol and Ro 25-6981 treatment.

Alcohol induced differential gene expression is largely independent of NR2B inhibition

Our results suggest that many transcriptome changes produced by acute ethanol were largely independent of NR2B antagonism. By removing those DEGs associated with Ro 25-6981 induced alterations we isolated ethanol induced DEGs not directly related to NMDAR inhibition. We identified 853 DEGs independent of NR2B antagonism (Fig. 3.3a). These genes displayed molecular function gene ontologies enriched for mRNA 3'UTR binding, mRNA binding, and MAPK signaling (Fig. 3.3b). RNA binding proteins are crucial for the trafficking of mRNAs to synapses and influence protein translation that underlies synaptic plasticity[85, 86]. Furthermore, mitogen-activated protein kinase (MAPK) signaling also plays a key role in regulating transcription and synaptic plasticity[188]. These ontologies may indicate an increased role in mRNA trafficking and local translation in synapses. The modulation of genes with these ontologies likely

contributes to the synaptic changes seen upon both acute ethanol treatment and after repeated exposures[189]. The DEGs with the greatest fold changes are displayed in a bar graph with red and blue bars indicating up- and down-regulated directionality respectively (Fig. 3.3c). These genes contain several protein coding genes involved in RNA binding and MAPK signaling[188] (Fig. 3.3c). A similar graph for genes associated with Ro 25-6981 is displayed in Supplemental Fig. 3.4. Alterations in gene expression were observed with acute ethanol and Ro 25-6981 treatment independently, but simultaneous gene expression alterations with both treatments were limited. Alterations in synaptic plasticity and synaptic function have been identified for both alcohol[80, 96, 186, 187] and rapid antidepressants[13, 76, 190, 191], therefore we sough to find an answer to why parallel transcriptional changes were not robust in our analysis by exploring differential exon usage that could direct expression of alternative protein isoforms.

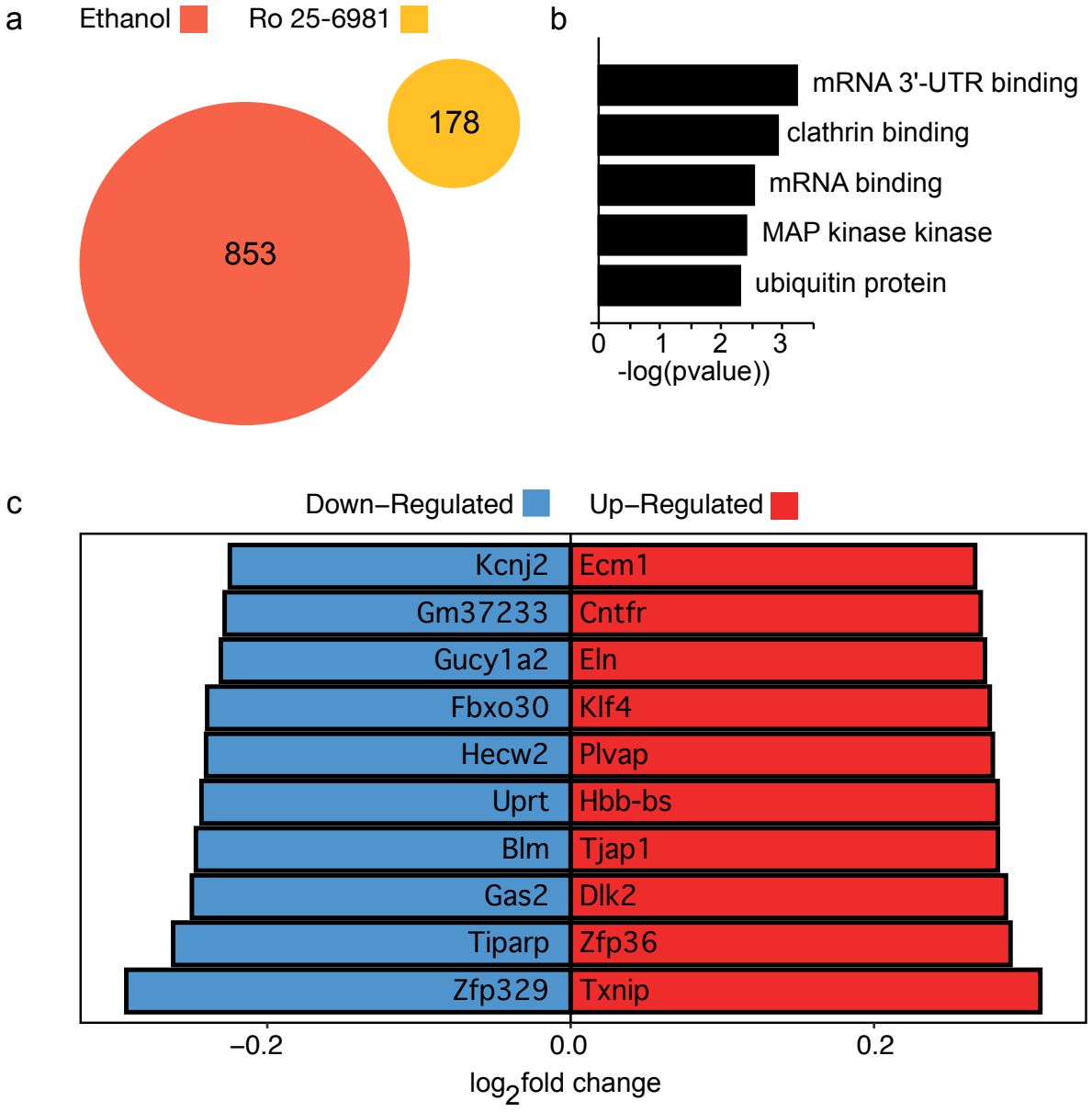

Figure 3.3. Ethanol DEGs independent of NR2B antagonism

DEGs with Ro 25-6981 treatment were removed from the DEGs with ethanol treatment ($p \leq 0.05$), to identified transcriptional changes independent of NMDAR inhibition. a) The Venn diagram illustrates that 853 genes are differentially expressed with ethanol ($p \leq 0.05$) independent of the 178 genes that are also differentially expressed with NR2B inhibition ($p \leq 0.05$), suggesting these genes may be implicated in acute ethanol alterations independent of NMDAR inhibition. b) Molecular component gene ontologies for these 853 DEGs were identified with Enrichr gene enrichment analysis software. The 5 most significant ontologies

determined by p value are shown in the summary bar graphs. c) Summary bar graph indicates the top 10 up- and down-regulated genes according to log_2fold change identified with acute ethanol independent Ro 25-6981 DEGs. Blue indicates down-regulated while red indicates up-regulated fold changes.

Alcohol and rapid antidepressant induce differential exon usage

To address the hypothesis that RNA splicing may be altered by alcohol and antidepressant treatments, we utilized DEXSeq to detect differentially expressed exons (DEEs). Many exons were differentially expressed with both ethanol and Ro 25-6981 as indicated by the summary bar graph (Fig. 3.1a). Corresponding volcano plots of exon expression for both ethanol and Ro 25-6981 show fold change variability and significant genes as colored points (Supplemental Fig. 3.4). DEEs for ethanol and Ro 25-6981 treatment were compared to identify co-occurring single exon changes with each treatment, and a significant population of exons were identified (Fig. 3.4b). We identified the genes where these exon-specific changes originated, summarized the number of significant genes with DEEs in a bar graph (Fig. 3.4c), and then overlapped these genes to identify those with co-occurring significant alternative exon use with both ethanol and Ro 25-6981. We discovered 2976 genes with alternative exon use with ethanol exposure, and 6082 genes with alternative exon use with Ro 25-6981. We then identified 1630 shared genes with alternative exon use in both ethanol and Ro 25-6981 treated mice, comprising ~55% of the ethanol induced genes with DEEs, and ~27% of the Ro 25-6981 induced genes with DEEs (Fig. 3.4d). These 1630

overlapping genes were enriched for cellular component gene ontologies linked to cytosolic and synaptic associated genes (Fig. 3.4e). These alternative exons may lead to alterations in synaptic isoforms contributing to the synaptic plasticity and alterations in synaptic activity observed with ethanol and rapid antidepressants[79]. This is in line with previous studies demonstrating altered isoforms in individuals with MDD or AUD[118, 125], diseases hallmarked by altered synaptic function and neuroadaptation[76, 96]. Our analysis revealed pathway ontologies enriched for genes associated with GTPase binding and ATP binding, including ATP9B (Fig. 3.4f) a gene previous implicated in MDD[118]. Specifically, ATP9B and EIF3K genes undergo extensive exon use alterations in both MDD individuals, and in the present study, upon acute ethanol and Ro 25-6981 treatment. Furthermore, we identified several genes with DEEs previously found to have alternative splice patterning in AUD including key synaptic receptors such as NDMAR[121] and $GABA_BR$[123]. These and other genes identified in our analysis represent novel genes that may contribute to the high degree of comorbidity observed between AUD and MDD. This overlap may reveal new treatment avenues for individuals suffering from comorbid AUD and MDD and allow for the development pharmacological intervention. Finally, our analysis highlights the effect acute NR2B inhibition exerts on differential exon use at the synapse. This altered exon use likely contributes to the mechanism of Ro 25-6981 and other NMDAR antagonists providing important context for their biological and pharmacological implications.

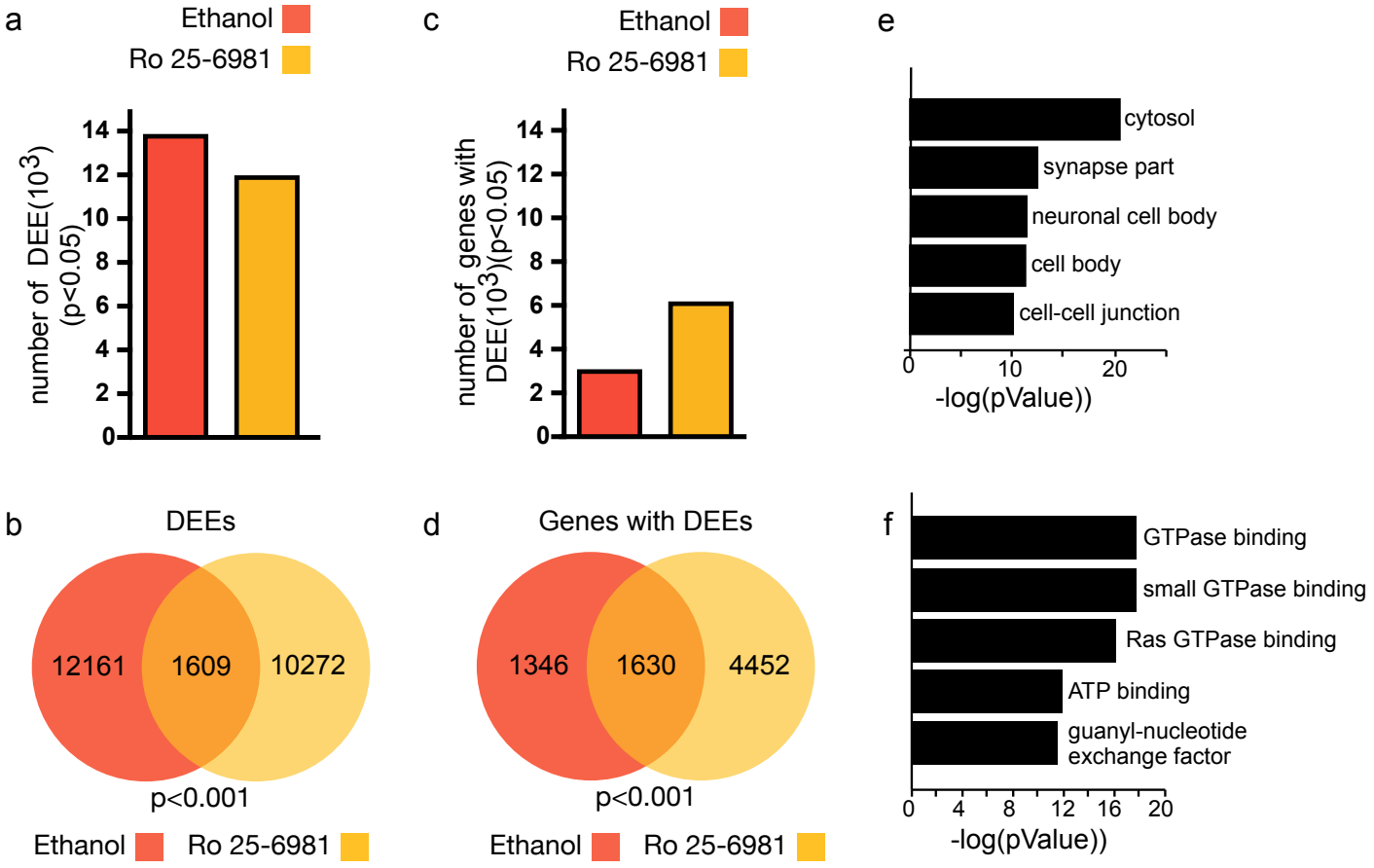

Figure 3.4. RNA-seq results of differentially expressed exons (DEEs) from synaptoneurosomes

mice (C57BL/6) were acutely treated with vehicle (saline; n=8), ethanol (2.5g/kg; n=7), or Ro 25-6981 (10mg/kg; n=8). a) Summary bar graph illustrates the total number of DEEs found with ethanol (13770; red) and Ro 25-6981 (11881; yellow) treatment ($p \leq 0.05$). b) Venn diagram compared DEEs found in ethanol and Ro 25-6981 treatment groups, and identified 1609 exons that overlapped between both treatment groups ($p \leq 0.0001$), suggesting these exons may be implicated in the acute antidepressant like effects of alcohol exposure. c) Genes containing differentially expressed exons were identified. The number of genes with DEEs for ethanol (2976; red) and Ro 25-6981 (6082; yellow) acute treatment were identified and displayed in the summary bar graph. d) Venn diagram compared genes with DEEs found in ethanol (red) and Ro 25-6981(yellow) treatment groups, and identified 1630 genes with DEEs that overlapped between both treatment groups ($p \leq 0.0001$), suggesting these exons may be implicated in the acute antidepressant like effects of alcohol exposure. e) Molecular component gene ontologies for these 1630 overlapping genes with DEEs were identified with

Enrichr gene enrichment analysis software. The 5 most significant ontologies determined by p value are shown in the summary bar graph. f) Cellular component gene ontologies for these 1630 overlapping genes with DEEs were identified with Enrichr gene enrichment analysis software. The 5 most significant ontologies determined by p value are shown in the summary bar graph.

Acute alcohol and Ro 25-6981 induce differential exon use in genes implicated in AUD and MDD

To take a closer look at differential exon usage produced by ethanol and Ro 25-6981, we focused on genes previously identified for their importance in splice variation with AUD (NMDAR), and MDD (ATP9B). DEEs appear with both treatments for Grin1, which encodes the NR1 subunit of the NMDAR (Fig. 3.5a-b). Ethanol induces an up-regulation in the expression of exon 5, which encodes the N1 splice cassette in some NR1 isoforms, and Ro 25-6981 induced an up-regulation in exon 4. The N1 splice cassette forms a surface loop, which can affect affinities for NMDA and glutamate[124, 192], potentiate receptor function[193], and accelerate the deactivation time course of NR1[194]. Studies of the modulation of NR1 splice variants with ethanol found differential exon 5 expressions, but reports are inconsistent and differ with dose, time, and brain region[125]. It is possible that differential exon use in this region of NR1 occurs with acute ethanol to counteract the inhibitory effects on the NMDAR. Both exon 4 and exon 5 are located in a ligand-binding domain of the NMDAR in mice, and alterations in this region may alter function of the synaptic NMDAR with ethanol and Ro 25-6981. Splice variants observed in the c-terminal domain of the NR1 can affect

localization and endoplasmic reticulum retention, affecting surface expression[195]. Differential exon expression in this region may increase surface targeting of NR1, and ethanol exposure altered exon use in this region of Grin1 (Fig. 3.5a); however more research is necessary to identify the effects of the differential regulation of these exons.

ATP9B encodes the ATPase Class II Type 9B protein, and has been implicated in pathways related to ion channel transport[196]. Ethanol and Ro 25-6981 acute treatment both induced DEE in the ATP9B gene; however, ethanol and Ro 25-6981 did not affect expression of the same exons (Fig. 3.5c-d). This may be a product of the differences between ethanol and Ro 25-6981 binding specificity and affinity. The pathophysiological consequences of ATP9B alternative splicing are unknown. It is critical to note that common DEEs can be discovered between acute treatments of ethanol and rapid antidepressant in mice that correspond the same genes with DEEs in AUD and MDD in humans. By examining different isoforms it may be possible to discover other targets to investigate underlying changes associated with the high comorbidity of AUD and MDD in humans.

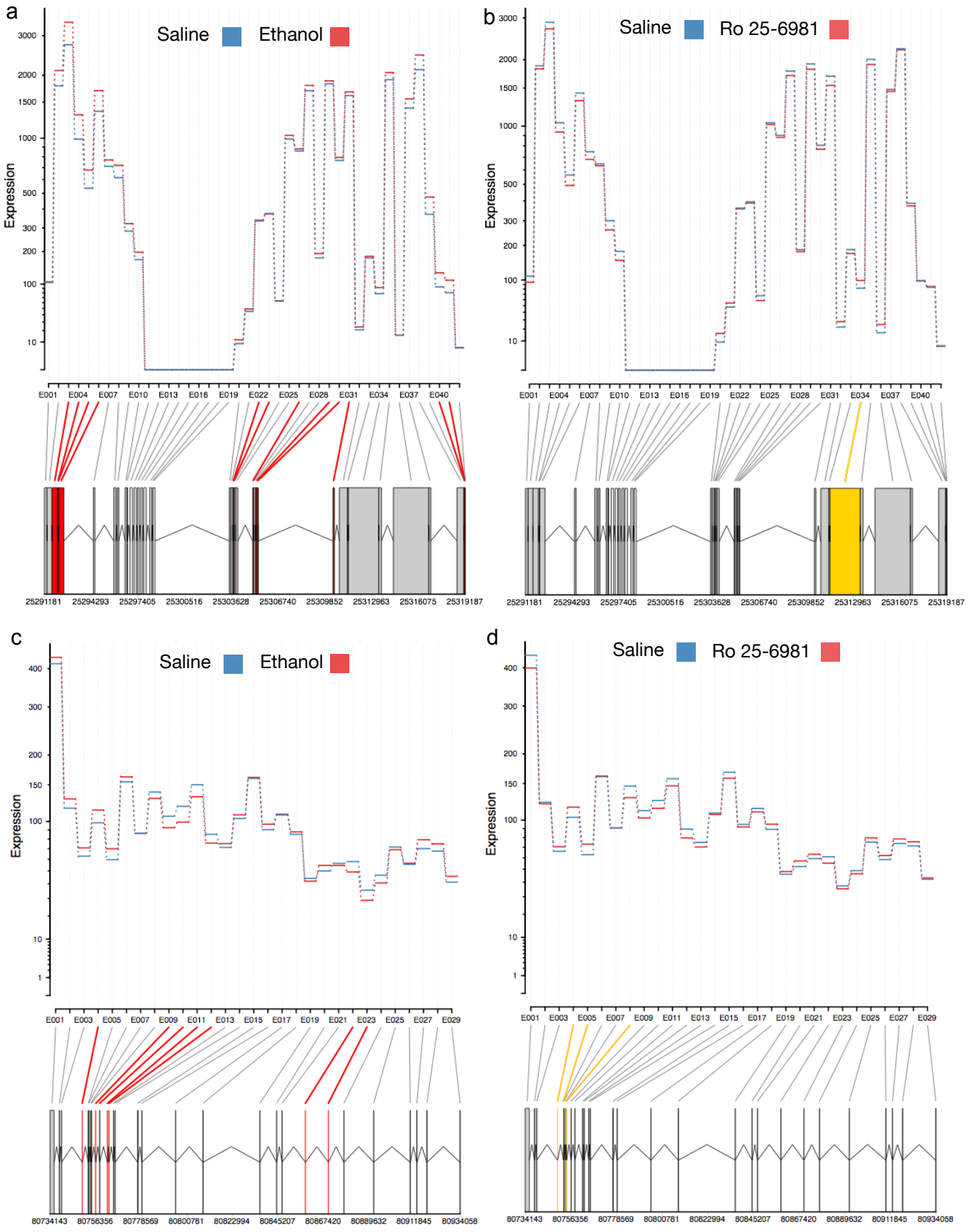
a
Saline
Ethanol
Expression
3000
2000
1500
1000
500
300
200
100
10
E001 E004 E007 E010 E013 E016 E019 E022 E025 E028 E031 E034 E037 E040
25291181 25294293 25297405 25300516 25303628 25306740 25309852 25312963 25316075 25319187
b
Saline
Ro 25-6981
Expression
3000
2000
1500
1000
500
300
200
100
10
E001 E004 E007 E010 E013 E016 E019 E022 E025 E028 E031 E034 E037 E040
25291181 25294293 25297405 25300516 25303628 25306740 25309852 25312963 25316075 25319187
c
Saline
Ethanol
Expression
400
300
200
150
100
10
1
E001 E003 E005 E007 E009 E011 E013 E015 E017 E019 E021 E023 E025 E027 E029
80734143 80756356 80778569 80800781 80822994 80845207 80867420 80889632 80911845 80934058
d
Saline
Ro 25-6981
Expression
400
300
200
150
100
10
1
E001 E003 E005 E007 E009 E011 E013 E015 E017 E019 E021 E023 E025 E027 E029
80734143 80756356 80778569 80800781 80822994 80845207 80867420 80889632 80911845 80934058

Figure 3.5. Expression of exons in NR1 and ATP9B with ethanol and Ro 25-6981 treatment

a-b) Graph represents normalized exon expression on the x-axis with exon IDs on the y-axis, and bellow the exon IDs is a NR1 transcript with corresponding gene locations labeled bellow. The dotted blue line represents vehicle (saline) while the red dotted line represents either ethanol expression or Ro 25-6981 expression. a) Red exons on the NR1 transcript indicate those significantly differentially expressed with ethanol treatment. b) Yellow exons on the NR1 transcript indicate those significantly differentially expressed with Ro 25-6981 treatment ($p \leq 0.05$). c-d) Graph represents normalized exon expression on the x-axis with exon IDs on the y-axis, and bellow the exon IDs is a ATP9B transcript with corresponding gene locations labeled bellow. The dotted blue line represents vehicle (saline) while the red dotted line represents either ethanol expression or Ro 25-6981 expression. a) Red exons on the ATP9B transcript indicate those significantly differentially expressed with ethanol treatment. b) Yellow exons on the ATP9B transcript indicate those significantly differentially expressed with Ro 25-6981 treatment ($p \leq 0.05$).

Discussion

NMDAR antagonists have gained acceptance as rapid acting antidepressants. Their fast acting and long lasting effects are due in part to alterations in synaptic plasticity and synaptic protein composition[70, 74, 78]. Alcohol induces similar antidepressant-like effects in behavioral tests for antidepressant efficacy and induced synaptic signaling pathways that could lead to plasticity[79]. Continued alcohol abuse may induce neuroadaptive changes to counteract these initial effects, and the self-medication hypothesis suggests that the initial antidepressant effects of alcohol will shift to depressant allostatic states with continued abuse leading to addiction[101]. Despite the high comorbidity of AUD and

MDD[14], the underlying mechanism for the dual development of these disorders is relatively unknown. In this study we investigated the synaptic transcriptome, hypothesizing that parallel alterations in synaptic gene expression would occur with acute ethanol and rapid antidepressant treatment.

We identified differential gene expression shared by ethanol and Ro 25-6981 treatments, but found that many transcriptional changes are distinct within the two treatments. We discovered that ethanol induced gene expression changes are largely independent of acute NR2B inhibition, emphasizing the important of investigating novel targets. We also predict that the dissimilarities observed between ethanol and Ro 25-6981 may be due to the potent and selective nature of Ro 25-6981 or the time point that we chose. Ethanol may induce greater and more pronounced gene expression changes with increased treatment time, as chronic ethanol consumption is known to produce more changes in gene expression in synaptoneurosomes than we found here[197]. More similarities between ethanol and Ro 25-6981 may also be observed with longer treatment times. One hypothesis to explain this phenomena is that altering the abundance of splice variants at the synapse, through either localization of previously transcribed RNAs or alternative splicing of *de novo* transcripts generated from transcriptionally active genes, may occur more rapidly than reprogramming of transcriptional routines to alter the steady state levels of different transcripts apparent in chronic AUD.

Our data suggest that isoform differences may be a key player in the inducing the molecular and behavior changes observed with acute ethanol and rapid antidepressant treatments. Ethanol and Ro 25-6981 share similarities in exon use patterns with acute treatment and display differential exon expression in genes identified in AUD and MDD. Altered exon usage suggests differences in splicing, isoforms, and subsequently protein sequences and function[177]. Although we observed limited overlap in gene expression between ethanol and Ro 25-6981 treatments, the abundant similarities in exon usage and genes containing DEEs suggests that shared alterations in protein function occur with both treatments. These co-occurring changes observed at 30 minutes might contribute to changes in synaptic function following induction of translation and activity of these new proteins, and be important for the initial antidepressant activity of ethanol. We highlighted two proteins where this might occur, NMDAR and ATP9B. NR1 acute expression displays increases in exon patterns thought to be involved in NMDAR function. ATP9B exon specific splicing is less well understood, but it is interesting that Ro 25-6981 increases some exons whereas MDD decreases others, identifying alternative splicing as an important avenue of research for the treatment of MDD or AUD.

Although we did not observe many parallel changes in gene expression, perhaps the DEGs we did discover had important protein interactions. We further assessed the 50 shared DEGs found with ethanol and Ro 25-6981 by comparing our gene expression results with key genes identified among our genes with

DEEs (NMDAR1, $GABA_BR1$, $GABA_AR5$, ATP9B, and EIF3K) and found many protein-protein interactions important to predominant genes and pathways in the fields (Fig. 3.6). By using a protein network approach, we found that our DEGs (displayed in color) are related to key genes known to be important to AUD or MDD (displayed in red), and secondary interacting proteins (grey). DEGs that are highly connected may be important for downstream changes in other proteins with treatment, such as Rhob[198] involved in GTP binding and GPCR signaling, and Dlg a scaffolding protein related to ion channel binding[71]. This network contains proteins involved in AUD and MDD as well as not well-characterized proteins. Even though few genes were similarly expressed with ethanol and Ro 25-6981, many interact with key proteins and pathways of interest. This opens new avenues for exploring these targets with ethanol and/or rapid antidepressants.

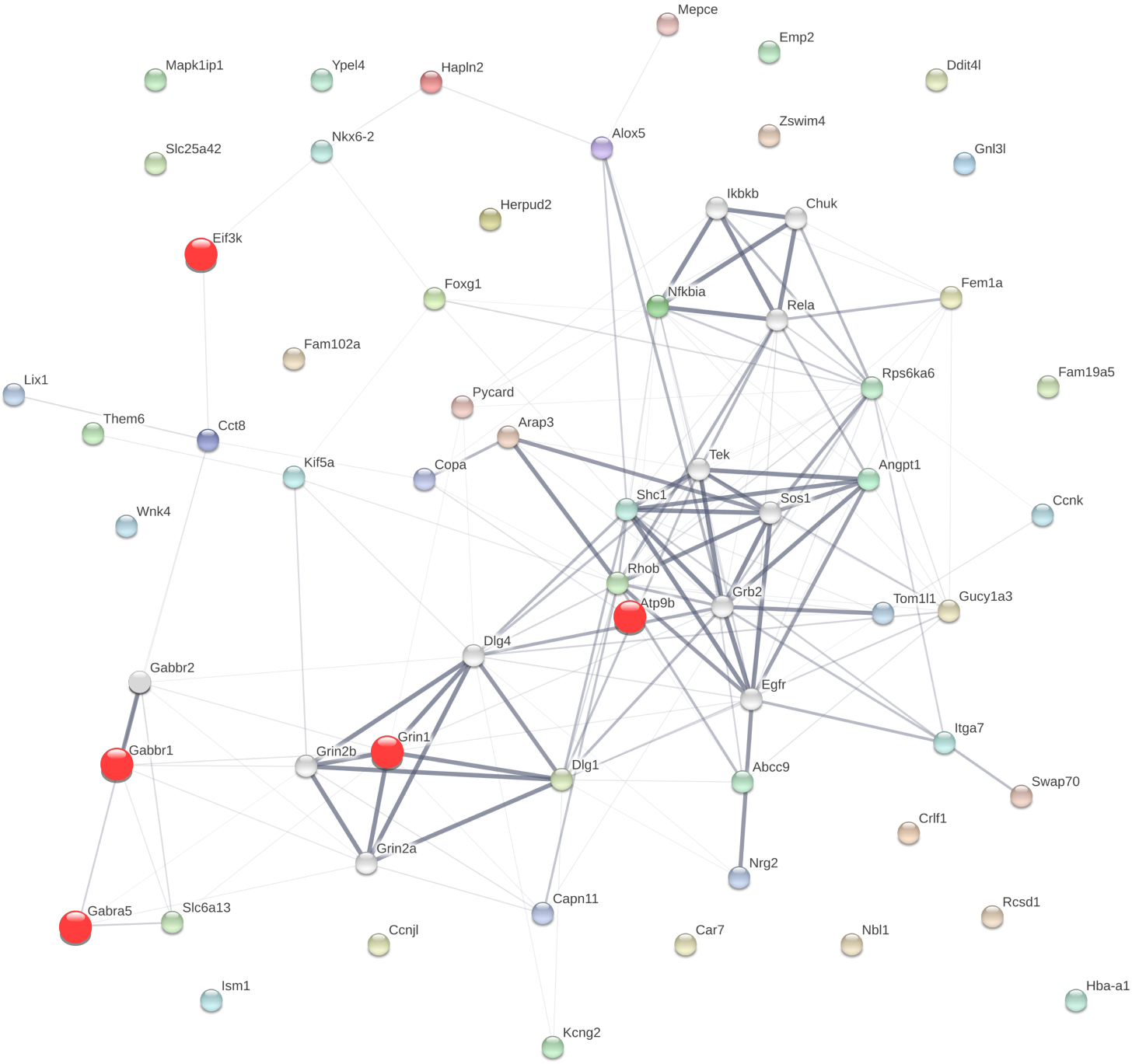

Figure 3.6. Protein interaction network of DEGs and proteins of interest

This protein interaction network is of the 50 simultaneously regulated DEGs between ethanol and Ro 25-6981 acute treatment. This network generated using String (version10.0) depicts the possible interactions of the 50 co-occurring

differentially expressed genes in addition to five proteins of interest important to AUD and MDD and found within the genes containing DEEs shown in red (Eif3k, Atp9b, Gabbr1, Grin1, and Gabra5). The 50 genes are shown in color while secondary shell interacting proteins are shown in grey. These secondary proteins may indicate pathways or interacting proteins of interest related to the DEGs we identified. Line thickness indicates the strength of data to support the interaction.

Overall this work implicates alternative splicing as an important mechanism for altering synaptic function with acute treatment of alcohol or rapid antidepressants. Parallel alterations in exon use were identified with ethanol and Ro 25-6981 treatment. This altered exon use likely contributes to the mechanism of Ro 25-6981 and other NMDAR antagonists providing important context for their biological and pharmacological implications. Some of these changes coincide with evidence of alternative splicing in human AUD and MDD. By examining different isoforms it may be possible to discover other targets to investigate underlying changes associated with the high comorbidity of AUD and MDD.

CHAPTER 4: DISCUSSION

The comorbidity between alcohol and psychiatric disorders is astounding[14, 36]; however very little is known about the molecular basis for this co-occurrence. This novel study identified that acute alcohol exposure elicits an antidepressant-like behavior that can persist up to 24 hours after exposure, suggesting that

ethanol can initiate a lasting antidepressant response. Furthermore we found that ethanol has a shared molecular pathway with rapid antidepressant that may explain these phenomena. Rapid antidepressant and ethanol inhibit NMDAR[52, 58, 128, 175] activity and induce two key molecular changes that produce the observed antidepressant response, including (1) an increase in $GABA_BR$ protein synthesis and (2) a shift in $GABA_BR$ function that increases dendritic calcium signaling[13, 78, 79]. Additionally, we identified FMRP as a key regulator of the induced protein synthesis of $GABA_BR$ upon acute RAAD and ethanol exposure[79]. Next we expanded our study by using RNA sequencing to identify synaptic changes on a more global scale that may be related to our pathway of interest. We identified a few select genes that displayed parallel expression changes with both acute ethanol and Ro 25-6981, suggesting that many acute ethanol changes are independent of NR2B inhibition. However, our findings suggested that exon use and alternative splicing may have a greater impact on the transcriptome with alcohol and RAAD exposure rather than differential gene expression.

Based on our data we proposed a mechanism from transcription to translation that could occur with acute ethanol and RAAD exposure. We envision two waves of translation occurring upon ethanol or RAAD exposure. The first wave would initiate translation of synaptic mRNAs already present at the synapse[81, 82]. These mRNAs would include those involved in the initiation of synaptic signaling and translation such as the $GABA_BR2$[13, 79] and mTOR[61, 74]. The second wave of translation would initiate protein translation of those

differentially expressed genes and exons identified with acute ethanol and Ro 25-6981 exposure. These possible alternatively spliced transcripts may be translated, have non-canonical function or localization, and affect synaptic function. Further research is needed to identify the nature of these changes.

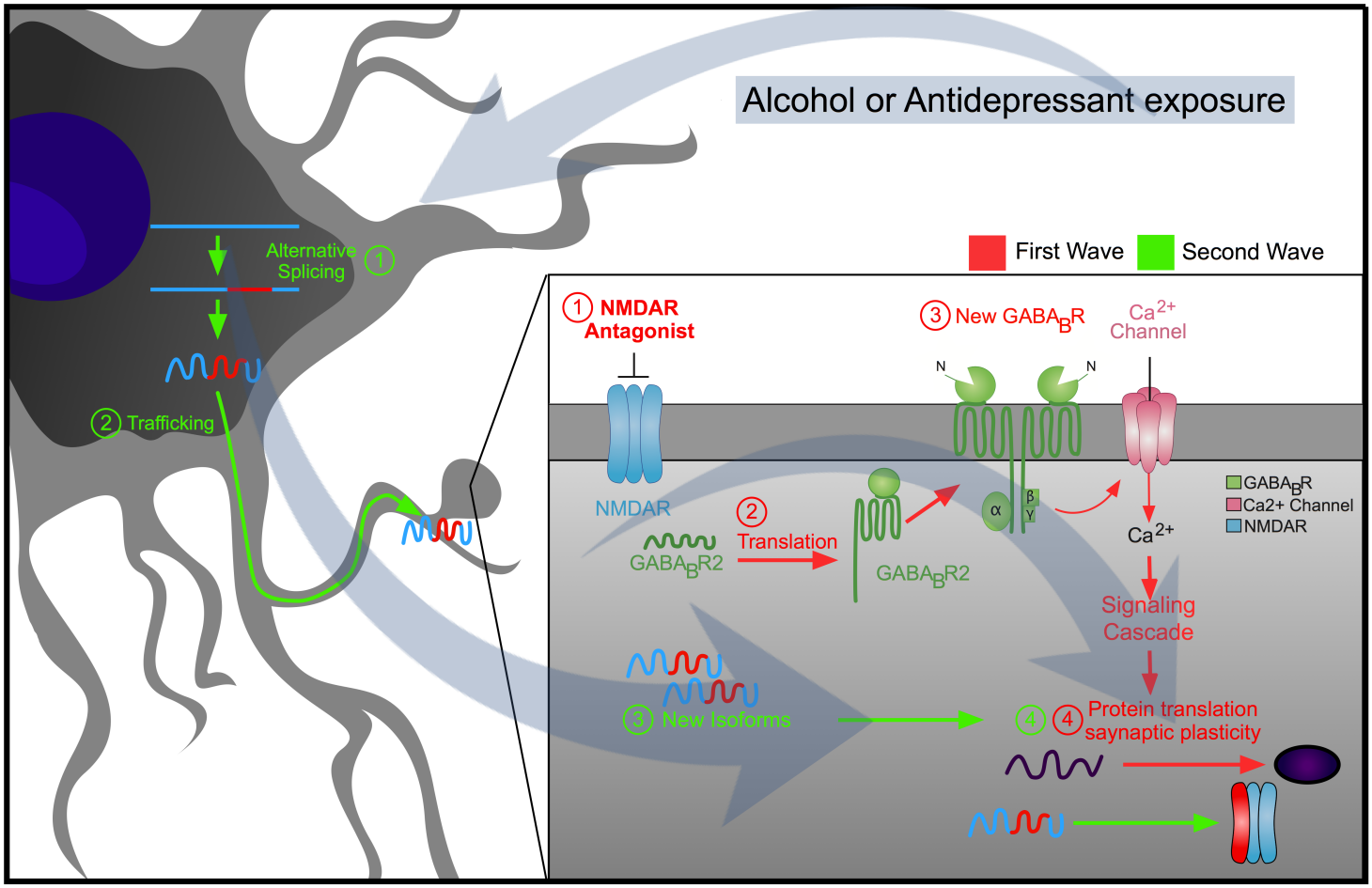

Figure 4.1. Proposed model for the shared acute actions of ethanol and Ro 25-6981

Arrows in red represent data from chapter 2 in which NMDAR inhibition induces release of FMRP binding allowing translation of GABA$_B$R2 and new GABA$_B$Rs

facilitate calcium entry and signaling to activate protein translation. Arrows in green represent data from chapter 3 in which NMDAR inhibition triggers alternative splicing/exon usage which leads to new translation of these new splice variants. Both these pathway lead to translation of alternative proteins and induction of synaptic plasticity.

Limitations

Some limitations of our study exist that could be addressed in the future. One is that we only explored pathways in the hippocampus. We focused on alterations in the hippocampus due to previous studies of ethanol and antidepressants affecting this brain region in both humans and animals[60, 113, 95]. Additionally, our previous work identified molecular mechanisms induced by Ro 25-6981 as well as other NMDAR inhibitors in the hippocampus[79]. However, it would be interesting to identify if this pathway is conserved between brain regions. We would also like to ask if other NMDAR antagonist such as Ketamine have the same effect as Ro 25-6981. We chose Ro 25-6981 for it's highly selective and potent inhibition of the NR2B subunit of the NMDAR[31, 32], as opposed to other rapid antidepressants that have adverse side effects[27], or alternative convoluting mechanisms of action[175]. However, disadvantages to using Ro 25-6981 are that it is not FDA approved and further away from being a pharmaceutical treatment option. We also limited our experiments to an acute time point for feasibility, but extending our findings from acute to chronic and withdrawal would give further insight into the development of the initial use of alcohol to lasting chronic use and addiction.

Future Direction

Several avenues of interest emerge from this research for future studies including neuroadaptive changes with chronic and withdrawal alcohol use, further characterization of the antidepressant effects of alcohol, and continued exploration of splice patterning in AUD and MDD.

Future directions will test the hypothesis that regulation of $GABA_BR$ function will contribute to dendritic neuroadaptation from acute to chronic and withdrawal ethanol states. Preliminary results suggest that dendritic $GABA_BR$ expression decreases with chronic exposure, and increases with ethanol withdrawal. We propose that $GABA_BR$ signaling is differentially regulated with acute, chronic, and withdrawal ethanol to regulate protein translation and synaptic protein composition; causing or counteracting neuroadaptations that occur with ethanol[62, 94]. Downstream changes in synaptic protein composition and synaptic plasticity induced by activation of this antidepressant pathway[13, 78, 79] would be interesting to explore at chronic and withdrawal states of antidepressant and ethanol use. This data would further our understanding of the mechanisms of this pathway and the behaviors they provoke. Further research on mechanisms of comorbidity may reveal new targets for the development of comorbid treatments, and eventually aid in development of much needed therapeutic options for individuals with dual diagnosis.

One immediate question that comes to rise is how does one dose of ethanol or RAAD induce the lasting antidepressant like effect we observed, and how long does that effect last. Studies with the rapid antidepressant Ketamine have varying results, but identified Ketamine as eliciting an antidepressant effect for up to a week in behavioral test for antidepressant efficacy[70, 71, 199]. The mechanism for action for this lasting effect of Ketamine are still under scrutiny, but focus on a cascade of neurochemical events initiated immediately after treatment[26]. It would be of interest to expand our shared molecular changes by first interrogating these potential neurochemical events since Ketamine, ethanol, and Ro 25-6981 all induce changes via NMDAR inhibition. We could predict that Ketamine changes such as activation of mTOR dependent pathways[74] and BDNF[73] would be conserved with acute treatment of ethanol and Ro 25-6981, and may increase our understanding of the actions of Ketamine as well. Additionally, we would like to see if ethanol and/or Ro 25-6981 elicit an antidepressant like response for up to a week, and the time of onset of the antidepressant effects. This will further characterize the self-medication effect, by identifying if more alcohol administration is needed to maintain an antidepressant like response. This progressive increase in alcohol consumption may lead to increased alcohol abuse and dependence[101].

Numerous targets for further exploration are present in our RNA-seq data for ethanol, antidepressant, or shared molecular changes. Here we took a particular interest in NMDAR1 and ATP9B exon usage and their implications for

protein and synaptic function, but other targets such as $GABA_BR1$, $GABA_AR$, and EIF3K and numerous others of interest to the field. Additionally, novel targets of interest can be identified for further exploration. It will be important to identify if altered exon use and thus splicing occurs in protein domains that will affect their function or localization and/or cellular function[200]. An immediate next step is to verify that these proposed spliceforms are translated, when they are translated, and if their respective alteration in expression is lasting. Translation and function of these isoforms may play a role in the lasting antidepressant effects of ethanol and Ro 25-6981. We did identify differentially expressed exons in genes previously shown to be involved in AUD and MDD. Pairing our results with an animal model of depression may be revealing. By exploring similarities and differences in an animal model of depression with and without ethanol or Ro 25-6981 expression we may find increasing evidence of splice variants and their role in AUD and MDD.

Conclusion

AUD and MDD are two devastating and complex disorders, and have been closely linked through epidemiological and clinical studies[14, 36]. but the high rate of comorbidity is not well understood. These results indicate that an underlying mechanism may increase the likelihood of developing comorbid AUD and MDD, and possibly other psychiatric disorders and substance abuse disorders. Further research is need to identify the extent of the molecular changes that we observed with ethanol and Ro 25-6981, and how downstream changes induced by this

pathway affect synaptic plasticity, neuroadaptation, and behavior. Additionally it will be imperative to assess the effects of alternative splicing with acute alcohol and RAADs. Specifically, do the splice events we identified acutely lead to neuroadaptation, produce lasting alterations in synaptic protein composition, or alter functions at the synapse and thus behavior? Other shared molecular changes may also exist between RAADs and ethanol that may further our understanding of comorbidity. Our research implicates several pathways and genes of interest for further investigation, including those targetable for potential therapeutic avenues.

SUPPLEMENTARY FIGURES

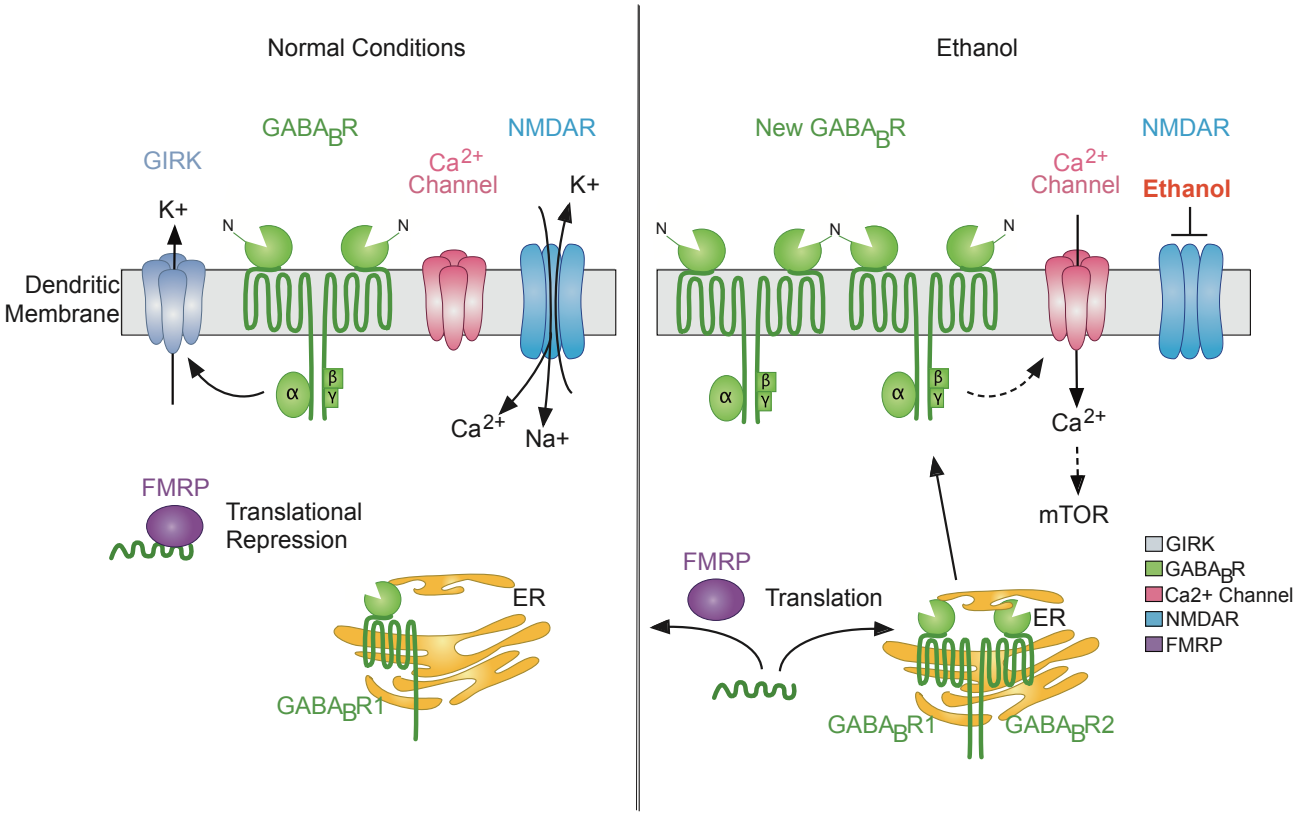

Supplemental Figure 2.1. Working model of ethanol-induced GABA$_B$R plasticity

Under normal conditions (on left) FMRP represses translation of target mRNA (e.g., GABA$_B$R2), and GABA$_B$R signaling is inhibitory via activation of G-protein inwardly rectifying potassium channels (Kir3/GIRK) in dendrites. Ethanol exposure (on right) inhibits NMDARs, causing FMRP to release GABA$_B$R2 mRNA, allowing for its translation. Newly synthesized GABA$_B$R2 assembles as a functional heterodimer with GABA$_B$R1 and is transported to the dendritic membrane. Upon activation, new surface GABA$_B$Rs facilitate calcium channel activity and may activate mTOR.

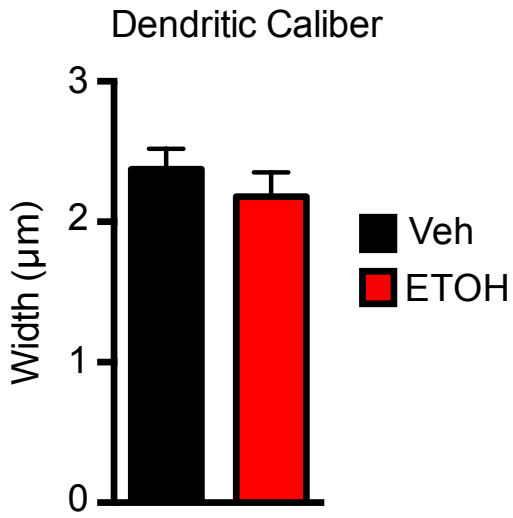

Supplemental Figure 2.2. Dendritic caliber is unaffected by acute ethanol

a) The width of cultured hippocampal dendrites proximal to the soma was measured using ImageJ software, and no significant changes in dendrite caliber were observed. Veh=2.38 ± 0.14 µm, n=28 dendrites; ETOH=2.18 ± 0.17 µm, n=38 dendrites; values represent mean ± SEM.

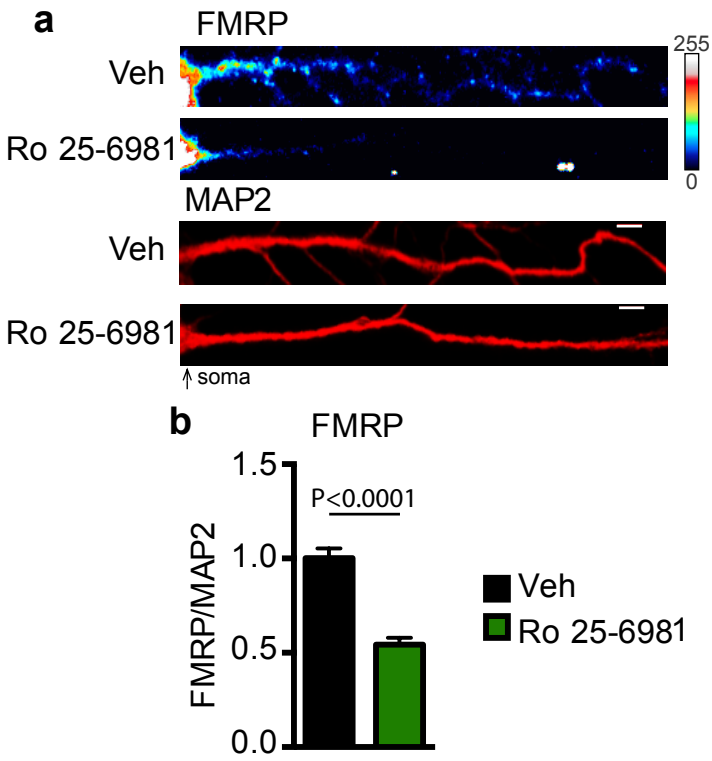

Supplemental Figure 2.3. Ro 25-6981 reduces dendritic expression of FMRP

(a) Representative immunofluorescent images and (b) summary graph of dendrites from cultured hippocampal neurons treated with Ro 25-6981 (10 μM, 2 hours) showing decreased dendritic FMRP expression (0.54 ± 0.04, n=40 dendrites) compared to vehicle (Veh)-treated neurons (H_2O, 2 hours; 1.00 ± 0.05, n=49 dendrites) normalized to MAP2. Significance determined by Student's t-test. Values represent mean ± SEM. Scale bar=5 μm.

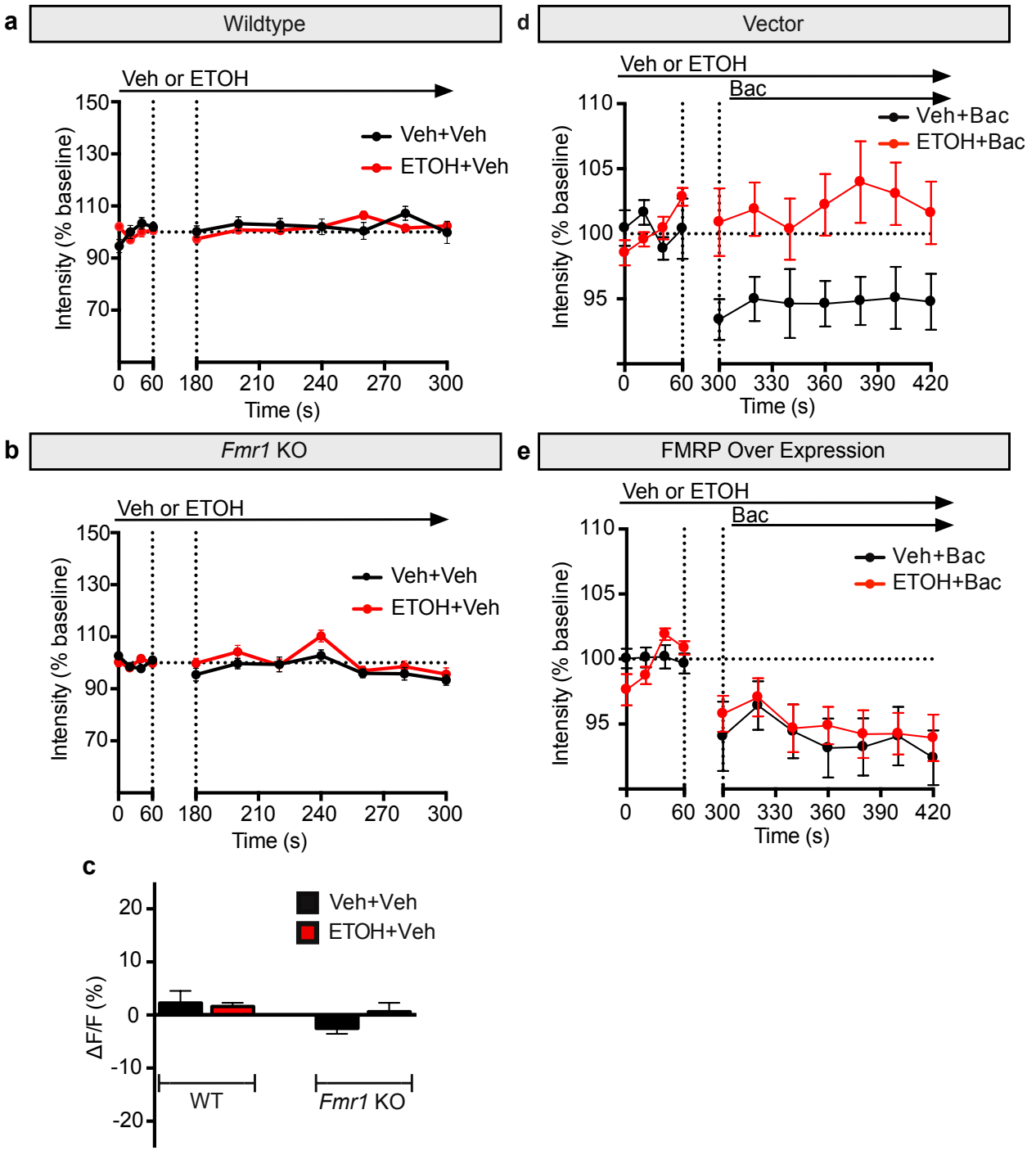

Supplemental Figure 2.4. Excess FMRP represses ethanol-induced $GABA_BR$ plasticity

(a-c) Mouse hippocampal cultured neurons were pretreated for 2 hours with vehicle (Veh: H_2O) or ethanol (ETOH: 30 mM). Line graphs represent the average fluorescent calcium signal over time in dendrites from (a) wildtype and (b) *Fmr1* KO mice. Baseline was established for 1 minute before the addition of vehicle and equilibrated as indicated by the break between dotted lines. (c) Summary graph shows that calcium remains at baseline in dendrites imaged (ΔF/F) in wildtype (WT) and *Fmr1* KO neurons treated with vehicle or ethanol. WT: Veh+Veh=2.25 ± 2.29, n=14; ETOH+Veh=1.60 ± 0.71, n=24. *Fmr1* KO : Veh+Veh=-2.50 ± 1.05, n=12; ETOH+Veh=0.64 ± 1.68, n=12. Related to Figure 7a-c. (d-e) Dendritic calcium imaging in hippocampal cultured neurons infected with vector (rAAV:mSYN-tdTomato) or showing FMRP overexpression (rAAV:mSYN-FMRP and rAAV:mSYN-tdTomato). Line graph illustrates the average fluorescent calcium signal in (d) vector and (e) FMPR overexpressing neurons pre-treated for 2 hours with vehicle or ethanol. Ethanol-induced increase in dendritic calcium is blocked by FMRP overexpression. Related to Figure 7d. Significance determined by two-way ANOVA and Tukey's multiple comparison test. Values represent mean ± SEM.

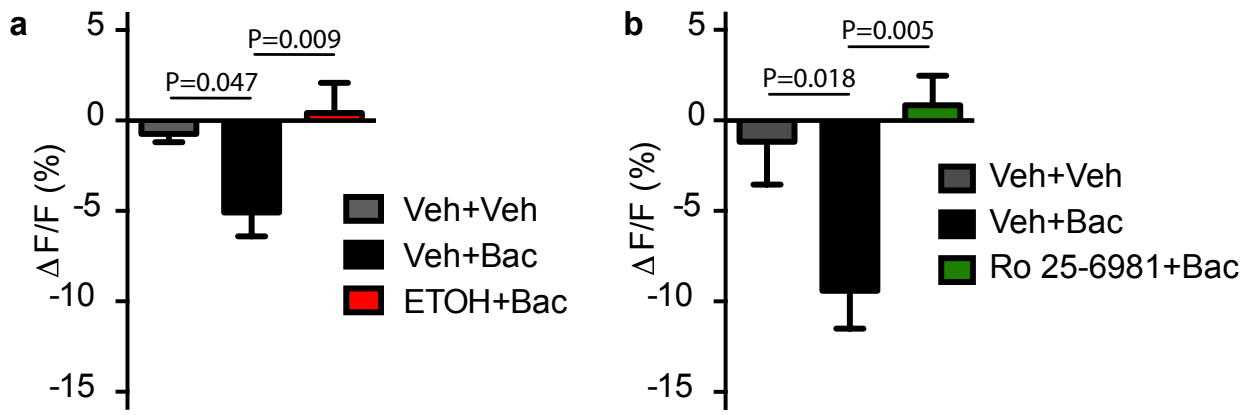

Supplemental Figure 2.5. $GABA_BR$ elevates dendritic Ca^{2+} with ethanol and Ro 25-6981

Calcium imaging in dendrites from rat hippocampal neurons. (a) Summary graph of ΔF/F of dendritic calcium in vehicle- (Veh: H_2O) and ethanol- (ETOH: 30 mM) treated neurons for 2 hours with the addition of vehicle or baclofen (Bac, 50 μM). ΔF/F between vehicle and ethanol do not significantly change relative to baseline. Baclofen decreases dendritic calcium in vehicle-treated neurons but not in ethanol-treated neurons. Veh+Veh=- 0.007 ± 0.004, n=11; Veh+Bac=-0.05 ± 0.01, n=11; ETOH+Bac=0.004 ± 0.02, n=12. Significance determined by one-way ANOVA with Dunnett's multiple comparison test. Values represent mean ± SEM. (b) Summary graph of dendritic calcium in neurons pre-treated with either vehicle (Veh: H2O, 2 hours) or Ro 25-6981 (Ro; 10 μM, 2 hours) in the presence of vehicle or baclofen (Bac, 50 μM). Baclofen reduces the calcium signal in vehicle-treated neurons but produces no significant change over baseline in the Ro 25-6981-treated neurons. Veh+Veh=-0.01 ± 0.02, n=10; Veh+Bac=-0.09 ± 0.02, n=9; Ro 25-698+Bac=0.01 ± 0.02, n=8. Significance determined by one-way ANOVA and Dunnett's multiple comparison test. Values represent mean ± SEM.

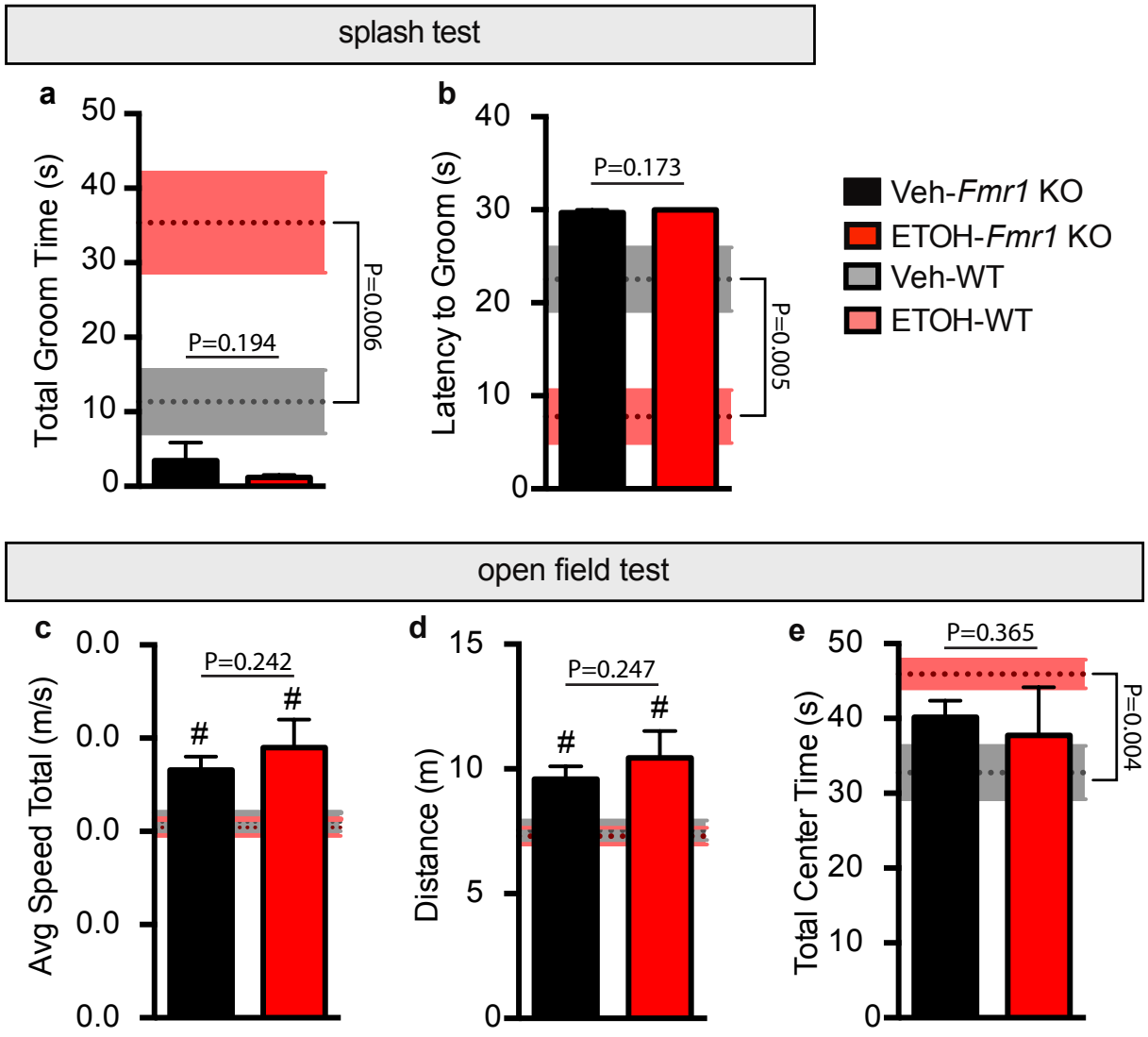

Supplemental Figure 2.6. Ethanol's antidepressant effect is absent in *Fmr1* KO

Fmr1 KO mice subjected to the splash test displayed no behavioral differences in (a) groom time or (b) latency to initiate grooming 24 hours post-ethanol (ETOH: 2.5 g kg^{-1}, i.p.) compared to vehicle (Veh; saline, i.p.) treatment. Data from wildtype (WT) C57BL/6 mice from Fig. 1b and c are shown as the mean (horizontal dotted lines) ± SEM (horizontal shaded area in v=Veh=grey or ETOH=pink). Data for *Fmr1* KO as indicated in bar graph (Veh=black or ETOH=red): Total groom time: Veh=3.44 ± 2.43 s, n=5; ETOH=1.20 ± 0.32 s, n=5. Latency to groom: Veh=297.0 ± 3.05 s, n=5; ETOH=300 ± 0.0 s, n=5. (c-e) Total center time, speed, and distance were measured in the open field test 24 hours post-injection in *Fmr1* KO mice. Ethanol-treated (2.5 g kg^{-1}, i.p.) *Fmr1* KO mice lacked the ethanol-induced increase in center time seen in WT mice (data

taken from Fig. 1b and c). Speed and distance traveled of *Fmr1* KO mice were unaffected by ethanol treatment, but both measures were increased compared to WT due to hyperexcitability in *Fmr1* KO mice. Total center time: Veh=401.6 ± 22.01 s, n=6; ETOH=377.4 ± 64.24 s, n=6. Average speed: Veh=0.05 ± 0.003 m/s, n=6; ETOH=0.06 ± 0.006 m/s, n=6. Total distance: Veh=95.89 ± 5.24 m, n=6; ETOH=104.4 ± 10.79 m, n=6. Significance determined by one-tailed t-test. Significance between genotypes designated by #. Average speed total: WT-Veh vs. KO-Veh P=0.006, WT-ETOH vs. KO-ETOH P=0.010. Distance: WT-Veh vs. KO-Veh P=0.005, WT-ETOH vs. KO-ETOH P=0.009. Values represent mean ± SEM.

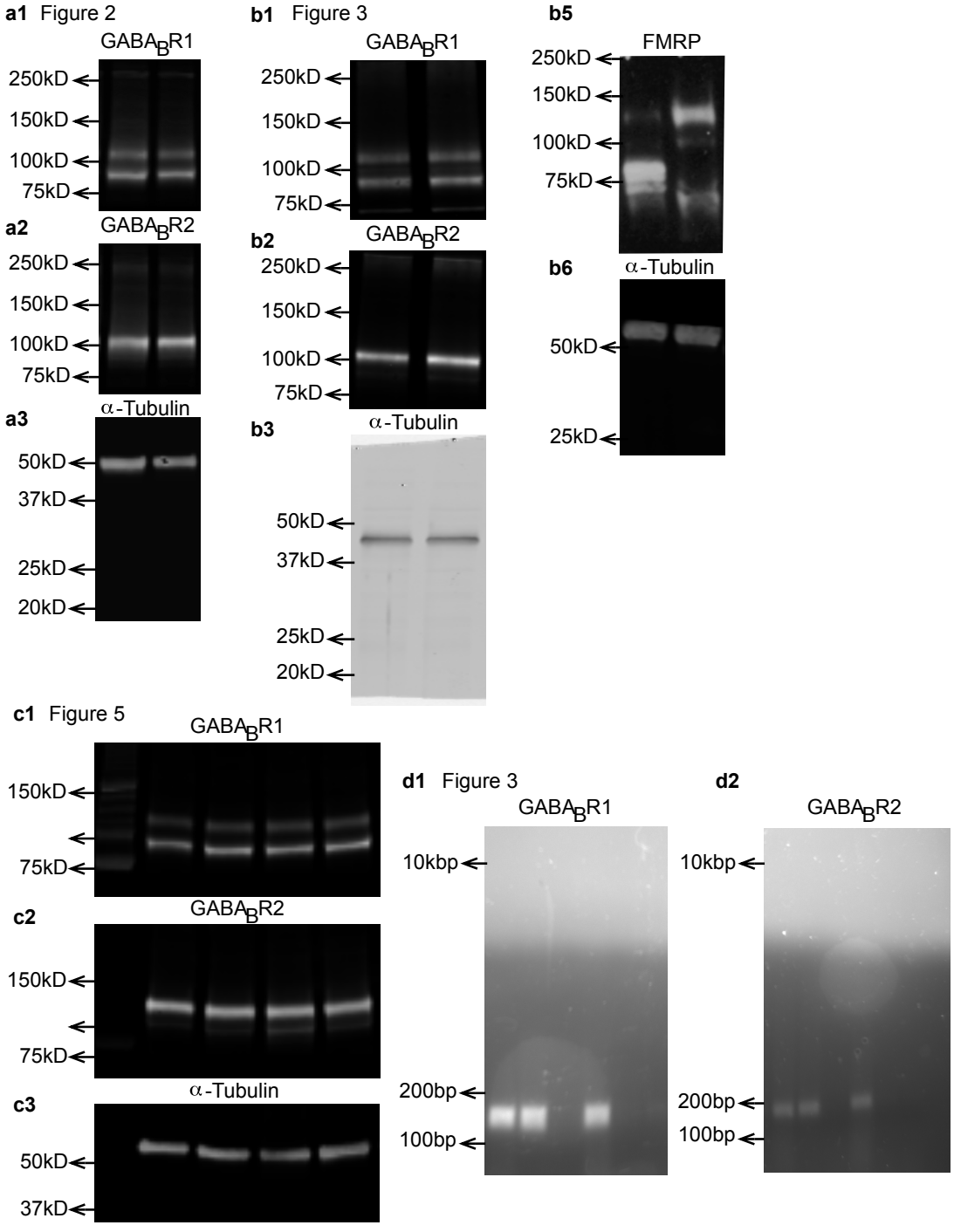

Supplemental Figure 2.7. Full uncropped images for representative blots

Full Western blots for all representative images are shown. Blots were cut to optimize staining. (a) Western blot for (a1) GABA$_B$R1, (a2) GABA$_B$R2, and

corresponding (a3) α-Tubulin are shown for Figure 2. (a1-3) Blot was probed for (a1) rabbit anti-$GABA_BR1$ and (a2) mouse anti-$GABA_BR2$ simultaneously and imaged with Licor Odyssey imaging system. Prior to Western blot membrane was cut just below 75kD and probed for (a3) α-Tubulin. (b) Western blot of (b1) $GABA_BR1$, (b2) $GABA_BR2$, and corresponding (b3) α-Tubulin; and (b5) FMRP and corresponding (b4) α-Tubulin are shown for Figure 3. (b1-3) Blot was probed for (b1) rabbit anti-$GABA_BR1$ and (b2) mouse anti-$GABA_BR2$ simultaneously and was cut just below 75kD and probed for (b3) α-Tubulin. (b5-6) Western blot was probed for (b5) FMRP and cut and probed below 75kD for (b6) α-Tubulin. (c) Western blot for $GABA_BR1$, $GABA_BR2$, and corresponding α-Tubulin in WT and *Fmr1* KO mice are shown for Figure 5. (c1-3) Blot was probed for (c1) rabbit anti-$GABA_BR1$ and (c2) mouse anti-$GABA_BR2$ simultaneously and was cut just below 75kD and probed for (c3) α-Tubulin. Molecular weight marker is shown to the left of all images. (d1-2) Full representative gels showing RT-qPCR amplified product of input sample, FMRP RIP, and IgG control are shown for (d1) $GABA_BR1$ and (d2) $GABA_BR2$.

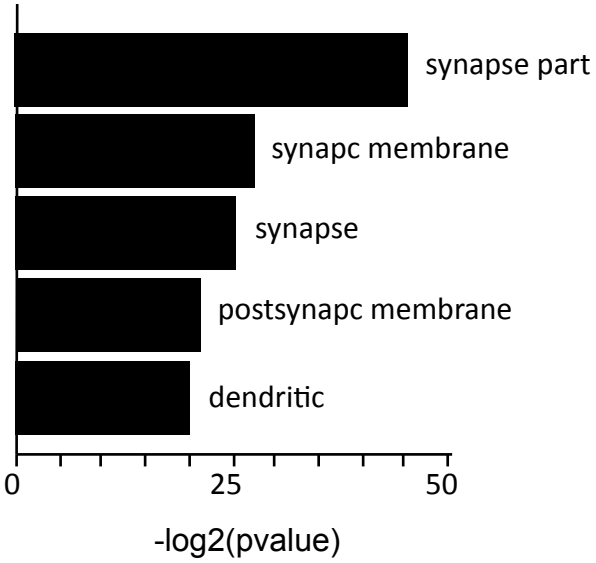

Supplemental Figure 3.1. Synaptoneurosomal enrichment analysis

The top 500 most abundant genes identified from the average normalized counts of RNA sequenced from saline (n=8) treated C57Bl/6 mice were analyzed for synaptic enrichment as a control for synaptoneurosome isolation. Cellular component gene ontologies for these 500 most abundant genes were identified with Enrichr gene enrichment analysis tool. The 5 most significant ontologies determined by p value are shown in the summary bar graphs, all are synaptic related.

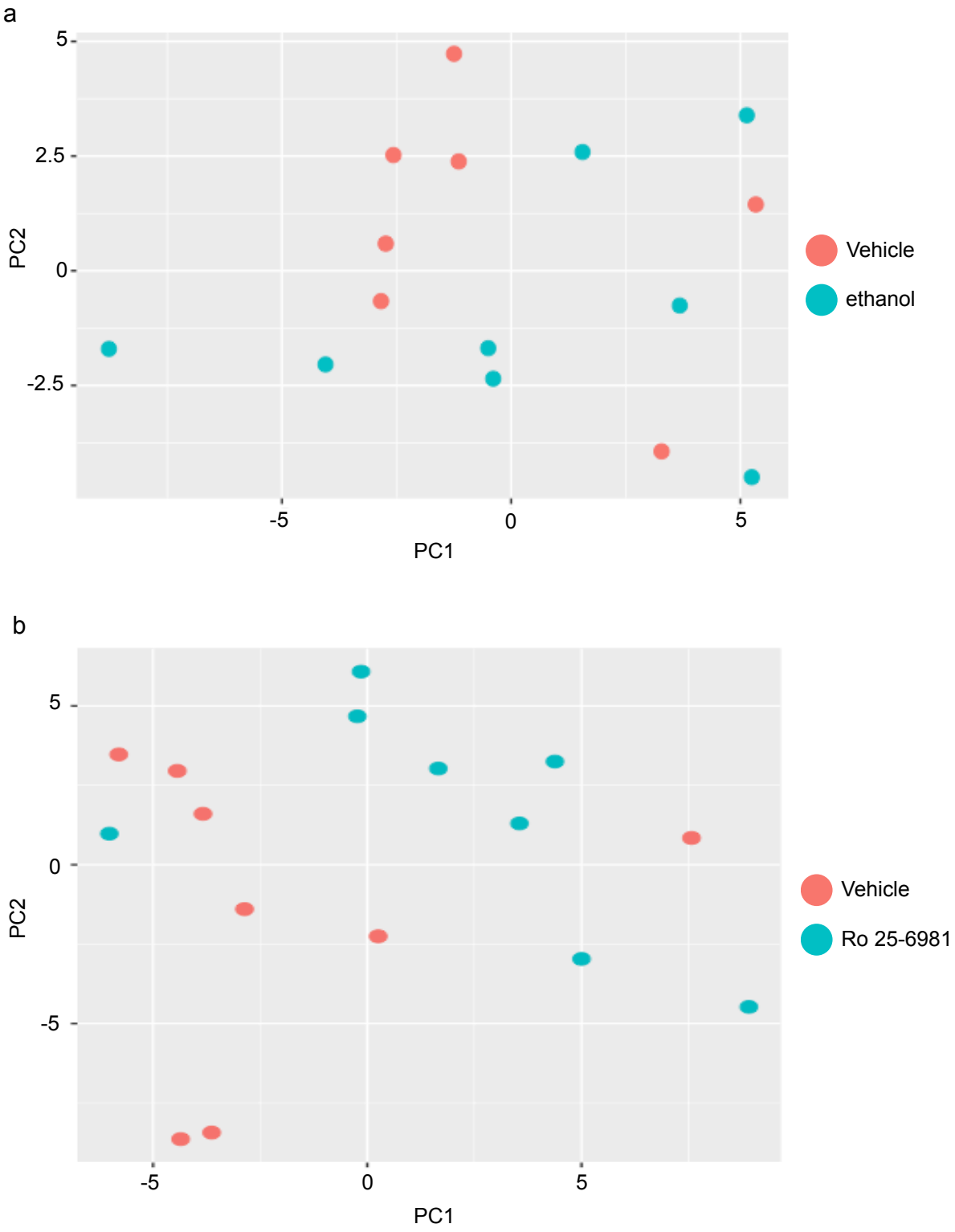
a
5
2.5
0
-2.5
PC2
-5
0
5
PC1
Vehicle
ethanol
b
5
0
-5
PC2
-5
0
5
PC1
Vehicle
Ro 25-6981

Supplemental Figure 3.2. Principle component analysis (PCA) of saline, ethanol and Ro 25-6981

a) PCA for vehicle (saline; blue, n=8) and ethanol (red, n=7) treatment shows no batch effect differences or outliers between samples. b) PCA for vehicle (saline; blue, n-8) and Ro 25-6981 (red, n=8) treatment shows now batch effect differences or outliers between samples.

a

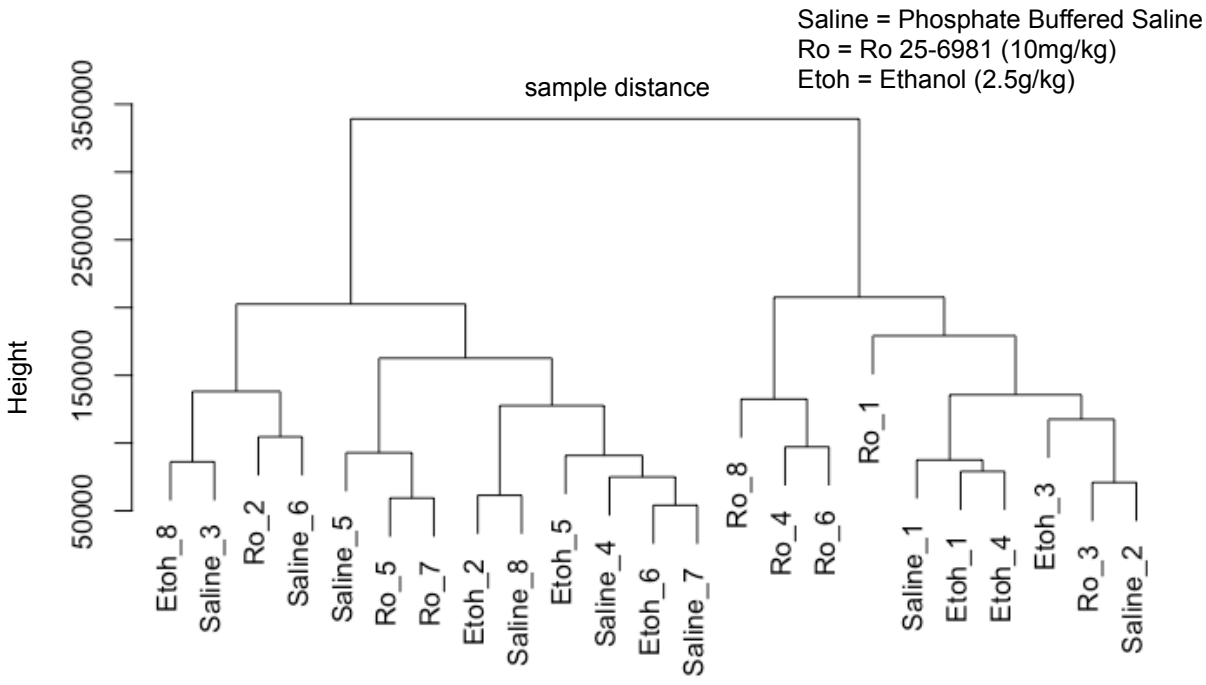
Saline = Phosphate Buffered Saline
Ro = Ro 25-6981 (10mg/kg)
Etoh = Ethanol (2.5g/kg)
sample distance
Height
350000
250000
150000
50000
Etoh_8
Saline_3
Ro_2
Saline_6
Saline_5
Ro_5
Ro_7
Etoh_2
Saline_8
Etoh_5
Saline_4
Etoh_6
Saline_7
Ro_8
Ro_4
Ro_6
Ro_1
Saline_1
Etoh_1
Etoh_4
Etoh_3
Ro_3
Saline_2

b

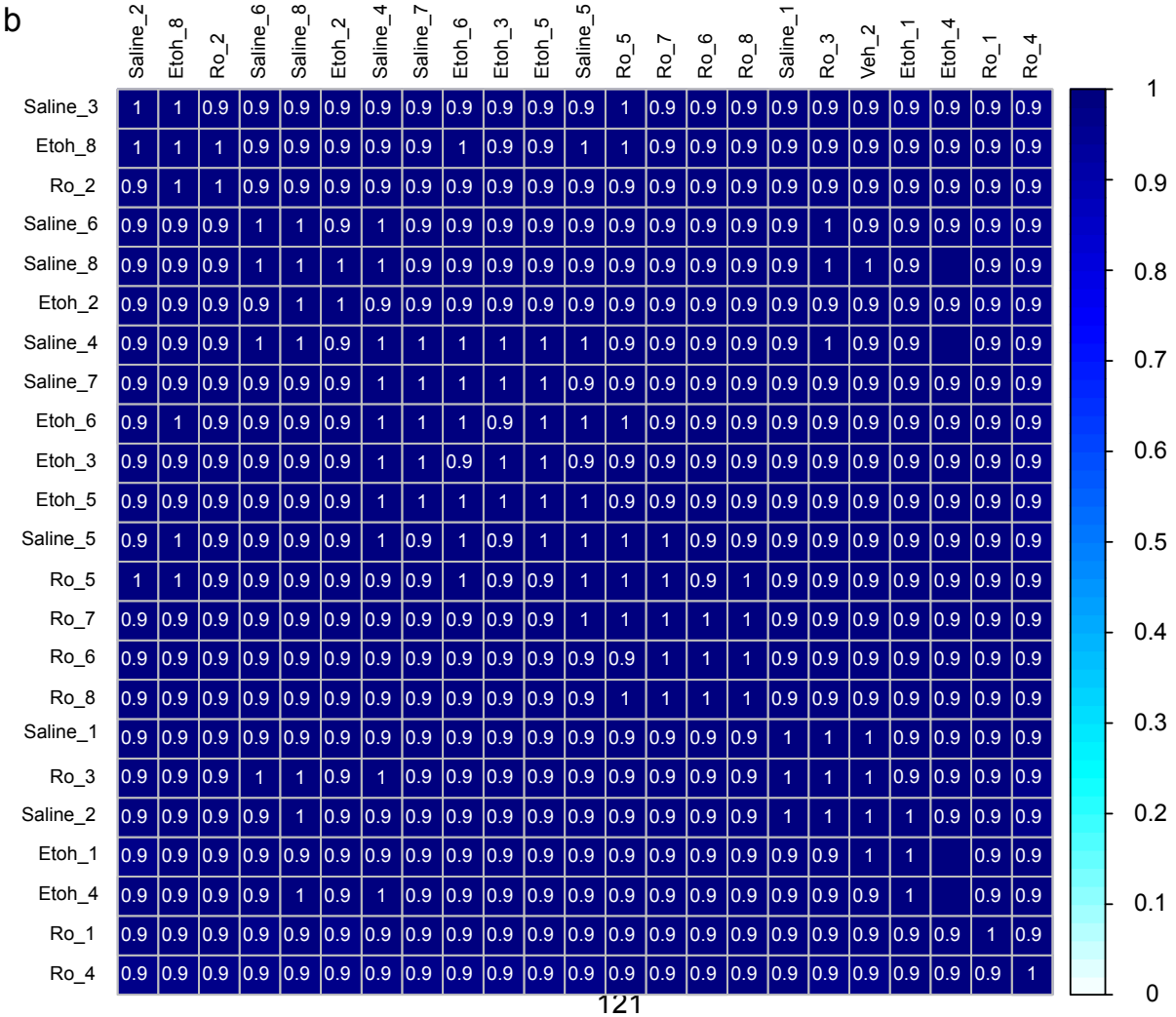
Saline_2 Etoh_8 Ro_2 Saline_6 Saline_8 Etoh_2 Saline_4 Saline_7 Etoh_6 Etoh_3 Etoh_5 Saline_5 Ro_5 Ro_7 Ro_6 Ro_8 Saline_1 Ro_3 Veh_2 Etoh_1 Etoh_4 Ro_1 Ro_4
Saline_3 1 1 0.9 0.9 0.9 0.9 0.9 0.9 0.9 0.9 0.9 0.9 1 0.9 0.9 0.9 0.9 0.9 0.9 0.9 0.9 0.9 0.9
Etoh_8 1 1 1 0.9 0.9 0.9 0.9 0.9 1 0.9 0.9 1 1 0.9 0.9 0.9 0.9 0.9 0.9 0.9 0.9 0.9 0.9
Ro_2 0.9 1 1 0.9 0.9 0.9 0.9 0.9 0.9 0.9 0.9 0.9 0.9 0.9 0.9 0.9 0.9 0.9 0.9 0.9 0.9 0.9 0.9
Saline_6 0.9 0.9 0.9 1 1 0.9 1 0.9 0.9 0.9 0.9 0.9 0.9 0.9 0.9 0.9 0.9 1 0.9 0.9 0.9 0.9 0.9
Saline_8 0.9 0.9 0.9 1 1 1 1 0.9 0.9 0.9 0.9 0.9 0.9 0.9 0.9 0.9 0.9 1 1 0.9 0.9 0.9
Etoh_2 0.9 0.9 0.9 0.9 1 1 0.9 0.9 0.9 0.9 0.9 0.9 0.9 0.9 0.9 0.9 0.9 0.9 0.9 0.9 0.9 0.9 0.9
Saline_4 0.9 0.9 0.9 1 1 0.9 1 1 1 1 1 1 0.9 0.9 0.9 0.9 0.9 1 0.9 0.9 0.9 0.9
Saline_7 0.9 0.9 0.9 0.9 0.9 0.9 1 1 1 1 1 0.9 0.9 0.9 0.9 0.9 0.9 0.9 0.9 0.9 0.9 0.9 0.9
Etoh_6 0.9 1 0.9 0.9 0.9 0.9 1 1 1 0.9 1 1 1 0.9 0.9 0.9 0.9 0.9 0.9 0.9 0.9 0.9 0.9
Etoh_3 0.9 0.9 0.9 0.9 0.9 0.9 1 1 0.9 1 1 0.9 0.9 0.9 0.9 0.9 0.9 0.9 0.9 0.9 0.9 0.9 0.9
Etoh_5 0.9 0.9 0.9 0.9 0.9 0.9 1 1 1 1 1 1 0.9 0.9 0.9 0.9 0.9 0.9 0.9 0.9 0.9 0.9 0.9
Saline_5 0.9 1 0.9 0.9 0.9 0.9 1 0.9 1 0.9 1 1 1 1 0.9 0.9 0.9 0.9 0.9 0.9 0.9 0.9 0.9
Ro_5 1 1 0.9 0.9 0.9 0.9 0.9 0.9 1 0.9 0.9 1 1 1 0.9 1 0.9 0.9 0.9 0.9 0.9 0.9 0.9
Ro_7 0.9 0.9 0.9 0.9 0.9 0.9 0.9 0.9 0.9 0.9 0.9 1 1 1 1 1 0.9 0.9 0.9 0.9 0.9 0.9 0.9
Ro_6 0.9 0.9 0.9 0.9 0.9 0.9 0.9 0.9 0.9 0.9 0.9 0.9 0.9 1 1 1 0.9 0.9 0.9 0.9 0.9 0.9 0.9
Ro_8 0.9 0.9 0.9 0.9 0.9 0.9 0.9 0.9 0.9 0.9 0.9 0.9 1 1 1 1 0.9 0.9 0.9 0.9 0.9 0.9 0.9
Saline_1 0.9 0.9 0.9 0.9 0.9 0.9 0.9 0.9 0.9 0.9 0.9 0.9 0.9 0.9 0.9 0.9 1 1 1 0.9 0.9 0.9 0.9
Ro_3 0.9 0.9 0.9 1 1 0.9 1 0.9 0.9 0.9 0.9 0.9 0.9 0.9 0.9 0.9 1 1 1 0.9 0.9 0.9 0.9
Saline_2 0.9 0.9 0.9 0.9 1 0.9 0.9 0.9 0.9 0.9 0.9 0.9 0.9 0.9 0.9 0.9 1 1 1 1 0.9 0.9 0.9
Etoh_1 0.9 0.9 0.9 0.9 0.9 0.9 0.9 0.9 0.9 0.9 0.9 0.9 0.9 0.9 0.9 0.9 0.9 0.9 1 1 0.9 0.9
Etoh_4 0.9 0.9 0.9 0.9 1 0.9 1 0.9 0.9 0.9 0.9 0.9 0.9 0.9 0.9 0.9 0.9 0.9 0.9 1 0.9 0.9
Ro_1 0.9 0.9 0.9 0.9 0.9 0.9 0.9 0.9 0.9 0.9 0.9 0.9 0.9 0.9 0.9 0.9 0.9 0.9 0.9 0.9 1 0.9
Ro_4 0.9 0.9 0.9 0.9 0.9 0.9 0.9 0.9 0.9 0.9 0.9 0.9 0.9 0.9 0.9 0.9 0.9 0.9 0.9 0.9 0.9 1
1
0.9
0.8
0.7
0.6
0.5
0.4
0.3
0.2
0.1
0

Supplemental Figure 3.3. Hierarchical cluster and correlation plot of all samples

a) Hierarchical cluster of samples indicates that there are no outliers (saline, n=8; ethanol, n=7; Ro 25-6981, n=8). b) Correlation plot of gene count per sample indicate no outliers, number indicates correlation coefficient between samples, scale coincides with correlation coefficient from 0 (white) to 1 (blue).

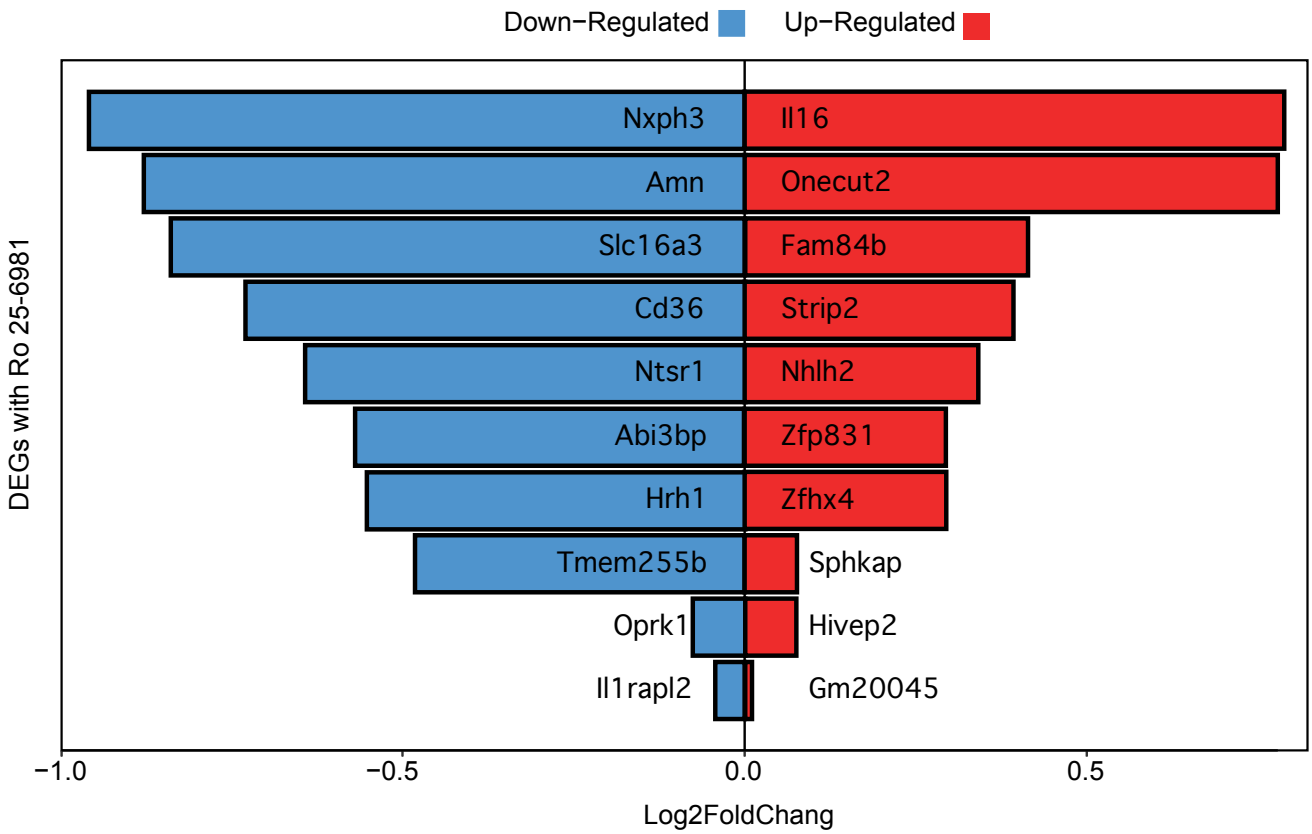

Supplemental Figure 3.4. Up-regulated and down-regulated genes with Ro 25-6981 acute treatment

Summary bar graph indicates the top 10 up- and down- regulated DEGs according to log_2fold change identified with acute Ro 25-6981 DEGs ($p \leq 0.05$). Blue indicates down-regulated while red indicates up-regulated fold changes.

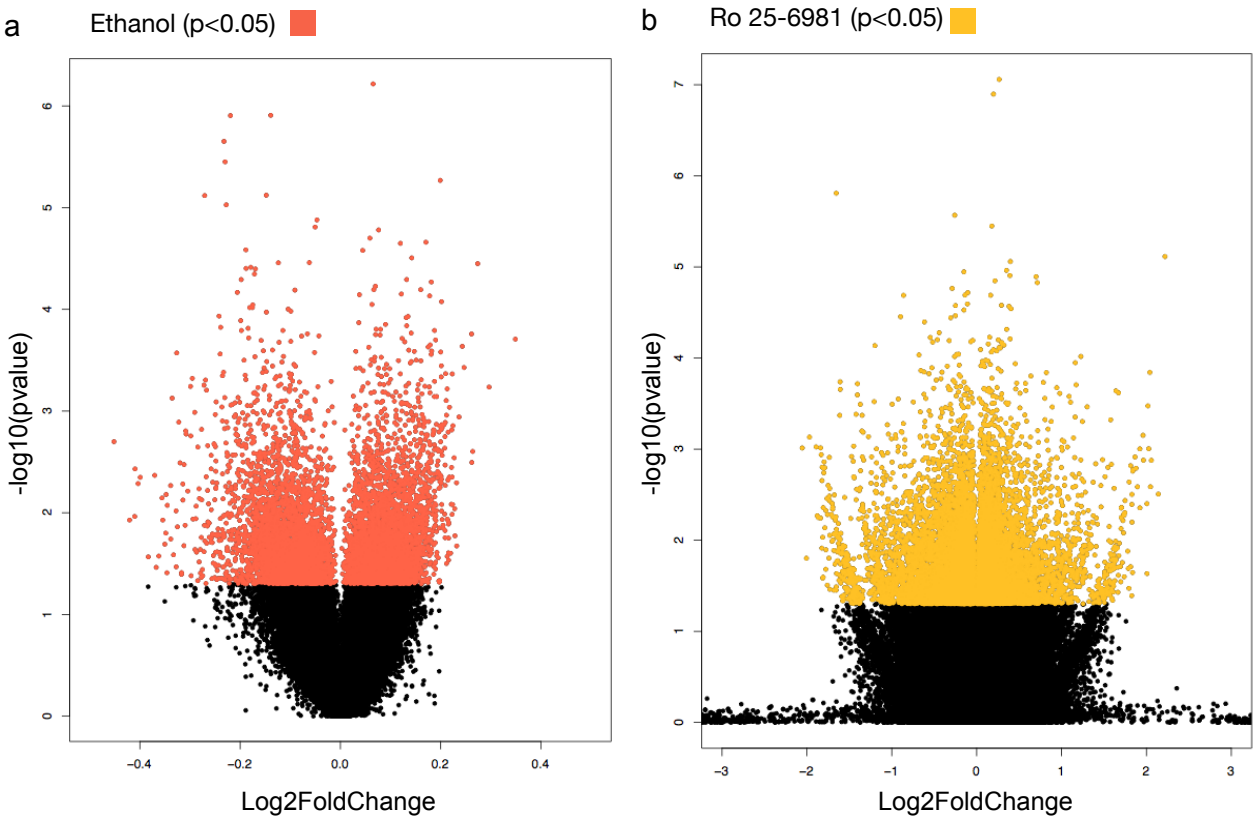

Supplemental Figure 3.5. Volcano plots of exons identified with DEXSeq with ethanol and Ro 25-6981 treatment

a) Volcano plot of differentially expressed exons with ethanol (n=7) compared to vehicle (saline, n=8) reveal a significant number of exons (red) both up- and down-regulated with ethanol exposure shown as positive of negative log_2fold change with treatment ($p \leq 0.05$). b) Volcano plot of differentially expressed exons with Ro 25-6981 compared to vehicle reveal a significant number of exons (yellow) both up- and down-regulated with Ro 25-6981 exposure shown as positive of negative log_2fold change with treatment ($p \leq 0.05$).

REFERENCES

1. Koob, G.F. & Le Moal, M. Addiction and the brain antireward system. *Annu Rev Psychol* **59**, 29-53 (2008).
2. Hoffman, P.L. & Tabakoff, B. Alcohol dependence: a commentary on mechanisms. *Alcohol Alcohol* **31**, 333-340 (1996).
3. Max Bayard, J.M., Keith Hill, Jack Woodside Alcohol Withdrawal syndrome. *American family Physician* **69**, 1443-1450 (2004).
4. Larson, E.W., Olincy, A., Rummans, T.A. & Morse, R.M. Disulfiram treatment of patients with both alcohol dependence and other psychiatric disorders: a review. *Alcohol Clin Exp Res* **16**, 125-130 (1992).
5. Volpicelli, J.R., Alterman, A.I., Hayashida, M. & O'Brien, C.P. Naltrexone in the treatment of alcohol dependence. *Arch Gen Psychiatry* **49**, 876-880 (1992).
6. Terenius, L., Wahlstrom, A. & Agren, H. Naloxone (Narcan) treatment in depression: clinical observations and effects on CSF endorphins and monoamine metabolites. *Psychopharmacology (Berl)* **54**, 31-33 (1977).
7. Mason, B.J. & Heyser, C.J. Acamprosate: a prototypic neuromodulator in the treatment of alcohol dependence. *CNS Neurol Disord Drug Targets* **9**, 23-32 (2010).
8. Mason, B.J. & Ownby, R.L. Acamprosate for the treatment of alcohol dependence: a review of double-blind, placebo-controlled trials. *CNS Spectr* **5**, 58-69 (2000).
9. Ralevski, E. *et al.* Treatment With Acamprosate in Patients With Schizophrenia Spectrum Disorders and Comorbid Alcohol Dependence. *J Dual Diagn* **7**, 64-73 (2011).
10. Whitworth, A.B. *et al.* Comparison of acamprosate and placebo in long-term treatment of alcohol dependence. *Lancet* **347**, 1438-1442 (1996).
11. Zarate, C., Jr. *et al.* Glutamatergic modulators: the future of treating mood disorders? *Harv Rev Psychiatry* **18**, 293-303 (2010).
12. American Psychiatric Association. & American Psychiatric Association. DSM-5 Task Force. *Diagnostic and statistical manual of mental disorders : DSM-5*, Edn. 5th. (American Psychiatric Association, Washington, D.C.; 2013).
13. Workman, E.R., Niere, F. & Raab-Graham, K.F. mTORC1-dependent protein synthesis underlying rapid antidepressant effect requires GABABR signaling. *Neuropharmacology* **73**, 192-203 (2013).
14. Boden, J.M. & Fergusson, D.M. Alcohol and depression. *Addiction* **106**, 906-914 (2011).
15. Krishnan, V. & Nestler, E.J. The molecular neurobiology of depression. *Nature* **455**, 894-902 (2008).
16. Berman, R.M. & Charney, D.S. Models of antidepressant action. *J Clin Psychiatry* **60 Suppl 14**, 16-20; discussion 31-15 (1999).
17. Murrough, J.W. & Charney, D.S. Is there anything really novel on the antidepressant horizon? *Curr Psychiatry Rep* **14**, 643-649 (2012).
18. Sellers, E.M. Biobehavioural basis of pharmacologic treatment of alcohol dependence. *Alcohol Alcohol Suppl* **2**, 517-521 (1994).
19. Cornelius, J.R. *et al.* Fluoxetine in depressed alcoholics. A double-blind, placebo-controlled trial. *Arch Gen Psychiatry* **54**, 700-705 (1997).

20. Cornelius, J.R. *et al.* Disproportionate suicidality in patients with comorbid major depression and alcoholism. *Am J Psychiatry* **152**, 358-364 (1995).
21. Horst, W.D. & Preskorn, S.H. Mechanisms of action and clinical characteristics of three atypical antidepressants: venlafaxine, nefazodone, bupropion. *J Affect Disord* **51**, 237-254 (1998).
22. Kranzler, H.R. & Rosenthal, R.N. Dual diagnosis: alcoholism and co-morbid psychiatric disorders. *Am J Addict* **12 Suppl 1**, S26-40 (2003).
23. Donovan, S. *et al.* Deliberate self-harm and antidepressant drugs. Investigation of a possible link. *Br J Psychiatry* **177**, 551-556 (2000).
24. Jick, H., Kaye, J.A. & Jick, S.S. Antidepressants and the risk of suicidal behaviors. *JAMA* **292**, 338-343 (2004).
25. Abdallah, C.G., Sanacora, G., Duman, R.S. & Krystal, J.H. in Annual review of medicine, Vol. 66 509-523 (NIH Public Access, 2015).
26. Browne, C.A. & Lucki, I. Antidepressant effects of ketamine: mechanisms underlying fast-acting novel antidepressants. *Front Pharmacol* **4**, 161 (2013).
27. De Luca, M.T., Meringolo, M., Spagnolo, P.A. & Badiani, A. The role of setting for ketamine abuse: clinical and preclinical evidence. *Rev Neurosci* **23**, 769-780 (2012).
28. Kew, J.N., Trube, G. & Kemp, J.A. A novel mechanism of activity-dependent NMDA receptor antagonism describes the effect of ifenprodil in rat cultured cortical neurones. *J Physiol* **497 (Pt 3)**, 761-772 (1996).
29. Williams, K. Extracellular Modulation of NMDA Receptors, in *Biology of the NMDA Receptor*. (ed. A.M. Van Dongen) (Boca Raton (FL); 2009).
30. Carter, C. *et al.* Ifenprodil and SL 82.0715 as cerebral anti-ischemic agents. II. Evidence for N-methyl-D-aspartate receptor antagonist properties. *J Pharmacol Exp Ther* **247**, 1222-1232 (1988).
31. Mutel, V. *et al.* In vitro binding properties in rat brain of [3H]Ro 25-6981, a potent and selective antagonist of NMDA receptors containing NR2B subunits. *J Neurochem* **70**, 2147-2155 (1998).
32. Fischer, G. *et al.* Ro 25-6981, a highly potent and selective blocker of N-methyl-D-aspartate receptors containing the NR2B subunit. Characterization in vitro. *J Pharmacol Exp Ther* **283**, 1285-1292 (1997).
33. Malherbe, P. *et al.* Identification of critical residues in the amino terminal domain of the human NR2B subunit involved in the RO 25-6981 binding pocket. *J Pharmacol Exp Ther* **307**, 897-905 (2003).
34. Kiselycznyk, C. *et al.* NMDA receptor subunits and associated signaling molecules mediating antidepressant-related effects of NMDA-GluN2B antagonism. *Behav Brain Res* **287**, 89-95 (2015).
35. Stephan, K.E., Baldeweg, T. & Friston, K.J. Synaptic plasticity and dysconnection in schizophrenia. *Biol Psychiatry* **59**, 929-939 (2006).
36. Grant, B.F. & Harford, T.C. Comorbidity between DSM-IV alcohol use disorders and major depression: results of a national survey. *Drug Alcohol Depend* **39**, 197-206 (1995).
37. Schuckit, M.A. *et al.* Comparison of induced and independent major depressive disorders in 2,945 alcoholics. *Am J Psychiatry* **154**, 948-957 (1997).
38. Hasin, D.S. & Grant, B.F. Major depression in 6050 former drinkers: association with past alcohol dependence. *Arch Gen Psychiatry* **59**, 794-800 (2002).

39. Greenfield, S.F. *et al.* The effect of depression on return to drinking: a prospective study. *Arch Gen Psychiatry* **55**, 259-265 (1998).
40. Conner, K.R. *et al.* Transitions to, and correlates of, suicidal ideation, plans, and unplanned and planned suicide attempts among 3,729 men and women with alcohol dependence. *J Stud Alcohol Drugs* **68**, 654-662 (2007).
41. Markou, A., Kosten, T.R. & Koob, G.F. Neurobiological similarities in depression and drug dependence: a self-medication hypothesis. *Neuropsychopharmacology* **18**, 135-174 (1998).
42. Cornelius, J.R., Bukstein, O., Salloum, I. & Clark, D. Alcohol and psychiatric comorbidity. *Recent Dev Alcohol* **16**, 361-374 (2003).
43. Sabino, V., Narayan, A.R., Zeric, T., Steardo, L. & Cottone, P. mTOR activation is required for the anti-alcohol effect of ketamine, but not memantine, in alcohol-preferring rats. *Behav Brain Res* **247**, 9-16 (2013).
44. Harris, R.A. Ethanol actions on multiple ion channels: which are important? *Alcohol Clin Exp Res* **23**, 1563-1570 (1999).
45. Lovinger, D.M. & Roberto, M. Synaptic effects induced by alcohol. *Curr Top Behav Neurosci* **13**, 31-86 (2013).
46. Zhou, Q., Verdoorn, T.A. & Lovinger, D.M. Alcohols potentiate the function of 5-HT3 receptor-channels on NCB-20 neuroblastoma cells by favouring and stabilizing the open channel state. *J Physiol* **507 (Pt 2)**, 335-352 (1998).
47. Welsh, B.T., Goldstein, B.E. & Mihic, S.J. Single-channel analysis of ethanol enhancement of glycine receptor function. *J Pharmacol Exp Ther* **330**, 198-205 (2009).
48. Sebe, J.Y., Eggers, E.D. & Berger, A.J. Differential effects of ethanol on GABA(A) and glycine receptor-mediated synaptic currents in brain stem motoneurons. *J Neurophysiol* **90**, 870-875 (2003).
49. Ziskind-Conhaim, L., Gao, B.X. & Hinckley, C. Ethanol dual modulatory actions on spontaneous postsynaptic currents in spinal motoneurons. *J Neurophysiol* **89**, 806-813 (2003).
50. Lu, S.M. & Yeh, H.H. Ethanol modulates AMPA-induced current responses of primary somatosensory cortical neurons. *Neurochem Int* **35**, 175-183 (1999).
51. Blanke, M.L. & VanDongen, A.M.J. Activation Mechanisms of the NMDA Receptor, in *Biology of the NMDA Receptor*. (ed. A.M. Van Dongen) (Boca Raton (FL); 2009).
52. Lovinger, D.M., White, G. & Weight, F.F. in Science, Vol. 243 1721-1724 (American Association for the Advancement of Science, 1989).
53. Lovinger, D.M., White, G. & Weight, F.F. NMDA receptor-mediated synaptic excitation selectively inhibited by ethanol in hippocampal slice from adult rat. *J Neurosci* **10**, 1372-1379 (1990).
54. Morrisett, R.A. & Swartzwelder, H.S. Attenuation of hippocampal long-term potentiation by ethanol: a patch-clamp analysis of glutamatergic and GABAergic mechanisms. *J Neurosci* **13**, 2264-2272 (1993).
55. Wang, J. *et al.* Ethanol induces long-term facilitation of NR2B-NMDA receptor activity in the dorsal striatum: implications for alcohol drinking behavior. *J Neurosci* **27**, 3593-3602 (2007).
56. McBain, C.J. & Mayer, M.L. N-methyl-D-aspartic acid receptor structure and function. *Physiol Rev* **74**, 723-760 (1994).

57. McBain, C.J., DiChiara, T.J. & Kauer, J.A. Activation of metabotropic glutamate receptors differentially affects two classes of hippocampal interneurons and potentiates excitatory synaptic transmission. *J Neurosci* **14**, 4433-4445 (1994).
58. Fink, K. & Gothert, M. Both ethanol and ifenprodil inhibit NMDA-evoked release of various neurotransmitters at different, yet proportional potency: potential relation to NMDA receptor subunit composition. *Naunyn Schmiedebergs Arch Pharmacol* **354**, 312-319 (1996).
59. Swartzwelder, H.S., Wilson, W.A. & Tayyeb, M.I. Differential sensitivity of NMDA receptor-mediated synaptic potentials to ethanol in immature versus mature hippocampus. *Alcohol Clin Exp Res* **19**, 320-323 (1995).
60. Zhou, Z., Yuan, Q., Mash, D.C. & Goldman, D. Substance-specific and shared transcription and epigenetic changes in the human hippocampus chronically exposed to cocaine and alcohol. *Proc Natl Acad Sci U S A* **108**, 6626-6631 (2011).
61. Barak, S. *et al.* Disruption of alcohol-related memories by mTORC1 inhibition prevents relapse. *Nat Neurosci* **16**, 1111-1117 (2013).
62. Neasta, J., Ben Hamida, S., Yowell, Q., Carnicella, S. & Ron, D. Role for mammalian target of rapamycin complex 1 signaling in neuroadaptations underlying alcohol-related disorders. *Proc Natl Acad Sci U S A* **107**, 20093-20098 (2010).
63. Minami, K., Minami, M. & Harris, R.A. Inhibition of 5-hydroxytryptamine type 2A receptor-induced currents by n-alcohols and anesthetics. *J Pharmacol Exp Ther* **281**, 1136-1143 (1997).
64. Minami, K., Vanderah, T.W., Minami, M. & Harris, R.A. Inhibitory effects of anesthetics and ethanol on muscarinic receptors expressed in Xenopus oocytes. *Eur J Pharmacol* **339**, 237-244 (1997).
65. Aryal, P., Dvir, H., Choe, S. & Slesinger, P.A. A discrete alcohol pocket involved in GIRK channel activation. *Nat Neurosci* **12**, 988-995 (2009).
66. Lewohl, J.M. *et al.* G-protein-coupled inwardly rectifying potassium channels are targets of alcohol action. *Nat Neurosci* **2**, 1084-1090 (1999).
67. Blednov, Y.A., Stoffel, M., Chang, S.R. & Harris, R.A. in J Pharmacol Exp Ther, Vol. 298 521-530 (American Society for Pharmacology and Experimental Therapeutics, 2001).
68. Gonzales, R.A., Job, M.O. & Doyon, W.M. The role of mesolimbic dopamine in the development and maintenance of ethanol reinforcement. *Pharmacol Ther* **103**, 121-146 (2004).
69. Siggins, G.R., Roberto, M. & Nie, Z. The tipsy terminal: presynaptic effects of ethanol. *Pharmacol Ther* **107**, 80-98 (2005).
70. Autry, A.E. *et al.* NMDA receptor blockade at rest triggers rapid behavioural antidepressant responses. *Nature* **475**, 91-95 (2011).
71. Li, N. *et al.* Glutamate N-methyl-D-aspartate receptor antagonists rapidly reverse behavioral and synaptic deficits caused by chronic stress exposure. *Biol Psychiatry* **69**, 754-761 (2011).
72. Ibrahim, L. *et al.* Rapid decrease in depressive symptoms with an N-methyl-d-aspartate antagonist in ECT-resistant major depression. *Prog Neuropsychopharmacol Biol Psychiatry* **35**, 1155-1159 (2011).

73. Lepack, A.E., Fuchikami, M., Dwyer, J.M., Banasr, M. & Duman, R.S. BDNF release is required for the behavioral actions of ketamine. *Int J Neuropsychopharmacol* **18** (2014).
74. Li, N. *et al.* mTOR-dependent synapse formation underlies the rapid antidepressant effects of NMDA antagonists. *Science* **329**, 959-964 (2010).
75. Raab-Graham, K.F., Workman, E.R., Namjoshi, S. & Niere, F. Pushing the threshold: How NMDAR antagonists induce homeostasis through protein synthesis to remedy depression. *Brain Res* (2016).
76. Duman, R.S., Aghajanian, G.K., Sanacora, G. & Krystal, J.H. Synaptic plasticity and depression: new insights from stress and rapid-acting antidepressants. *Nat Med* **22**, 238-249 (2016).
77. Mony, L., Kew, J.N., Gunthorpe, M.J. & Paoletti, P. Allosteric modulators of NR2B-containing NMDA receptors: molecular mechanisms and therapeutic potential. *Br J Pharmacol* **157**, 1301-1317 (2009).
78. Workman, E.R. *et al.* Rapid antidepressants stimulate the decoupling of GABA receptors from GIRK/Kir3 channels through increased protein stability of 14-3-3eta. *Mol Psychiatry* (2015).
79. Wolfe, S.A. *et al.* FMRP regulates an ethanol-dependent shift in GABABR function and expression with rapid antidepressant properties. *Nat Commun* **7**, 12867 (2016).
80. Kauer, J.A. & Malenka, R.C. Synaptic plasticity and addiction. *Nat Rev Neurosci* **8**, 844-858 (2007).
81. Fernandez-Moya, S.M., Bauer, K.E. & Kiebler, M.A. Meet the players: local translation at the synapse. *Front Mol Neurosci* **7**, 84 (2014).
82. Hanus, C. & Schuman, E.M. Proteostasis in complex dendrites. *Nat Rev Neurosci* **14**, 638-648 (2013).
83. Dahm, R. & Kiebler, M. Cell biology: silenced RNA on the move. *Nature* **438**, 432-435 (2005).
84. Holt, C.E. & Bullock, S.L. Subcellular mRNA localization in animal cells and why it matters. *Science* **326**, 1212-1216 (2009).
85. Doyle, M. & Kiebler, M.A. Mechanisms of dendritic mRNA transport and its role in synaptic tagging. *EMBO J* **30**, 3540-3552 (2011).
86. Di Liegro, C.M., Schiera, G. & Di Liegro, I. Regulation of mRNA transport, localization and translation in the nervous system of mammals (Review). *Int J Mol Med* **33**, 747-762 (2014).
87. Bassell, G.J. & Warren, S.T. in Neuron, Vol. 60 201-214 (2008).
88. Dictenberg, J.B., Swanger, S.A., Antar, L.N., Singer, R.H. & Bassell, G.J. in Developmental Cell, Vol. 14 926-939 (2008).
89. Zalfa, F., Achsel, T. & Bagni, C. mRNPs, polysomes or granules: FMRP in neuronal protein synthesis. *Curr Opin Neurobiol* **16**, 265-269 (2006).
90. Huttelmaier, S. *et al.* Spatial regulation of beta-actin translation by Src-dependent phosphorylation of ZBP1. *Nature* **438**, 512-515 (2005).
91. Steward, O. & Levy, W.B. Preferential localization of polyribosomes under the base of dendritic spines in granule cells of the dentate gyrus. *J Neurosci* **2**, 284-291 (1982).
92. Cajigas, I.J. *et al.* in Neuron, Vol. 74 453-466 (2012).
93. Neasta, J., Barak, S., Hamida, S.B. & Ron, D. mTOR complex 1: a key player in neuroadaptations induced by drugs of abuse. *J Neurochem* **130**, 172-184 (2014).

94. Most, D., Workman, E. & Harris, R.A. Synaptic adaptations by alcohol and drugs of abuse: changes in microRNA expression and mRNA regulation. *Front Mol Neurosci* **7**, 85 (2014).
95. Ficek, J. *et al.* Molecular profile of dissociative drug ketamine in relation to its rapid antidepressant action. *BMC Genomics* **17**, 362 (2016).
96. Chandler, L.J., Harris, R.A. & Crews, F.T. Ethanol tolerance and synaptic plasticity. *Trends Pharmacol Sci* **19**, 491-495 (1998).
97. Volk, L.J., Pfeiffer, B.E., Gibson, J.R. & Huber, K.M. Multiple Gq-coupled receptors converge on a common protein synthesis-dependent long-term depression that is affected in fragile X syndrome mental retardation. *J Neurosci* **27**, 11624-11634 (2007).
98. Hay, N. & Sonenberg, N. Upstream and downstream of mTOR. *Genes Dev* **18**, 1926-1945 (2004).
99. Hoeffer, C.A. & Klann, E. NMDA Receptors and Translational Control, in *Biology of the NMDA Receptor*. (ed. A.M. Van Dongen) (Boca Raton (FL); 2009).
100. Tang, S.J. *et al.* A rapamycin-sensitive signaling pathway contributes to long-term synaptic plasticity in the hippocampus. *Proc Natl Acad Sci U S A* **99**, 467-472 (2002).
101. Koob, G.F. & Le Moal, M. Drug addiction, dysregulation of reward, and allostasis. *Neuropsychopharmacology* **24**, 97-129 (2001).
102. Filip, M. & Frankowska, M. GABA(B) receptors in drug addiction. *Pharmacol Rep* **60**, 755-770 (2008).
103. Bettler, B., Kaupmann, K., Mosbacher, J. & Gassmann, M. Molecular structure and physiological functions of GABA(B) receptors. *Physiol Rev* **84**, 835-867 (2004).
104. Colombo, G. *et al.* The GABA(B) receptor agonists baclofen and CGP 44532 prevent acquisition of alcohol drinking behaviour in alcohol-preferring rats. *Alcohol Alcohol* **37**, 499-503 (2002).
105. Carai, M.A. *et al.* Withdrawal syndrome from gamma-hydroxybutyric acid (GHB) and 1,4-butanediol (1,4-BD) in Sardinian alcohol-preferring rats. *Brain Res Brain Res Protoc* **15**, 75-78 (2005).
106. Darnell, J.C. *et al.* FMRP stalls ribosomal translocation on mRNAs linked to synaptic function and autism. *Cell* **146**, 247-261 (2011).
107. Sidorov, M.S., Auerbach, B.D. & Bear, M.F. Fragile X mental retardation protein and synaptic plasticity. *Mol Brain* **6**, 15 (2013).
108. Farris, S.P. *et al.* Applying the new genomics to alcohol dependence. *Alcohol* **49**, 825-836 (2015).
109. Smith, L.N. *et al.* in Neuron, Vol. 82 645-658 (2014).
110. Katz, Y., Wang, E.T., Airoldi, E.M. & Burge, C.B. Analysis and design of RNA sequencing experiments for identifying isoform regulation. *Nat Methods* **7**, 1009-1015 (2010).
111. Barh, D., Zambare, V. & Azevedo, V. *Omics : applications in biomedical, agricultural, and environmental sciences*. (CRC Press, Boca Raton, FL; 2013).
112. Farris, S.P., Arasappan, D., Hunicke-Smith, S., Harris, R.A. & Mayfield, R.D. Transcriptome organization for chronic alcohol abuse in human brain. *Mol Psychiatry* (2014).

113. Enoch, M.A. *et al.* GABAergic gene expression in postmortem hippocampus from alcoholics and cocaine addicts; corresponding findings in alcohol-naive P and NP rats. *PLoS One* **7**, e29369 (2012).
114. Kerns, R.T. *et al.* Ethanol-responsive brain region expression networks: implications for behavioral responses to acute ethanol in DBA/2J versus C57BL/6J mice. *J Neurosci* **25**, 2255-2266 (2005).
115. Piechota, M. *et al.* The dissection of transcriptional modules regulated by various drugs of abuse in the mouse striatum. *Genome Biol* **11**, R48 (2010).
116. Farris, S.P., Wolen, A.R. & Miles, M.F. Using expression genetics to study the neurobiology of ethanol and alcoholism. *Int Rev Neurobiol* **91**, 95-128 (2010).
117. Darby, M.M., Yolken, R.H. & Sabunciyan, S. Consistently altered expression of gene sets in postmortem brains of individuals with major psychiatric disorders. *Transl Psychiatry* **6**, e890 (2016).
118. Pantazatos, S.P. *et al.* Whole-transcriptome brain expression and exon-usage profiling in major depression and suicide: evidence for altered glial, endothelial and ATPase activity. *Mol Psychiatry* (2016).
119. Kang, H.J. *et al.* Decreased expression of synapse-related genes and loss of synapses in major depressive disorder. *Nat Med* **18**, 1413-1417 (2012).
120. Lee, J.H. *et al.* Gene expression profile analysis of genes in rat hippocampus from antidepressant treated rats using DNA microarray. *BMC Neurosci* **11**, 152 (2010).
121. Koltchine, V., Anantharam, V., Wilson, A., Bayley, H. & Treistman, S.N. Homomeric assemblies of NMDAR1 splice variants are sensitive to ethanol. *Neurosci Lett* **152**, 13-16 (1993).
122. Samson, H.H. & Harris, R.A. Neurobiology of alcohol abuse. *Trends Pharmacol Sci* **13**, 206-211 (1992).
123. Lee, C., Mayfield, R.D. & Harris, R.A. Altered gamma-aminobutyric acid type B receptor subunit 1 splicing in alcoholics. *Biol Psychiatry* **75**, 765-773 (2014).
124. Durand, G.M. *et al.* Cloning of an apparent splice variant of the rat N-methyl-D-aspartate receptor NMDAR1 with altered sensitivity to polyamines and activators of protein kinase C. *Proc Natl Acad Sci U S A* **89**, 9359-9363 (1992).
125. Sasabe, T. & Ishiura, S. Alcoholism and alternative splicing of candidate genes. *Int J Environ Res Public Health* **7**, 1448-1466 (2010).
126. Skolnick, P., Popik, P. & Trullas, R. Glutamate-based antidepressants: 20 years on. *Trends Pharmacol Sci* **30**, 563-569 (2009).
127. Nosyreva, E. *et al.* Acute suppression of spontaneous neurotransmission drives synaptic potentiation. *J Neurosci* **33**, 6990-7002 (2013).
128. Raab-Graham, K.F., Workman, E.R, Namjoshi, S., Niere, F. Pushing the threshold: how NMDAR antagonists induce homeostasis through protein synthesis to remedy depression. *Brain Research* **in press** (2016).
129. Huber, K.M., Gallagher, S.M., Warren, S.T. & Bear, M.F. in PNAS, Vol. 99 7746-7750 (National Acad Sciences, 2002).
130. Vanderklish, P.W. & Edelman, G.M. Dendritic spines elongate after stimulation of group 1 metabotropic glutamate receptors in cultured hippocampal neurons. *Proc Natl Acad Sci U S A* **99**, 1639-1644 (2002).
131. Hou, L. *et al.* in Neuron, Vol. 51 441-454 (2006).

132. Nalavadi, V.C., Muddashetty, R.S., Gross, C. & Bassell, G.J. Dephosphorylation-induced ubiquitination and degradation of FMRP in dendrites: a role in immediate early mGluR-stimulated translation. *J Neurosci* **32**, 2582-2587 (2012).
133. Hagerman, R. & Hagerman, P. in The Lancet Neurology, Vol. 12 786-798 (2013).
134. Ron, D. & Messing, R.O. Signaling pathways mediating alcohol effects. *Curr Top Behav Neurosci* **13**, 87-126 (2013).
135. Placzek, A.N. *et al.* Translational control of nicotine-evoked synaptic potentiation in mice and neuronal responses in human smokers by eIF2alpha. *Elife* **5** (2016).
136. Luscher, C. & Malenka, R.C. Drug-evoked synaptic plasticity in addiction: from molecular changes to circuit remodeling. *Neuron* **69**, 650-663 (2011).
137. Niere, F., Wilkerson, J.R. & Huber, K.M. in J. Neurosci., Vol. 32 5924-5936 (Society for Neuroscience, 2012).
138. Chandler, L.J., Sumners, C. & Crews, F.T. Ethanol inhibits NMDA receptor-mediated excitotoxicity in rat primary neuronal cultures. *Alcohol Clin Exp Res* **17**, 54-60 (1993).
139. Sosanya, N.M. *et al.* Degradation of high affinity HuD targets releases Kv1.1 mRNA from miR-129 repression by mTORC1. *J Cell Biol* **202**, 53-69 (2013).
140. Varga, V. *et al.* Fast synaptic subcortical control of hippocampal circuits. *Science* **326**, 449-453 (2009).
141. tom Dieck, S. *et al.* Direct visualization of newly synthesized target proteins in situ. *Nat Methods* **12**, 411-414 (2015).
142. Quinlan, E.M., Olstein, D.H. & Bear, M.F. Bidirectional, experience-dependent regulation of N-methyl-D-aspartate receptor subunit composition in the rat visual cortex during postnatal development. *Proc Natl Acad Sci U S A* **96**, 12876-12880 (1999).
143. Jain, R. *et al.* RIP-Chip analysis: RNA-Binding Protein Immunoprecipitation-Microarray (Chip) Profiling. *Methods Mol Biol* **703**, 247-263 (2011).
144. Keene, J.D., Komisarow, J.M. & Friedersdorf, M.B. RIP-Chip: the isolation and identification of mRNAs, microRNAs and protein components of ribonucleoprotein complexes from cell extracts. *Nat Protoc* **1**, 302-307 (2006).
145. Pfaffl, M.W. A new mathematical model for relative quantification in real-time RT-PCR. *Nucleic Acids Res* **29**, e45 (2001).
146. Cohen, J. Statistical Power Analysis. *Current Directions in Psychological science* **1**, 98-101 (1992).
147. Treit, D. & Fundytus, M. in Pharmacology Biochemistry and Behavior, Vol. 31 959-962 (1988).
148. David, D.J. *et al.* Neurogenesis-dependent and -independent effects of fluoxetine in an animal model of anxiety/depression. *Neuron* **62**, 479-493 (2009).
149. Surget, A. *et al.* Drug-dependent requirement of hippocampal neurogenesis in a model of depression and of antidepressant reversal. *Biol Psychiatry* **64**, 293-301 (2008).
150. Porsolt, R.D., Bertin, A., Blavet, N., Deniel, M. & Jalfre, M. Immobility induced by forced swimming in rats: effects of agents which modify central catecholamine and serotonin activity. *Eur J Pharmacol* **57**, 201-210 (1979).
151. Blednov, Y.A. *et al.* Linking GABA(A) receptor subunits to alcohol-induced conditioned taste aversion and recovery from acute alcohol intoxication. *Neuropharmacology* **67**, 46-56 (2013).

152. Rhodes, J.S., Best, K., Belknap, J.K., Finn, D.A. & Crabbe, J.C. in Physiology & Behavior, Vol. 84 53-63 (2005).
153. Margeta-Mitrovic, M., Jan, Y.N. & Jan, L.Y. in Neuron, Vol. 27 97-106 (2000).
154. Ginsburg, B.C. *et al.* Mouse breathalyzer. *Alcohol Clin Exp Res* **32**, 1181-1185 (2008).
155. Graber, T.E. *et al.* Reactivation of stalled polyribosomes in synaptic plasticity. *Proc Natl Acad Sci U S A* **110**, 16205-16210 (2013).
156. Hendel, T. *et al.* Fluorescence changes of genetic calcium indicators and OGB-1 correlated with neural activity and calcium in vivo and in vitro. *J Neurosci* **28**, 7399-7411 (2008).
157. Jaso, B.A. *et al.* Therapeutic Modulation of Glutamate Receptors in Major Depressive Disorder. *Curr Neuropharmacol* (2016).
158. Muddashetty, R.S., Kelić, S., Gross, C., Xu, M. & Bassell, G.J. in J. Neurosci., Vol. 27 5338-5348 (Society for Neuroscience, 2007).
159. Soden, M.E. & Chen, L. Fragile X protein FMRP is required for homeostatic plasticity and regulation of synaptic strength by retinoic acid. *J. Neurosci.* **30**, 16910-16921 (2010).
160. Muddashetty, R.S. *et al.* in Mol. Cell, Vol. 42 673-688 (2011).
161. Antar, L.N., Li, C., Zhang, H., Carroll, R.C. & Bassell, G.J. Local functions for FMRP in axon growth cone motility and activity-dependent regulation of filopodia and spine synapses. *Mol Cell Neurosci* **32**, 37-48 (2006).
162. Christie, S.B., Akins, M.R., Schwob, J.E. & Fallon, J.R. The FXG: a presynaptic fragile X granule expressed in a subset of developing brain circuits. *J Neurosci* **29**, 1514-1524 (2009).
163. Gatto, C.L., Pereira, D. & Broadie, K. GABAergic circuit dysfunction in the Drosophila Fragile X syndrome model. *Neurobiol Dis* **65**, 142-159 (2014).
164. D'Hulst, C. *et al.* Decreased expression of the GABAA receptor in fragile X syndrome. *Brain Res* **1121**, 238-245 (2006).
165. Henderson, C. *et al.* Reversal of Disease-Related Pathologies in the Fragile X Mouse Model by Selective Activation of GABAB Receptors with Arbaclofen. *Science Translational Medicine* **4**, 152ra128-152ra128 (2012).
166. Qin, M. *et al.* R-Baclofen Reverses a Social Behavior Deficit and Elevated Protein Synthesis in a Mouse Model of Fragile X Syndrome. *International Journal of Neuropsychopharmacology* **18**, pyv034 (2015).
167. Gibson, J.R., Bartley, A.F., Hays, S.A. & Huber, K.M. in Journal of Neurophysiology, Vol. 100 2615-2626 (American Physiological Society, 2008).
168. Osterweil, E.K., Kind, P.C. & Bear, M.F. Lifting the mood on treating fragile X. *Biol Psychiatry* **72**, 895-897 (2012).
169. Kenny, P.J. Epigenetics, microRNA, and addiction. *Dialogues Clin Neurosci* **16**, 335-344 (2014).
170. Holmes, A., Spanagel, R. & Krystal, J.H. Glutamatergic targets for new alcohol medications. *Psychopharmacology* **229**, 539-554 (2013).
171. Krishnan-Sarin, S., O'Malley, S. & Krystal, J.H. Treatment implications: using neuroscience to guide the development of new pharmacotherapies for alcoholism. *Alcohol Res Health* **31**, 400-407 (2008).
172. Johnson, J.M. *et al.* Genome-wide survey of human alternative pre-mRNA splicing with exon junction microarrays. *Science* **302**, 2141-2144 (2003).

173. Vuong, C.K., Black, D.L. & Zheng, S. The neurogenetics of alternative splicing. *Nat Rev Neurosci* **17**, 265-281 (2016).
174. Warden, A.S. & Mayfield, R.D. Gene expression profiling in the human alcoholic brain. *Neuropharmacology* (2017).
175. Zanos, P. *et al.* NMDAR inhibition-independent antidepressant actions of ketamine metabolites. *Nature* **533**, 481-486 (2016).
176. Trapnell, C. *et al.* Differential gene and transcript expression analysis of RNA-seq experiments with TopHat and Cufflinks. *Nat Protoc* **7**, 562-578 (2012).
177. Anders, S., Reyes, A. & Huber, W. Detecting differential usage of exons from RNA-seq data. *Genome Res* **22**, 2008-2017 (2012).
178. Anders, S., Pyl, P.T. & Huber, W. HTSeq--a Python framework to work with high-throughput sequencing data. *Bioinformatics* **31**, 166-169 (2015).
179. Love, M.I., Huber, W. & Anders, S. Moderated estimation of fold change and dispersion for RNA-seq data with DESeq2. *Genome Biol* **15**, 550 (2014).
180. Reyes, A. *et al.* Drift and conservation of differential exon usage across tissues in primate species. *Proc Natl Acad Sci U S A* **110**, 15377-15382 (2013).
181. Chen, E.Y. *et al.* Enrichr: interactive and collaborative HTML5 gene list enrichment analysis tool. *BMC Bioinformatics* **14**, 128 (2013).
182. Kuleshov, M.V. *et al.* Enrichr: a comprehensive gene set enrichment analysis web server 2016 update. *Nucleic Acids Res* **44**, W90-97 (2016).
183. Martinowich, K., Jimenez, D.V., Zarate, C.A., Jr. & Manji, H.K. Rapid antidepressant effects: moving right along. *Mol Psychiatry* **18**, 856-863 (2013).
184. Malherbe, P. *et al.* Mutational analysis and molecular modeling of the allosteric binding site of a novel, selective, noncompetitive antagonist of the metabotropic glutamate 1 receptor. *J Biol Chem* **278**, 8340-8347 (2003).
185. Allgaier, C. Ethanol sensitivity of NMDA receptors. *Neurochem Int* **41**, 377-382 (2002).
186. Zorumski, C.F., Mennerick, S. & Izumi, Y. Acute and chronic effects of ethanol on learning-related synaptic plasticity. *Alcohol* **48**, 1-17 (2014).
187. McCool, B.A. Ethanol modulation of synaptic plasticity. *Neuropharmacology* **61**, 1097-1108 (2011).
188. Thomas, G.M. & Huganir, R.L. MAPK cascade signalling and synaptic plasticity. *Nat Rev Neurosci* **5**, 173-183 (2004).
189. Agoglia, A.E. *et al.* Alcohol alters the activation of ERK1/2, a functional regulator of binge alcohol drinking in adult C57BL/6J mice. *Alcohol Clin Exp Res* **39**, 463-475 (2015).
190. Fuchsova, B., Alvarez Julia, A., Rizavi, H.S., Frasch, A.C. & Pandey, G.N. Altered expression of neuroplasticity-related genes in the brain of depressed suicides. *Neuroscience* **299**, 1-17 (2015).
191. Raab-Graham, K.F., Workman, E.R., Namjoshi, S. & Niere, F. Pushing the threshold: How NMDAR antagonists induce homeostasis through protein synthesis to remedy depression. *Brain Res* **1647**, 94-104 (2016).
192. Dingledine, R., Borges, K., Bowie, D. & Traynelis, S.F. The glutamate receptor ion channels. *Pharmacol Rev* **51**, 7-61 (1999).
193. Traynelis, S.F., Burgess, M.F., Zheng, F., Lyuboslavsky, P. & Powers, J.L. Control of voltage-independent zinc inhibition of NMDA receptors by the NR1 subunit. *J Neurosci* **18**, 6163-6175 (1998).

194. Vicini, S. *et al.* Functional and pharmacological differences between recombinant N-methyl-D-aspartate receptors. *J Neurophysiol* **79**, 555-566 (1998).
195. Standley, S., Roche, K.W., McCallum, J., Sans, N. & Wenthold, R.J. PDZ domain suppression of an ER retention signal in NMDA receptor NR1 splice variants. *Neuron* **28**, 887-898 (2000).
196. Takatsu, H. *et al.* ATP9B, a P4-ATPase (a putative aminophospholipid translocase), localizes to the trans-Golgi network in a CDC50 protein-independent manner. *J Biol Chem* **286**, 38159-38167 (2011).
197. Most, D., Ferguson, L., Blednov, Y., Mayfield, R.D. & Harris, R.A. The synaptoneurosome transcriptome: a model for profiling the emolecular effects of alcohol. *Pharmacogenomics J* **15**, 177-188 (2015).
198. Vega, F.M. & Ridley, A.J. The RhoB small GTPase in physiology and disease. *Small GTPases*, 1-10 (2016).
199. Tizabi, Y., Bhatti, B.H., Manaye, K.F., Das, J.R. & Akinfiresoye, L. Antidepressant-like effects of low ketamine dose is associated with increased hippocampal AMPA/NMDA receptor density ratio in female Wistar-Kyoto rats. *Neuroscience* **213**, 72-80 (2012).
200. Li, Q., Lee, J.A. & Black, D.L. Neuronal regulation of alternative pre-mRNA splicing. *Nat Rev Neurosci* **8**, 819-831 (2007).